

The Institute of Paper Chemistry

Appleton, Wisconsin

Doctor's Dissertation

The Movement of a Soluble Material
During the Washing of a Bed of Packed Solids

William Roger Sherman

June, 1962

LOAN COPY
To be returned to
EDITORIAL DEPARTMENT

THE MOVEMENT OF A SOLUBLE MATERIAL
DURING THE WASHING OF A BED OF PACKED SOLIDS

A thesis submitted by

William Roger Sherman

B.S. 1956, Rensselaer Polytechnic Institute
M.S. 1958, Lawrence College

in partial fulfillment of the requirements
of The Institute of Paper Chemistry
for the degree of Doctor of Philosophy
from Lawrence College,
Appleton, Wisconsin

June, 1962

TABLE OF CONTENTS

	Page
INTRODUCTION	1
PRESENTATION OF THE PROBLEM	5
THEORY	7
The Irregular Movement of Solute in a Bed of Packed Solids	7
Predictions of the Diffusionlike Theory	16
Application of the Diffusionlike Differential Equation Using the Step Function Boundary Condition	20
Application of the Diffusionlike Differential Equation With a New Boundary Condition	26
EXPERIMENTAL EQUIPMENT	31
EXPERIMENTAL PROCEDURES	40
Characterization of Solid Particles	40
Bed Preparation	45
Washing Run	46
Preliminary Washing Runs	47
RESULTS AND DISCUSSION	58
SUMMARY AND CONCLUSIONS	79
SIGNIFICANCE OF RESULTS AND SUGGESTIONS FOR FUTURE RESEARCH	83
NOMENCLATURE	86
LITERATURE CITED	89
APPENDIX I. TABLE OF LAPLACE TRANSFORMS	91
APPENDIX II. SAMPLE CALCULATIONS	92
APPENDIX III. INTRAFIBER DIFFUSION	102

INTRODUCTION

In the washing of a bed of packed solid particles, saturated with a fluid containing soluble materials, certain complex transport phenomena may be involved. If the solid particles in the bed are porous, then the solute, which is to be removed from the bed during the washing process, may be initially contained both within the solid particles and in solution contained in the interparticle voids. In order for the solute, initially in the particle, to be removed from the bed, it must move from the internal structure of the particle to the external surface of the particle and then into solution in the fluid contained in the interparticle voids. This may involve molecular diffusion within the particle, adsorption and desorption on the internal surfaces of the particle, surface diffusion along the internal surfaces of the particle, and electrokinetic phenomena. In the ideal case of piston flow, the fluid in the interparticle voids will be removed by a simple displacement by the wash fluid. However, in any real bed the complex flow pattern, caused by the complex geometry of the bed, will cause the entering fluid to mix with the fluid originally in the bed. In addition to this mixing, caused by the flow pattern around and among the particles in the bed, an additional mixing may occur due to diffusion of the solute.

Although a complete mathematical description of the complex flow pattern in a bed of randomly oriented solid particles is not presently available, the over-all movement of a solute, in a bed of nonporous granular material, has been described using a diffusionlike differential equation. In this case, however, the diffusion coefficient is replaced

by a longitudinal dispersion coefficient which includes both the effect of molecular diffusion and the effect of the varying flow pattern in the bed.

While there have been numerous investigations of the washing of relatively simple beds of granular materials, few studies have been made with the more complex fibrous systems. There are several important differences between a bed of granular media and a bed of fibrous media. In the case of spherical particles (granular media), the particles are always geometrically similar, and with reasonable care the packing will also be similar. In the case of long cylindrical particles (fibrous media), the particles are not necessarily geometrically similar. It is also doubtful that geometrically similar packing is obtained when different size fibers are used. Another difference between a fiber system and a granular system is the porosity. The porosity of a granular bed is generally determined by the mode of packing. Since the packing of most granular beds is similar, most granular beds have about the same porosity, which is generally about 0.4. However, unlike granular systems which are incompressible, fibrous systems are compressible and therefore the porosity may vary over a wide range, depending upon the compacting force applied to the bed. Thus, the porosity of a fiber bed may vary from 0.6-0.7 at large compacting loads to 0.95 or higher under small compacting loads. A fourth difference between the two systems is the fact that the beds of fibrous media have a much wider pore size distribution. Thus, although the same basic mechanism should apply to the dispersion of solute in both beds of granular or fibrous media, the longitudinal dispersion coefficient will be affected by the differences between the two types of beds.

Engineers in the pulp and paper industry are interested in the movement of soluble materials during the washing of pulp fibers. Although much could be learned from a study of this system, an intensive fundamental investigation of this highly complex system appears overly ambitious at the present time. A more logical approach to the problem would be to study the least complex fibrous system first and then, by a stepwise process, to approach the more complex pulp fiber system. Thus, a suitable order of study would be to study (1) beds of well-defined nonporous fibers, (2) beds of well-defined, porous fibers, and finally, (3) beds of pulp fibers.

In order to use the differential equation, used to describe the movement of solute in a bed of packed solids, it is necessary to know the appropriate boundary conditions. Three types of boundary conditions (step, pulse, and sine wave) have been used in studies of granular media. In order to use the step function boundary condition, the input stream should instantaneously change from the solution initially saturating the bed to pure water. Although this ideal is never achieved, a number of investigations have been carried out on beds of granular material under the assumption that the actual change is abrupt enough so that the exit concentration data may be treated with the equations developed for the step change condition. This assumption may be valid for thick beds; however, for thin beds this assumption may be appreciably in error.

From an experimental standpoint it is not practical to use fiber beds which are several feet thick. This is so because (1) it would take a very long time to form a fiber bed of this thickness (since it must be formed

from a dilute slurry in order to avoid flocculation), and (2) an unduly large quantity of fiber would be necessary. Thus, rather than assume a step function boundary condition, which would be experimentally difficult to satisfy, the actual quasi-step input stream concentration history was used as a boundary condition.

PRESENTATION OF THE PROBLEM

In recent years a number of studies have been made on the movement of a solute in a bed of packed solids, while a fluid is flowing through the bed (and also the movement of heat in analogous heat transfer problems). Most of these studies have been made on thick beds of granular media. In the pulp and paper industry, however, the systems of specific interest are those consisting of beds of fibrous media.

The purpose of this thesis is to study the movement of a solute in a bed of packed solids, during the washing process, with particular emphasis on fibrous systems. In order to quantitatively describe the movement of the solute, it is necessary to develop an appropriate mathematical model. It appears reasonable to assume that the same diffusion-like differential equation, which is used to describe the dispersion of material in a bed of granular media, may be used to describe the dispersion of material in a bed of fibrous media. However, in order to avoid the experimental difficulties encountered in obtaining a satisfactory step function boundary condition (which is particularly difficult for thin beds, such as must be used with fibrous media), the equations were modified to include the actual quasi-step function input concentration history.

Since it was deemed impractical to form thick beds of fibrous media, this study was limited to thin beds of packed solids (glass beads, dacron fibers, and all-skin viscose fibers). The glass bead system was primarily used to check out the experimental system and verify the mathematical model. The dacron fiber system was investigated in order to indicate the

important variables in a nonporous fiber system and to show the differences between a fiber system and a granular system. The viscose fiber system was investigated in order to indicate the importance of a movement of solute within the fibers. In order to avoid any unnecessary complications, the beds of fibrous media were rendered effectively incompressible by applying an external compacting force on the bed during the washing runs. If the external compacting force is large compared to the fluid drag force across the bed during the washing run, then the fluid drag force will not further compact the bed during the washing run; thus, a uniform porosity should be maintained throughout the thickness of the bed.

THEORY

In order to develop the equations and techniques to describe and measure the washing of thin fiber beds, it is helpful to first understand the theories and techniques used to describe and measure the washing of thick beds of nonporous, granular materials.

Let us for the moment consider the flow of a liquid through a bed of nonporous particles. As a fluid element travels through the bed, around and among the solid particles, it will change its speed and direction many times. As the size of the channel changes, the speed of the fluid elements will change. When the streamline in which a fluid element is traveling approaches a solid particle, the direction of the fluid element will change. In this way, as the fluid elements travel through the bed, they will appear to have an irregular motion with respect to the average longitudinal motion of the fluid elements.

THE IRREGULAR MOVEMENT OF SOLUTE IN A BED OF PACKED SOLIDS

Let us now consider the irregular movement of solute molecules in a fluid which is flowing through a bed of packed solids.*

We will introduce a time interval, τ , in our discussion, which is to be very small compared with the observed time interval but, nevertheless, of such a magnitude that the movements executed by both fluid elements and solute molecules in two consecutive intervals of time, τ ,

* The following derivation is based upon a consideration of "The Irregular Movement of Particles Suspended in a Liquid and the Relation of This to Diffusion" by Einstein (1).

are to be considered as mutually independent phenomena. In order to satisfy this criterion, τ would probably correspond to the time it takes the fluid elements to travel through several layers of the bed (a layer of the bed is generally considered to be 1 particle diameter thick). We must also assume that each fluid element executes a movement with respect to the average flow, which is independent of the movement of all other particles for consecutive intervals of time, τ .

Suppose there are altogether N solute molecules and n fluid elements in the bed of packed solids. In an interval of time, τ , the z -coordinates of the fluid elements will increase by $\underline{u}\tau + \Delta$ ($\underline{u}\tau$ = average movement of the fluid elements) where \underline{u} is the pore velocity of the fluid and Δ has a different value (positive or negative) for each element. For the value of Δ , a certain probability law will hold (determined by the geometry of the void spaces in the bed of packed solids and the average fluid velocity). The number, dn , of fluid elements which experience, in the time interval, τ , a displacement which lies between $\underline{u}\tau + \Delta$ and $\underline{u}\tau + \Delta + d\Delta$, will be expressed by an equation of the form,

$$dn = n\phi(\Delta)d\Delta \quad (1)$$

where

$$\int_{-\infty}^{\infty} \phi(\Delta)d\Delta = 1 \quad (2)$$

and $\phi(\Delta)$ differs from zero only for small values of Δ and also fulfills the condition $\phi(\Delta) = \phi(-\Delta)$.

In this same time interval, τ , the z -co-ordinates of the solute molecules will, in addition, increase by δ , due to random molecular motion,

where δ has a different value (positive or negative) for each molecule. For the value of δ , a certain probability law will hold (determined by the random molecular motion of the solute molecules in the fluid, corrected for the tortuosity of the bed of packed solids). The number, dN , of solute molecules which experience in the time interval, τ , a displacement, due to random molecular motion, which lies between δ and $\delta + d\delta$, will be expressed by an equation of the form,

$$dN = N\phi(\delta)d\delta \quad (3)$$

where

$$\int_{-\infty}^{\infty} \phi(\delta)d\delta = 1 \quad (4)$$

and $\phi(\delta)$ only differs from zero for very small values of δ and also fulfills the condition $\phi(\delta) = \phi(-\delta)$.

The total increase in the z -co-ordinates of the solute molecules, in the time interval, τ , is not given by the displacement due to molecular motion alone but by the sum of the displacements due to the movement of fluid elements and that due to molecular motion. In other words, the total increase in the z -co-ordinates of the solute molecules, in the time interval, τ , is given by $u\tau + \Delta + \delta$. The probability that a solute molecule will experience both a displacement, $u\tau + \Delta$, due to the movement of the fluid elements, and a displacement, δ , due to molecular motion, is the product of the probabilities for each displacement. Thus, the number of solute molecules which experience in the time interval, τ , a total displacement between $u\tau + h$ and $u\tau + h + dh$, will be expressed by an equation of the form,

$$dN = N \psi(h) dh \quad (5)$$

where

$$\begin{aligned} \underline{h} &= \Delta + \delta, \text{ and} \\ \psi(h) &= \int_{-\infty}^{\infty} \Phi(\Delta) \delta(h - \Delta) d\Delta \end{aligned} \quad (6)$$

and again,

$$\int_{-\infty}^{\infty} \psi(h) dh = 1 \quad (7)$$

If we confine ourselves to the case where the number, v , of solute molecules per unit volume of fluid depends only on \underline{z} and \underline{t} , then $v = \underline{f}(\underline{z}, \underline{t})$. We will now calculate the number of solute molecules which are located, at the time $\underline{t} + \tau$, in the volume between two planes, of area ϵA , perpendicular to the \underline{z} -axis with abscissae \underline{z} and $\underline{z} + \underline{dz}$, from the distribution of solute molecules at time \underline{t} . The number of solute molecules at $\underline{z} - \underline{u}\tau - \underline{h}$, at time \underline{t} , is given by $\underline{f}(\underline{z} - \underline{u}\tau - \underline{h}, \underline{t}) \epsilon A \underline{dz}$. The number of these molecules that will move the distance $\underline{u}\tau + \underline{h}$ (in other words, to the point, \underline{z}), in the time interval τ , is given by $\underline{f}(\underline{z} - \underline{u}\tau - \underline{h}, \underline{t}) \epsilon A \underline{dz} \psi(\underline{h}) \underline{dh}$. If this expression is integrated over all values of \underline{z} (i.e., $-\infty$ to ∞), we will obtain the expression for the number of molecules which, during the time interval, τ , will have moved from all points in the system to the volume between the planes \underline{z} and $\underline{z} + \underline{dz}$. Thus,

$$\underline{f}(\underline{z}, \underline{t} + \tau) \epsilon A \underline{dz} = \int_{-\infty}^{\infty} \underline{f}(\underline{z} - \underline{u}\tau - \underline{h}, \underline{t}) \epsilon A \underline{dz} \psi(\underline{h}) \underline{dh} \quad (8)$$

Using Taylor's expansion, we may rewrite Equation (8) as

$$f(z, t) + \tau \frac{\partial f(z, t)}{\partial t} + \dots = \int_{-\infty}^{\infty} \left\{ f(z, t) + (-u\tau - h) \frac{\partial f(z, t)}{\partial z} + \frac{(-u\tau - h)^2}{2!} \frac{\partial^2 f(z, t)}{\partial z^2} + \dots \right\} \psi(h) dh \quad (9).$$

Since both $\Phi(\Delta)$ and $\varnothing(\delta)$ are even, $\psi(h)$ must be even. Thus, $\int_{-\infty}^{\infty} h^i \psi(h) dh = 0$ where i is an odd integer. Equation (9) thus becomes

$$\frac{\partial f(z, t)}{\partial t} = -u \frac{\partial f(z, t)}{\partial z} + \left[\frac{1}{2\tau} \int_{-\infty}^{\infty} h^2 \psi(h) dh \right] \frac{\partial^2 f(z, t)}{\partial z^2} \quad (10)$$

where terms containing τ to the first power or higher, or h to the 4th power or higher have been neglected.

If we now define

$$D_T = \frac{1}{2\tau} \int_{-\infty}^{\infty} h^2 \psi(h) dh \quad (11)$$

Equation (10) becomes

$$\frac{\partial f(z, t)}{\partial t} = -u \frac{\partial f(z, t)}{\partial z} + D_T \frac{\partial^2 f(z, t)}{\partial z^2} \quad (12).$$

However, since $f(z, t) = v$, the number of solute molecules per unit volume of fluid (in other words, concentration), we may rewrite Equation (12) as

$$\frac{\partial c}{\partial t} = -u \frac{\partial c}{\partial z} + D_T \frac{\partial^2 c}{\partial z^2} \quad (13)$$

which is the well-known diffusion-type differential equation which has been used by many workers [e.g., (2-7)] to describe the movement of material in a bed of packed solids. Ebach (2) and others have arrived at Equation (13) by assuming that the mass transfer rate in the bed may be expressed by $-\underline{D}_T \frac{dc}{dz}$ and performing a material balance for an increment of time dt and bed thickness dz . Although this technique provides us with the differential equation, it does not give us any insight into how \underline{D}_T may change as the variables in the system are changed. As we will see in the next section, however, the preceding derivation, of Equation (13), does provide us with considerable insight into how we may expect \underline{D}_T to change as the variables in the system are changed.

The constant, \underline{D}_T , is the total dispersion coefficient which we will now show to be the sum of the molecular dispersion coefficient, \underline{D}_{mol} , corrected for the tortuous path through the bed of packed solids and a longitudinal dispersion coefficient, \underline{D}_L , due to the flow pattern in the bed of packed solids.

From the definition of \underline{D}_T and $\psi(\underline{h})$, we may write

$$D_T = \frac{1}{2\tau} \int_{-\infty}^{\infty} \left[\int_{-\infty}^{\infty} \phi(\Delta) \psi(h - \Delta) d\Delta \right] h^2 dh \quad (14)$$

or,

$$D_T = \frac{1}{2\tau} \int_{-\infty}^{\infty} \phi(\Delta) \left[\int_{-\infty}^{\infty} \psi(h - \Delta) h^2 dh \right] d\Delta \quad (14a).$$

However, since $\underline{h} = \delta + \Delta$,

$$\int_{-\infty}^{\infty} \psi(h - \Delta) h^2 dh = \int_{-\infty}^{\infty} \psi(\delta) (\delta + \Delta)^2 d\delta = \int_{-\infty}^{\infty} \psi(\delta) \delta^2 d\delta + \Delta^2 \quad (15).$$

Now, according to the normal definition (1),

$$D_{\text{mol.}} = \frac{1}{2\tau} \int_{-\infty}^{\infty} \phi(\delta) \delta^2 d\delta \quad (16)$$

and by analogy,

$$D_L = \frac{1}{2\tau} \int_{-\infty}^{\infty} \phi(\Delta) \Delta^2 d\Delta \quad (17)$$

Substituting Equation (15) into Equation (14a) and then using the above definitions of $D_{\text{mol.}}$ and D_L , we find that

$$D_T = \frac{1}{2\tau} \int_{-\infty}^{\infty} \phi(\Delta) \left[2\tau D_{\text{mol.}} = \Delta^2 \right] d\Delta \quad (18)$$

or

$$D_T = D_{\text{mol.}} = \frac{1}{2\tau} \int_{-\infty}^{\infty} \phi(\Delta) \Delta^2 d\Delta \quad (19)$$

or

$$D_T = D_{\text{mol.}} + D_L \quad (20)$$

Thus, Equation (13) may be rewritten

$$\frac{\partial C}{\partial t} = -u \frac{\partial C}{\partial z} + (D_{\text{mol.}} + D_L) \frac{\partial^2 C}{\partial z^2} \quad (21).$$

There are two major assumptions in the above derivation. The first assumption is that the movement of a fluid element, after a time interval, τ , is independent of its movement before the time interval. When one considers the nature of flow through a bed of packed solids, it seems unlikely that the motion of a fluid element at time $t + \tau$ bears any relation to its motion at time t so long as the interval τ is long enough for the element to travel several particle diameters. Thus, if we confine our studies to beds many particle diameters thick, this assumption should be valid.

The second major assumption is that the dispersion of longitudinal velocities is symmetrical about the average longitudinal velocity, \bar{u} , or to be specific, that the function, $\phi(\Delta)$, is symmetrical. The best verification of the validity of this assumption is offered by experimental work with pulse-type concentration changes (2, 3) in which the symmetry of the dispersion process has been observed.

The experimental verification of the symmetry of the dispersion process, and presumably of the function, $\phi(\Delta)$, does not, however, prove the symmetry of the dispersion mechanism itself. For example, consider the cell mixing model of dispersion in a bed of packed solids. In this model (4, 5, 10), it is assumed that the bed of packed solids consists of n perfect mixing cells in which the concentration at every point within the cell has a concentration equal to the exit concentration. From this model, Aris and Amundson (10) have derived an equation for the probability that a molecule introduced into the bed at time $t = 0$ will be in the n th cell at time t and found that it corresponds to Poisson's probability law. For a small number of such mixing cells, the dispersion is decidedly nonsymmetrical; however, as n becomes large, the distribution approaches a Gaussian distribution which is symmetrical. Thus, if the bed of packed solids is many particle diameters thick (a mixing cell is considered to be about 1 particle diameter long), then our assumption of symmetry will be valid even though the individual processes themselves do not produce symmetrical dispersions. This again points out the fact that the above derivation may be seriously questioned when the bed is only a few particle diameters thick.

It should also be emphasized that Equation (21) has been derived for a one-dimensional system. If macroscopic radial concentration gradients exist in the bed, then radial dispersion must be accounted for. With proper boundary conditions, it is doubtful that macroscopic radial concentration gradients will occur unless there are serious radial velocity variations. If the ratio of tube diameter to particle diameter is over 30, then serious radial velocity variations should not exist (11). Thus, if the ratio of the tube diameter to particle diameter is maintained at 30 or more, Equation (21) should be satisfactory.

In review, then, we have seen that the dispersion of a solute in a fluid flowing through a bed of packed solids is due mainly to the dispersion of fluid elements brought about by the flow pattern in the bed of packed solids. It was then shown that this dispersion process can be described by a diffusionlike differential equation such as

$$\frac{\partial C}{\partial t} = -u \frac{\partial C}{\partial z} + (D_{\text{mol.}} + D_L) \frac{\partial^2 C}{\partial z^2} \quad (21).$$

It now seems pertinent to discuss the factors which affect $D_{\text{mol.}}$ and D_L . As we have previously noted, the molecular diffusivity coefficient, $D_{\text{mol.}}$, is not the same as the normal molecular diffusion coefficient of the solute in the solvent. This coefficient, $D_{\text{mol.}}$, is the molecular diffusion coefficient corrected in such a way as to account for the complex geometry of the pore structure of the bed of packed solids. This correction is discussed by Wyllie (12) and Peterson (13). Experimentally, $D_{\text{mol.}}$ may be determined by measuring the diffusion of solute in the bed of packed solids, with no flow occurring, such as was done by Raimondi, et al. (3).

The longitudinal diffusivity coefficient, \underline{D}_L , accounts for the dispersion of solute, due to the dispersion of fluid elements, caused by the nonuniform flow of fluid through the bed of packed solids. The flow pattern in the bed affects the dispersion of fluid elements in three ways. These are:

1. Under the same pressure gradient, fluid elements in large pores will travel more rapidly than fluid elements in small pores;
2. At the same flow rate, fluid elements may travel different longitudinal distances due to the orientation of their respective channels; and finally,
3. Fluid elements in the center of a channel will move more rapidly than fluid elements near a solid surface.

The first of these effects, that of the pore size distribution, has been shown to be quite important by the work of Raimondi, et al. (3) and Orlob, et al. (8) on granular systems. The second effect has been shown to be important by the calculations of de Josselin de Jong (9). Raimondi, et al. (3) have shown the third effect to be comparatively insignificant for longitudinal dispersion. Thus, we may conclude that the dispersion of fluid elements is mainly due to the orientation and size distribution of the pores in the bed of packed solids.

PREDICTIONS OF THE DIFFUSIONLIKE THEORY

It has previously been stated that one advantage of the preceding derivation of Equation (13) is the fact that it gives us some insight into how \underline{D}_T (or, more specifically, \underline{D}_L) changes as we change some of the variables in the system. We have stated that

$$D_L = \frac{1}{2\tau} \int_{-\infty}^{\infty} \Delta^2 \Phi(\Delta) d\Delta \quad (17)$$

where $\Phi(\Delta)$ represents the dispersion of material, in the time interval, τ , due to nonuniform fluid element velocities. It should be noted that $\Phi(\Delta)$ should really be written as $\Phi(\Delta, \tau)$ since the value of $\Phi(\Delta)$ depends upon the value of τ . In fact, $\Phi(\Delta)$ changes, as τ changes, so that $\underline{D_L}$, defined by Equation (17), is independent of τ . With the above facts in mind, let us consider the effects of (1) the average pore velocity, \underline{u} , (2) changing from streamline to turbulent flow, and (3) particle size on the longitudinal dispersion coefficient, $\underline{D_L}$.

Consider the movement of a fluid element from point A to point B in a bed of packed solids. Let us pick A and B such that the fluid element travels from A to B in the time interval, τ_1 , when the average pore velocity of the fluid is \underline{u}_1 . Now, let us ask ourselves what happens if the average pore velocity is changed to \underline{u}_2 . If streamline flow is maintained, the element will travel along the same streamline between A and B but the time of passage will be changed to $\tau_2 = \underline{u}_1 \tau_1 / \underline{u}_2$, since the speed of the fluid element at any point along the streamline will be changed by the ratio, $\underline{u}_2 / \underline{u}_1$. This same argument holds for every fluid element in the bed. Since the movement of each and every fluid element in the interval τ_1 (when $\underline{u} = \underline{u}_1$) is the same as the movement in τ_2 (when $\underline{u} = \underline{u}_2$), the function $\Phi(\Delta, \tau_1)_1 = \Phi(\Delta, \tau_2)_2$. In other words, $\Phi(\Delta)$ is independent of \underline{u} if the product, $\underline{u}\tau$, is kept constant. Dividing Equation (17) by \underline{u} gives

$$\frac{D_L}{u} = \frac{1}{2\tau u} \int_{-\infty}^{\infty} \Delta^2 \Phi(\Delta) d\Delta \quad (22).$$

Since the product, $\underline{u}\tau$, may be maintained constant by changing τ as \underline{u} changes, and under these conditions, $\Phi(\Delta)$ is constant, $\underline{D}_L/\underline{u}$ must be a constant. In other words, \underline{D}_L must be directly proportional to \underline{u} , so long as streamline flow is maintained. This relationship has been theoretically predicted by a number of workers (14, 3, 4, 9, 10). Experimentally, Raimondi, et al. (3) found that \underline{D}_L was proportional to \underline{u} . Ebach (2) found that \underline{D}_L was proportional to $\underline{u}^{1.08}$. Liles, et al. (15) found that \underline{D}_L was proportional to $\underline{u}^{0.93}$.

In changing from streamline to turbulent flow, the effect of the orientation of the pores should remain unchanged; however, dispersion due to the pore size distribution will be decreased. In order to understand this, consider the average velocities, \underline{u}_1 and \underline{u}_2 , in two capillaries of diameters, \underline{d}_1 and \underline{d}_2 , respectively. If the pressure gradient is the same in both capillaries, and the flow is streamline, then, according to Poiseuille's law, $\underline{u}_1/\underline{u}_2$ is proportional to $(\underline{d}_1/\underline{d}_2)^2$. Under turbulent flow conditions, $\underline{u}_1/\underline{u}_2$ is proportional to $(\underline{d}_1/\underline{d}_2)^n$ where n is less than 2 and, according to Blasius's formula (27), approaches 5/7 as the flow becomes fully turbulent. Obviously, the dispersion will be a minimum when $\underline{u}_1/\underline{u}_2 = 1$. Thus, it becomes clear that when n decreases, in changing from streamline to turbulent flow, less dispersion will occur. Experimentally, this results in a decrease in the ratio, $\underline{D}_L/\underline{u}$, or, more directly, in a sharper breakthrough curve. This relationship has been observed by a number of workers who have studied both the streamline and turbulent regions.

In order to illustrate the effect of the particle diameter, \underline{d}_p , on the longitudinal diffusivity coefficient, \underline{D}_L , let us divide Equation (22) by \underline{d}_p ; thus,

$$\frac{D_L}{ud_p} = \frac{1}{2\tau ud_p} \int_{-\infty}^{\infty} \Delta^2 \phi(\Delta) d\Delta \quad (23).$$

If we can assume that geometrical similarity is maintained in the bed of packed solids, as the particle size is changed, then by adjusting the fluid velocity, \underline{u} , to maintain the product, \underline{ud}_p , constant (or more generally, the Reynolds number), we will maintain dynamic similarity. If dynamic similarity is maintained, geometrically similar flow patterns will exist. Thus, for any given system, the dispersion of fluid elements is proportional to $\underline{u}\tau$. For geometrically similar flow patterns in different systems, the dispersion of fluid elements will be proportional to $\underline{u}\tau\underline{d}_p$, where \underline{d}_p is a scale factor for the system. Thus, if the product, $\tau\underline{ud}_p$, is maintained constant, $\phi(\Delta)$ will remain fixed. Under these conditions, the left-hand side of Equation (23) is fixed and we find that \underline{D}_L is directly proportional to \underline{ud}_p . Since we already know that \underline{D}_L is directly proportional to \underline{u} , \underline{D}_L must also be directly proportional to \underline{d}_p . This relationship has been predicted by several authors (3, 9, 16) and experimentally verified by Ebach (2) and Raimondi, et al. (3). Liles, et al. (15), on the other hand, were not able to verify this relationship (i.e., they found \underline{D}_L proportional to $\underline{d}_p^{0.73}$ for three particle sizes). It should be emphasized that the direct proportionality between \underline{D}_L and \underline{d}_p will only hold for geometrically similar beds. The mere fact that the particles in different beds of packed solids are geometrically similar does not guarantee that the beds themselves are geometrically similar. It is also necessary for the packing of the beds to be identical. In experimental systems in which a distribution of particle sizes exists, both the distribution and the packing must be identical for geometric similarity and for the consequent proportionality between \underline{D}_L and \underline{d}_p to hold.

Since we have introduced the dimensionless grouping, $\frac{D_L}{u d_p}$, in our discussion, it seems pertinent to discuss further its commonly used reciprocal, $\frac{u d_p}{D_L}$, or the Peclet number (Pe). As we have seen in our previous discussion, the Peclet number should be a constant for all beds of spherical particles, as long as (a) streamline flow is maintained, (b) the beds are similarly packed, and (c) the distribution of particle sizes is the same. Experimental values of the Peclet number for liquids are found to vary from 0.3 to 1.5 for a variety of granular materials. Considering the possible variations in packing and distribution of particle sizes and the numerous experimental techniques used, this variation in the Peclet number is not surprising.

By comparing the cell mixing model with the diffusionlike model, ~~Aris and Amundson (10)~~ have predicted that the value of the Peclet number should be about 2 for a bed of spherical particles.

Since the cell mixing model assumes perfect mixing within each "cell," this prediction should be best when the flow is highly turbulent. From our discussion of the effect of turbulent flow versus streamline flow on $\frac{D_L}{u}$, we know that the Peclet number will decrease as we change from turbulent flow to streamline flow. Thus, it is not surprising that the experimental values of Pe are less than 2 when the flow is not highly turbulent.

APPLICATION OF THE DIFFUSIONLIKE DIFFERENTIAL EQUATION
USING THE STEP FUNCTION BOUNDARY CONDITION

Equation (21) has been derived in order to describe the longitudinal dispersion of solute in a bed of nonporous solids. If the solid particles

are porous, or if the solute is adsorbed by the solid particles, then an additional term must be added to Equation (21) to account for the accumulation (or depletion) of material sorbed by the solid. Equation (21) thus becomes

$$(D_{\text{mol.}} + D_L) \frac{\partial^2 C}{\partial z^2} - u \frac{\partial C}{\partial z} = \frac{\partial C}{\partial t} + \frac{1 - \epsilon}{\epsilon} \frac{\partial \eta}{\partial t} \quad (24)$$

where

$D_{\text{mol.}}$ = effective molecular diffusion coefficient in axial direction, sq. cm./sec.,

D_L = longitudinal dispersion coefficient, sq. cm./sec.,

C = concentration of solute in solution, g. solute/cc. solution,

z = distance variable in the direction of flow, cm.,

u = average pore velocity in axial direction, cm./sec.,

t = time, sec.,

ϵ = porosity of the bed of packed solids, cc. void space/cc. bed, dimensionless, and

η = quantity of solute sorbed by the solid per unit volume of the solid, g. solute/cc. solid.

Equation (24) was proposed by Lapidus and Amundson (17). The first term on the left-hand side of Equation (24) represents the dispersion of solute due to both molecular diffusion and the dispersion of fluid elements caused by the irregular flow pattern within the bed of packed solids. The second term represents the bulk movement of solute due to the flow of the fluid through the bed. The first term on the right-hand side of Equation (24) represents the depletion (or accumulation) of solute in solution at a given level in the bed. The last term in Equation (24) represents the depletion (or accumulation) of solute sorbed by the solid at a given level in the bed.

Before Equation (24) can be solved, it is necessary to express η in terms of C . This may be done in a number of ways, depending upon the system in question; however, we will consider only those cases where

$$\eta = K_0 + KC \quad (25).$$

Three special cases where Equation (25) applies are: (1) no sorption, $\eta = 0$, (2) equilibrium between the solution absorbed by the solid and the surrounding solution, $\eta = KC$, and (3) adsorption with a linear isotherm, $\eta = K_0 + KC$. If Equation (25) applies, then $\partial\eta/\partial t = K(\partial C/\partial t)$, and Equation (24) becomes

$$(D_{\text{mol.}} + D_L) \frac{\partial^2 C}{\partial z^2} - u \frac{\partial C}{\partial z} = \frac{\partial C}{\partial t} + \frac{(1 - \epsilon)K}{\epsilon} \frac{\partial C}{\partial t} \quad (26)$$

or

$$(D_{\text{mol.}} + D_L) \frac{\partial^2 C}{\partial z^2} - u \frac{\partial C}{\partial z} = \frac{1}{\lambda} \frac{\partial C}{\partial t} \quad (27)$$

where

$$\lambda = 1/(1 - \underline{K} + \underline{K}/\epsilon).$$

This may be further simplified to

$$D_L \frac{\partial^2 C}{\partial z^2} - u \frac{\partial C}{\partial z} = \frac{1}{\lambda} \frac{\partial C}{\partial t} \quad (28)$$

if $D_{\text{mol.}}$ is small compared to D_L . (This is true except for very low flow rates.) Equation (28) can be used if the proper boundary conditions are known. The boundary conditions are determined by the experimental system in question. The experimental systems which have been used may be grouped into three classes. These are: (1) a harmonic variation of input concentration, (2) a pulse change in the input concentration (a concentrated

solution of solute is injected into the input stream for a very short time), and (3) an instantaneous step change in the input concentration. From the standpoint of mathematical simplicity, the step function is the most desirable. Lapidus and Amundson (17) have solved Equation (28) for the case where the boundary condition is a step function. Their solution is

$$\frac{C}{C_0} = 1 - \frac{1}{2} \left[\operatorname{erfc}\left(\frac{1 - R\lambda}{2\sqrt{R\lambda S}}\right) + e^{1/S} \operatorname{erfc}\left(\frac{1 + R\lambda}{2\sqrt{R\lambda S}}\right) \right] \quad (29)$$

where

C_0 = the concentration of solution initially in the bed of packed solids, g./cc.,

$R = \frac{ut}{z}$,

$S = \frac{D_L}{uz}$, and

C , u , t , z , λ , and D_L have their previous meanings.

Ebach (2) attempted to use this solution, but experimental difficulties in obtaining a step function led him to use the pulse and harmonic frequency boundary conditions instead. Orlob and Radhakrishna (8) used the step function solution; however, they neglected the term, $e^{1/S} \operatorname{erfc}[(1 + R\lambda)/(2\sqrt{R\lambda S})]$. Under this assumption, Equation (29) becomes

$$\frac{C}{C_0} = 1 - \frac{1}{2} \operatorname{erfc}\left(\frac{1 - R\lambda}{2\sqrt{R\lambda S}}\right) \quad (30).$$

Carberry and Bretton (4), in a review of the literature, state that Rafai (18) and Dankwerts (19) also used this approximation. If D_L is estimated from the slope of a relative concentration (C/C_0) versus reduced time (R) plot at $R = 1$, then this approximation will be valid (since the derivative of

$$e^{1/S} \operatorname{erfc}\left(\frac{1 + R\lambda}{2\sqrt{R\lambda S}}\right)$$

with respect to \underline{R} at $\underline{R} = 1$ and $\lambda = 1$ is zero). On the other hand, Equation (30) gives a value of $\underline{C}/\underline{C}_0$ at $\underline{R} = 1$ which is appreciably in error unless the bed is very thick. This is shown in Table I and Fig. 1. The calculations were based upon a value of $\underline{D}_L/\underline{u}$ that was obtained in this study, using 3-mm. glass beads. The values for the various particle sizes were calculated on the assumption that the Peclet number is a constant. In practice, the experimental curve of $\underline{C}/\underline{C}_0$ versus \underline{R} may agree with Equation (30) even though the term,

$$e^{1/S} \operatorname{erfc} \left(\frac{1 + R\lambda}{2 \sqrt{R\lambda S}} \right),$$

is not negligible. This may occur when a true step function is not obtained. In this case, Equation (29) is not complete and the correction for the true input condition may cancel the effect of neglecting the term,

$$e^{1/S} \operatorname{erfc} \left(\frac{1 + R\lambda}{2 \sqrt{R\lambda S}} \right).$$

TABLE I

A COMPARISON OF EQUATIONS (29) and (30)

\underline{S}^a			6-mm. Beads		3-mm. Beads		1.5-mm. Beads	
	(1)	(2)	\underline{z} , cm.	(3)	\underline{z} , cm.	(3)	\underline{z} , cm.	(3)
0.040	0.445	0.500	2.65	12.4	5.3	12.4	10.6	12.4
0.020	0.460	0.500	5.3	8.7	10.6	8.7	21.2	8.7
0.010	0.472	0.500	10.6	5.9	21.2	5.9	42.4	5.9
0.005	0.480	0.500	21.2	4.2	42.4	4.2	84.8	4.2

^a Value of \underline{S} obtained in studies on 3-mm. beads.

Note: (1) $\underline{C}/\underline{C}_0$ from Equation (29) with $\underline{R} = 1$, $\lambda = 1$ (no sorption).

(2) $\underline{C}/\underline{C}_0$ from Equation (30) with $\underline{R} = 1$, $\lambda = 1$ (no sorption).

(3) Per cent error = $100[(2) - (1)]/(1)$.

\underline{z} = bed length.

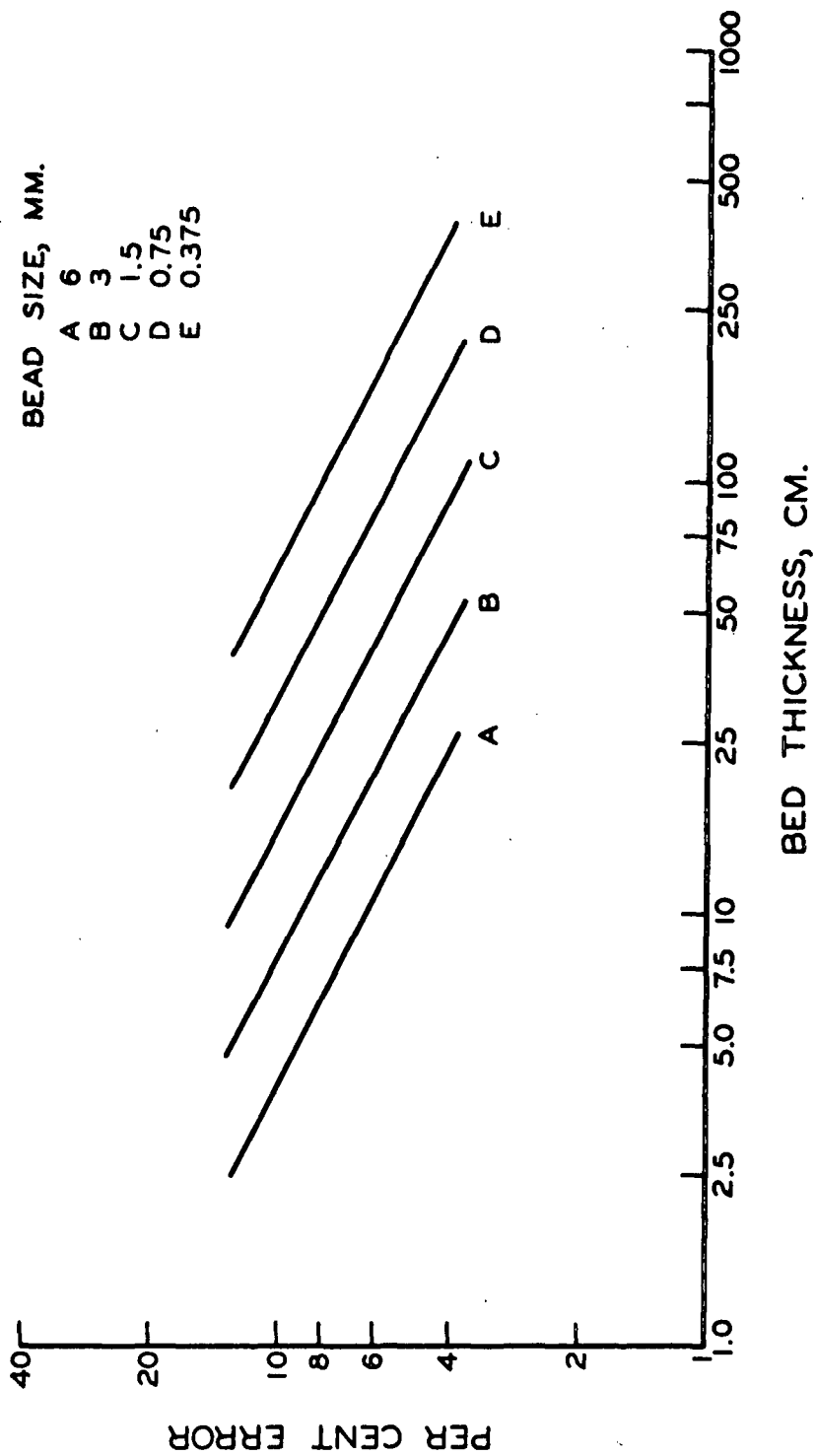


Figure 1. A Comparison of Equations (29) and (30)

APPLICATION OF THE DIFFUSIONLIKE DIFFERENTIAL EQUATION WITH A NEW BOUNDARY CONDITION

The experimental procedure used in this study consisted of saturating a bed of packed solids with an aqueous diacetyl solution and then washing the pad with water. A procedure of this type is generally described by a step-function boundary condition. With thick beds, the use of this assumption may lead to fairly accurate results; however, with thin beds, such as those used in this study, the assumption can result in errors of appreciable magnitude. Rather than make this assumption and then become involved in the experimental difficulties generally encountered in satisfying this assumption, the following boundary conditions were used.

$$C = C_0, \text{ for } z > 0, \text{ at } t = 0 \quad (31);$$

$$C = f(t) = C_0 (k_0 + k_1 t + k_2 t^2 + k_3 t^3 + k_4 t^4) e^{-\gamma t} \quad (32)$$

at $\underline{z} = 0, \underline{t} = 0.$

Equation (31) represents the condition that the concentration in the bed is uniform at $\underline{t} = 0.$ Equation (32) is an empirical representation of the concentration at the top of the bed ($\underline{z} = 0$) as a function of time. The constants, $\underline{k}_0, \underline{k}_1, \underline{k}_2, \underline{k}_3, \underline{k}_4,$ and $\gamma,$ are adjusted so that Equation (32) accurately describes the experimentally determined condition at $\underline{z} = 0$ as a function of time.

The differential equation describing the movement of solute in the bed of packed solids has been given as

$$D_L \frac{\partial^2 C}{\partial z^2} - u \frac{\partial C}{\partial z} = \frac{1}{\lambda} \frac{\partial C}{\partial t} \quad (28).$$

The Laplace transform of Equation (28) is obtained by multiplying by e^{-pt} and integrating from $\underline{t} = 0$ to $\underline{t} = \infty$. This gives

$$\frac{\partial^2 \bar{C}}{\partial z^2} - \frac{u}{D_L} \frac{\partial \bar{C}}{\partial z} - \frac{p}{\lambda D_L} \bar{C} = \frac{1}{\lambda D_L} [C(z, t)]_{\underline{t}=0} \quad (33)$$

where \bar{C} = the Laplace transform of C .

Equation (31) states that $C(\underline{z}, \underline{t})_{\underline{t}=0} = C_0$ if $\underline{z} > 0$. Therefore, Equation (33) becomes

$$\frac{\partial^2 \bar{C}}{\partial z^2} - \frac{u}{D_L} \frac{\partial \bar{C}}{\partial z} - \frac{p}{\lambda D_L} \bar{C} = - \frac{C_0}{\lambda D_L} \quad (34).$$

Equation (34) is a second-order nonhomogeneous partial differential equation whose solution is

$$\bar{C} = \frac{C_0}{p} + K_\alpha e^{\alpha z} + K_\beta e^{\beta z} \quad (35),$$

where

$$\alpha = \frac{u}{2D_L} - \sqrt{\left(\frac{u}{2D_L}\right)^2 + \frac{p}{\lambda D_L}} \quad (36),$$

and

$$\beta = \frac{u}{2D_L} + \sqrt{\left(\frac{u}{2D_L}\right)^2 + \frac{p}{\lambda D_L}} \quad (37),$$

and K_α and K_β are to be determined by the boundary conditions. $C(\underline{z}, \underline{t})$ approaches C_0 at any \underline{t} if \underline{z} approaches ∞ , but $C(\underline{z}, \underline{t})$ approaches 0 at any \underline{z} if \underline{t} approaches ∞ . Thus, \bar{C} must be bounded and therefore K_β must equal zero. Equation (35) thus reduces to

$$\bar{C} = \frac{C_0}{p} + K_\alpha e^{\alpha z} \quad (38).$$

In order to solve for \underline{K}_α in Equation (38), we need to make use of the boundary condition represented by Equation (32). The Laplace transform of Equation (32) is

$$\bar{C} = C_o \left[\frac{k_o}{(\gamma + p)} + \frac{k_1}{(\gamma + p)^2} + \frac{2k_2}{(\gamma + p)^3} + \frac{6k_3}{(\gamma + p)^4} + \frac{24k_4}{(\gamma + p)^5} \right] \quad (39)$$

at $\underline{z} = 0$; $\underline{t} = 0$.

Since Equation (38) must approach Equation (39) as \underline{z} approaches 0, \underline{K}_α must be represented by Equation (40).

$$\underline{K}_\alpha = -\frac{C_o}{p} + C_o \left[\frac{k_o}{(\gamma + p)} + \frac{k_1}{(\gamma + p)^2} + \frac{2k_2}{(\gamma + p)^3} + \frac{6k_3}{(\gamma + p)^4} + \frac{24k_4}{(\gamma + p)^5} \right] \quad (40).$$

Substitution of this value of \underline{K}_α in Equation (38) gives

$$\bar{C} = \frac{C_o}{p} + C_o \left[\frac{-1}{p} + \frac{k_o}{(\gamma + p)} + \frac{k_1}{(\gamma + p)^2} + \frac{2k_2}{(\gamma + p)^3} + \frac{6k_3}{(\gamma + p)^4} + \frac{24k_4}{(\gamma + p)^5} \right] e^{\alpha z} \quad (41)$$

A short table of inverse transforms is contained in the Appendix.

From this table, the inverse transform of Equation (41) becomes

$$\frac{C}{C_o} = 1 - \frac{z \exp[uz/2D_L]}{2 \sqrt{D_L \lambda \pi}} \int_0^t \frac{\exp\left[-\frac{u^2 \lambda \tau}{4D_L} - \frac{z^2}{4D_L \lambda \tau}\right] d\tau}{\tau^{3/2}} + \frac{z \exp[uz/2D_L]}{2 \sqrt{D_L \lambda \pi}} \int_0^t \left[k_o + k_1(t - \tau) + k_2(t - \tau)^2 + k_3(t - \tau)^3 + k_4(t - \tau)^4 \right] \frac{\exp[-\gamma(t - \tau)] \exp\left[-\frac{u^2 \lambda \tau}{4D_L} - \frac{z^2}{4D_L \lambda \tau}\right] d\tau}{\tau^{3/2}} \quad (42).$$

Equation (42) may be rearranged in terms of the dimensionless quantities, $\underline{C}/\underline{C}_0$, $\underline{R} = \underline{ut}/\underline{z}$, and $\underline{S} = \underline{D}_L/\underline{uz}$, to give

$$\frac{\underline{C}}{\underline{C}_0} = 1 - \frac{1}{2} \left[\operatorname{erfc} \left(\frac{1 - \underline{R}\lambda}{2\sqrt{\underline{R}\lambda\underline{S}}} \right) + e^{1/\underline{S}} \operatorname{erfc} \left(\frac{1 + \underline{R}\lambda}{2\sqrt{\underline{R}\lambda\underline{S}}} \right) \right] + \frac{1}{\sqrt{\pi\lambda\underline{R}\underline{S}}} \int_1^{\infty} [k_0 + k_1' \omega_1 + k_2' \omega_1^2 + k_3' \omega_1^3 + k_4' \omega_1^4] \exp \left[\frac{1}{2\underline{S}} - \gamma' \omega_1 - \frac{\underline{R}\lambda}{4\underline{S}\omega^2} - \frac{\omega^2}{4\underline{R}\lambda\underline{S}} \right] d\omega \quad (43)$$

where

$$\begin{aligned} \omega_1 &= \left(1 - \frac{1}{\omega^2} \right) \underline{R}, \\ \underline{k}_1' &= \underline{k}_1 (\underline{z}/\underline{u}), \\ \underline{k}_2' &= \underline{k}_2 (\underline{z}/\underline{u})^2, \\ \underline{k}_3' &= \underline{k}_3 (\underline{z}/\underline{u})^3, \\ \underline{k}_4' &= \underline{k}_4 (\underline{z}/\underline{u})^4, \text{ and} \\ \gamma' &= \gamma (\underline{z}/\underline{u}). \end{aligned}$$

It should be noted that \underline{k}_1' , \underline{k}_2' , \underline{k}_3' , \underline{k}_4' , and γ' may be obtained directly from a plot of $\underline{C}/\underline{C}_0$ vs. \underline{R} since Equation (32) may be rearranged to give

$$\underline{C}/\underline{C}_0 = (k_0 + k_1' \underline{R} + k_2' \underline{R}^2 + k_3' \underline{R}^3 + k_4' \underline{R}^4) e^{-\gamma' \underline{R}} \quad (44).$$

The first two terms in Equation (43) represent the solution to the step function boundary condition and are in agreement with Equation (29) given by Lapidus and Amundson (17). The last term in Equation (43) may be thought of as a correction due to the fact that a true step function was not obtained at $\underline{z} = 0$.

The advantage of Equation (43) is that it is possible to obtain the same information (generally \underline{D}_L is the unknown to be determined from the experimental data) as may be obtained from the step function solution without the experimental difficulties which are encountered in obtaining a step function. This is particularly important for thin beds, such as those used in this study.

EXPERIMENTAL EQUIPMENT

The primary pieces of experimental equipment used in this study are shown in Fig. 2. The flow system is shown schematically in Fig. 3. The essential features of this equipment were:

- A. a large area tank to maintain a constant head during the washing run,
- B. a removable sliding valve to form an interface (between the water and the aqueous solution saturating the bed) near the top of the bed,
- C. a permeable piston to compact the fiber beds (between the bottom of the sliding valve and the top of the piston),
- D. a solenoid valve to start and stop flow,
- E. a needle valve to control the flow rate of the wash fluid, and
- F. an adjustable outlet level control.

The details of the sliding valve are shown in Fig. 4 and 5. As the sliding member was pushed against the stop (a distance of $1/16$ inch) an interface was formed at the bottom of the sliding member (between the solution in the bed of packed solids and the wash fluid) immediately above the bed (a distance of $3/16$ inch above the screen at the top of the bed). No flow occurred at this time since the solenoid valve was not opened until just after the sliding valve was fully open.

The bottom member of the sliding valve, the piston which compacts the bed, and the tube containing the bed were constructed to allow one beam of light to be passed just above the bed and another beam of light

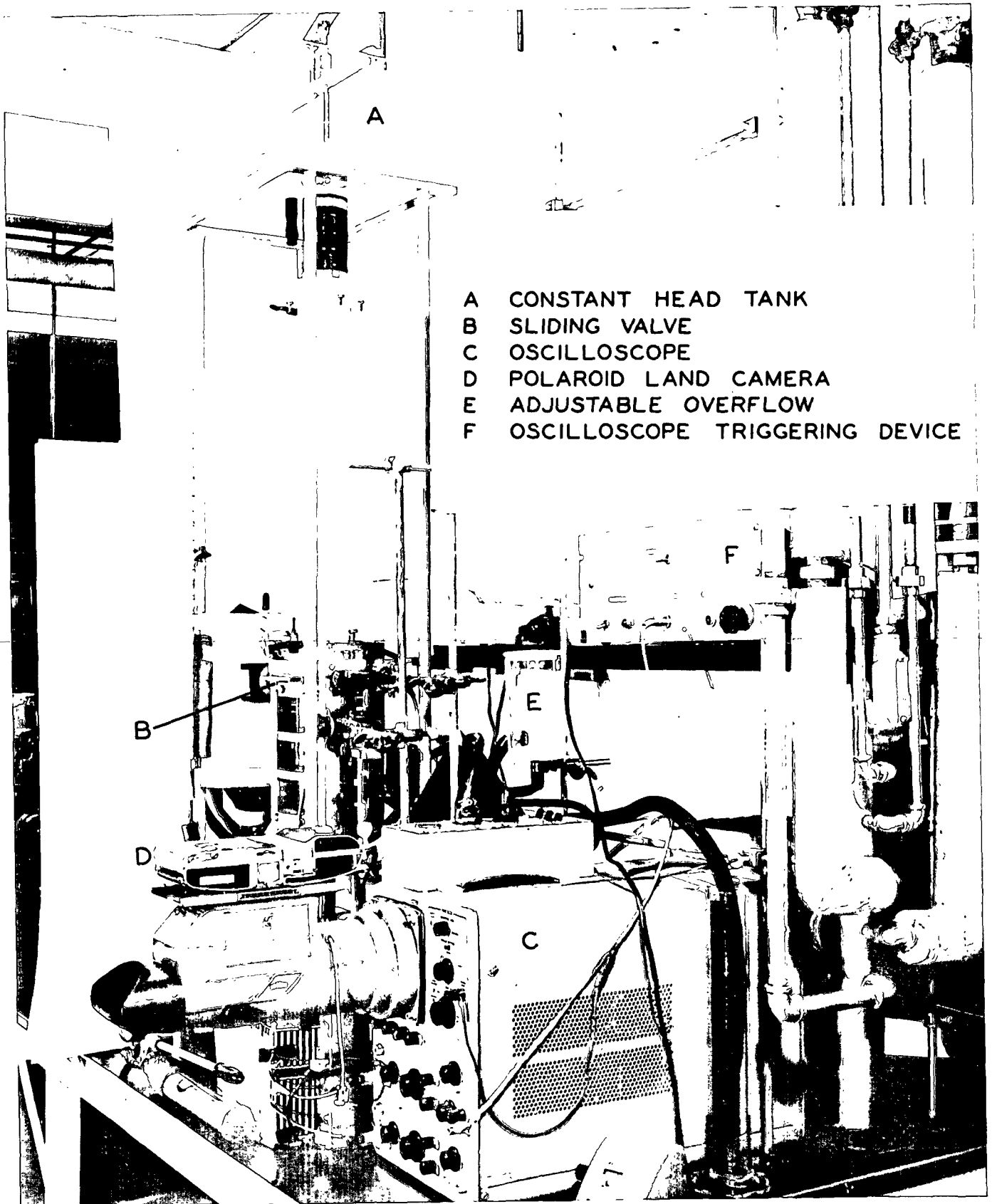


Figure 2. Primary Pieces of Experimental Equipment

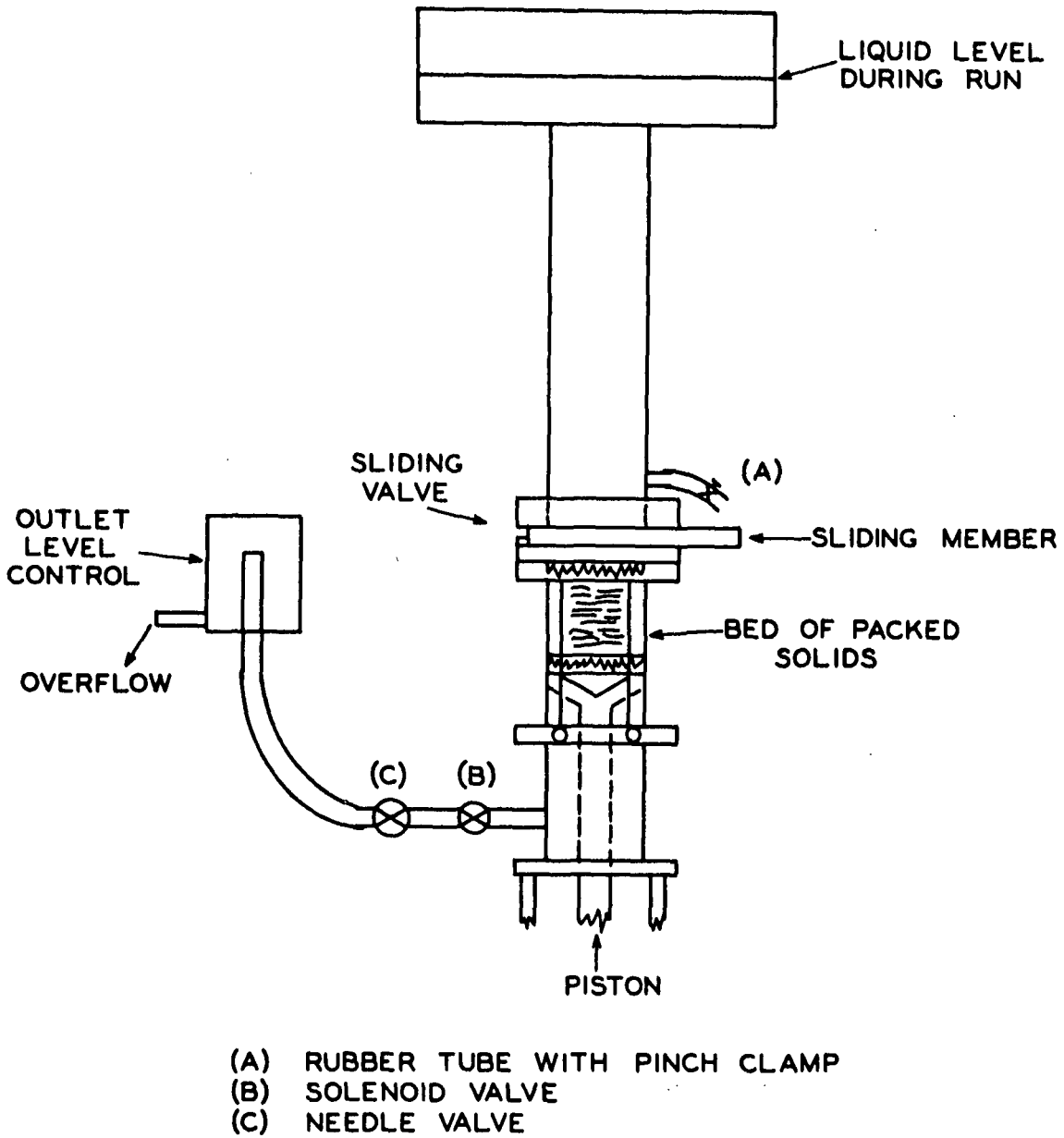
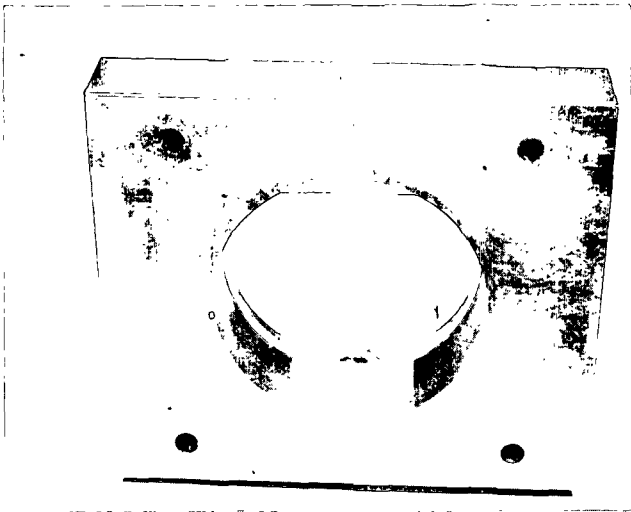
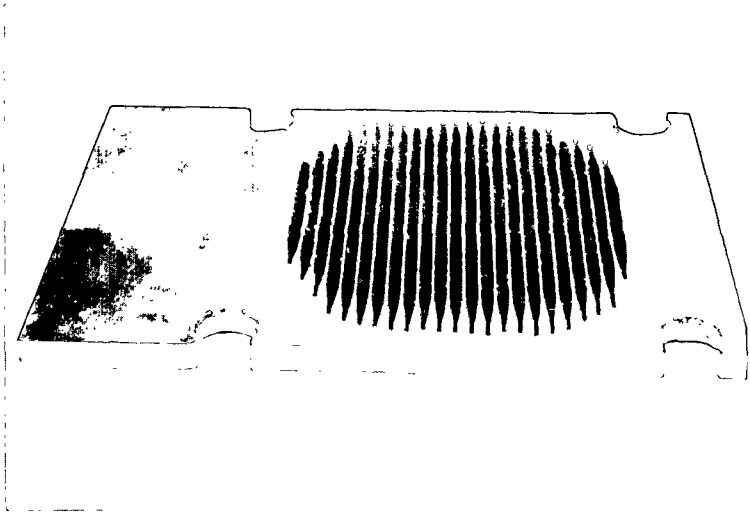


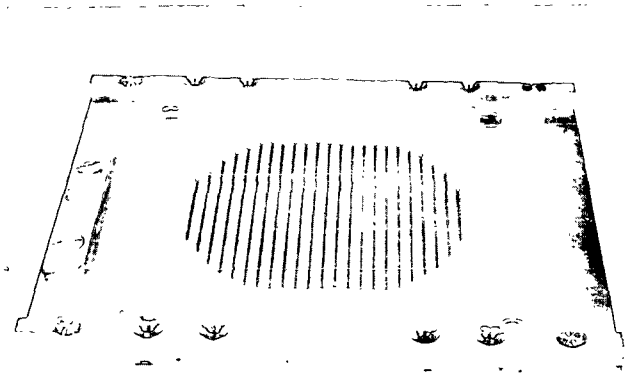
Figure 3. Schematic Diagram of Flow System



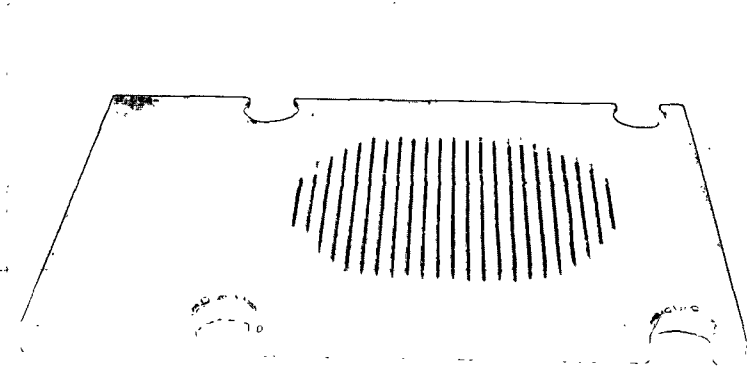
Upper Tube and Flange



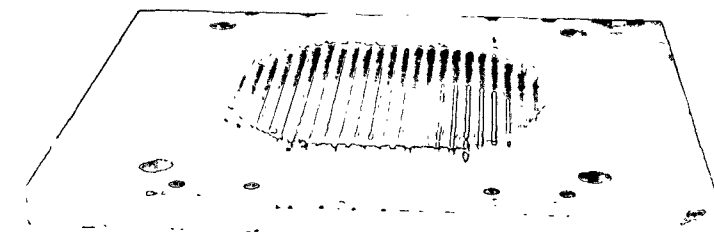
Top of Sliding Member



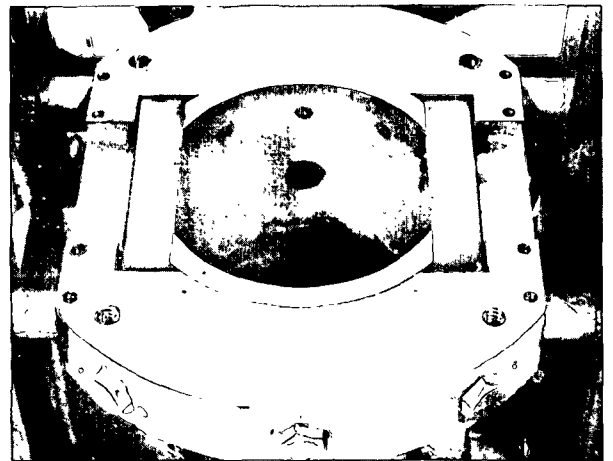
Top of Fixed Member



Bottom of Sliding Member



Bottom of Fixed Member



Lower Tube and Flange

Figure 4. Details of Sliding Valve

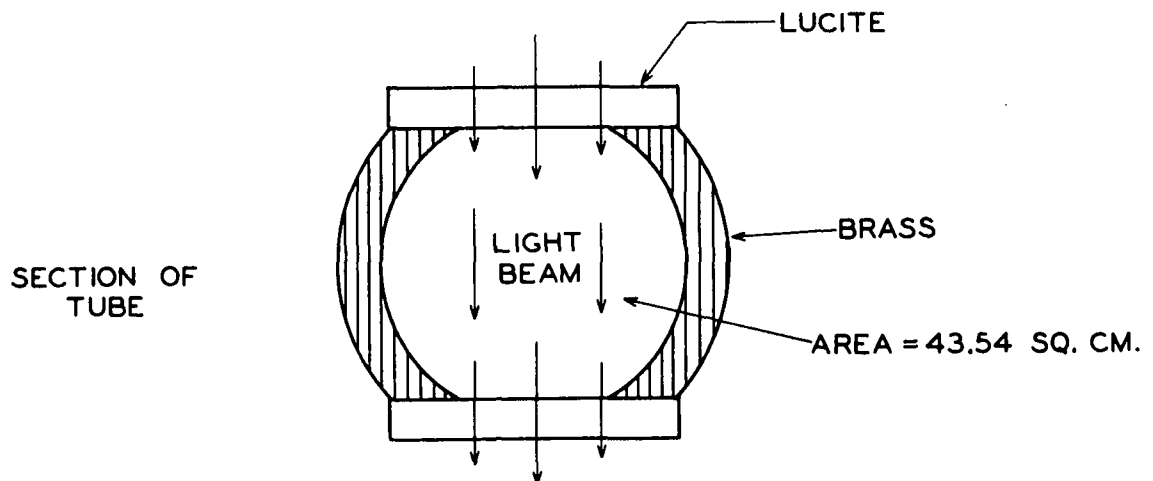
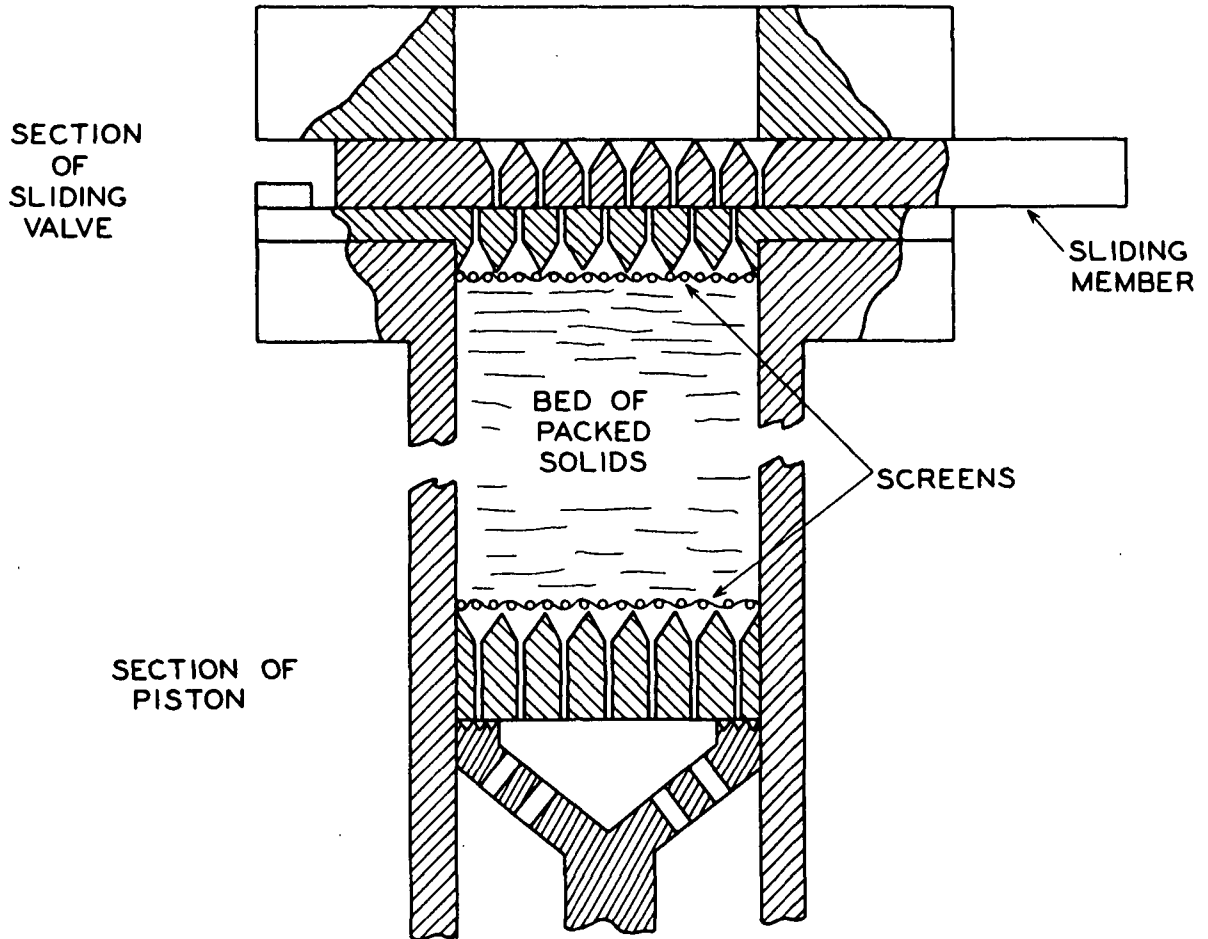
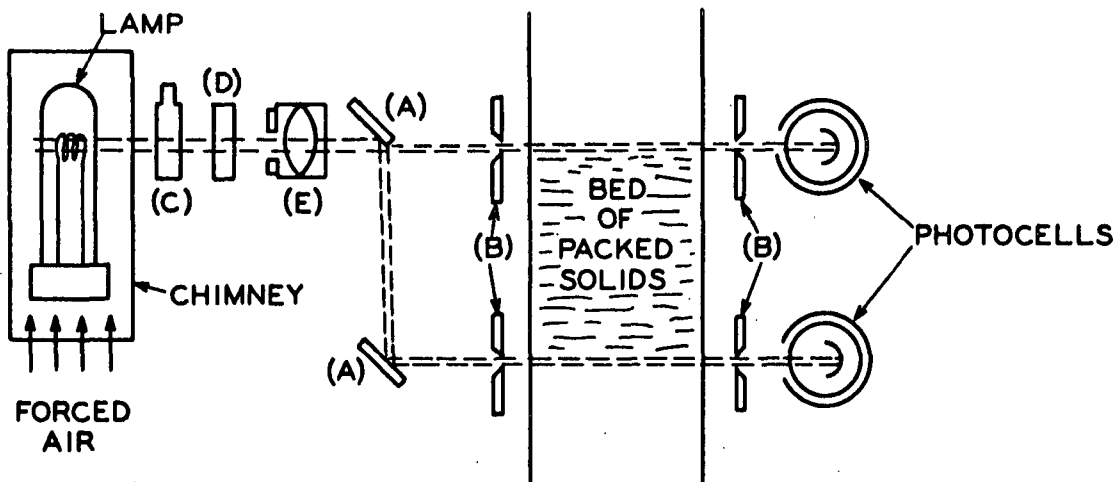


Figure 5. Details of Sliding Valve, Piston, and Tube

to be passed just below the bed. The details of this construction are shown in Fig. 5. The light beams passed through the triangular spaces between the screen and valve or piston.

The concentrations of the solution entering and leaving the bed were measured by application of Beer's law. The optical system for measuring optical transmission is shown in Fig. 6. The major elements of this system were an incandescent light source, a copper sulfate heat filter, a colored glass filter, a collimating lens, beam-splitting mirrors, 2 photocells, an oscilloscope, and a polaroid Land camera. For a system of this type it is desirable to have the light intensity (defined by the light source and the colored glass filter), solute absorption, and photocell response peak at the same wavelength. The characteristics of the light source, colored glass filter, diacetyl solution, and photocells are shown in Fig. 7.

During the course of a washing run, it was desirable to start the sweep of the oscilloscope, open the solenoid valve, and start a timer simultaneously. This was accomplished by the electrical circuit shown in Fig. 8. When the microswitch (A) in Fig. 8 was released, the relay was activated, the oscilloscope sweep was triggered, the solenoid valve was opened, and the timer was started.



- A MIRRORS
- B LIGHT-DEFINING SLITS
- C COPPER SULFATE HEAT FILTER
- D COLORED GLASS FILTER
- E LIGHT COLLIMATING LENS
- F PHOTOCELLS

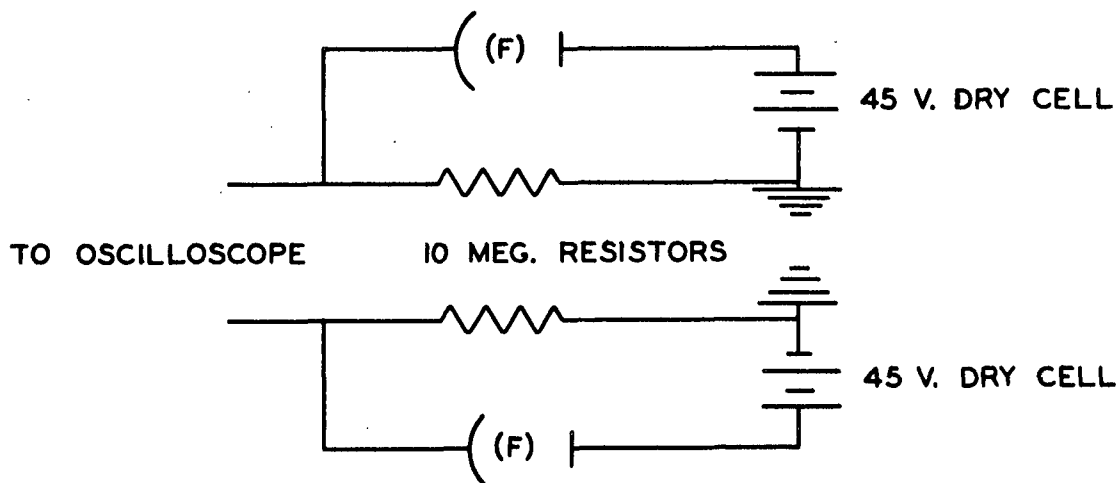


Figure 6. Optical System

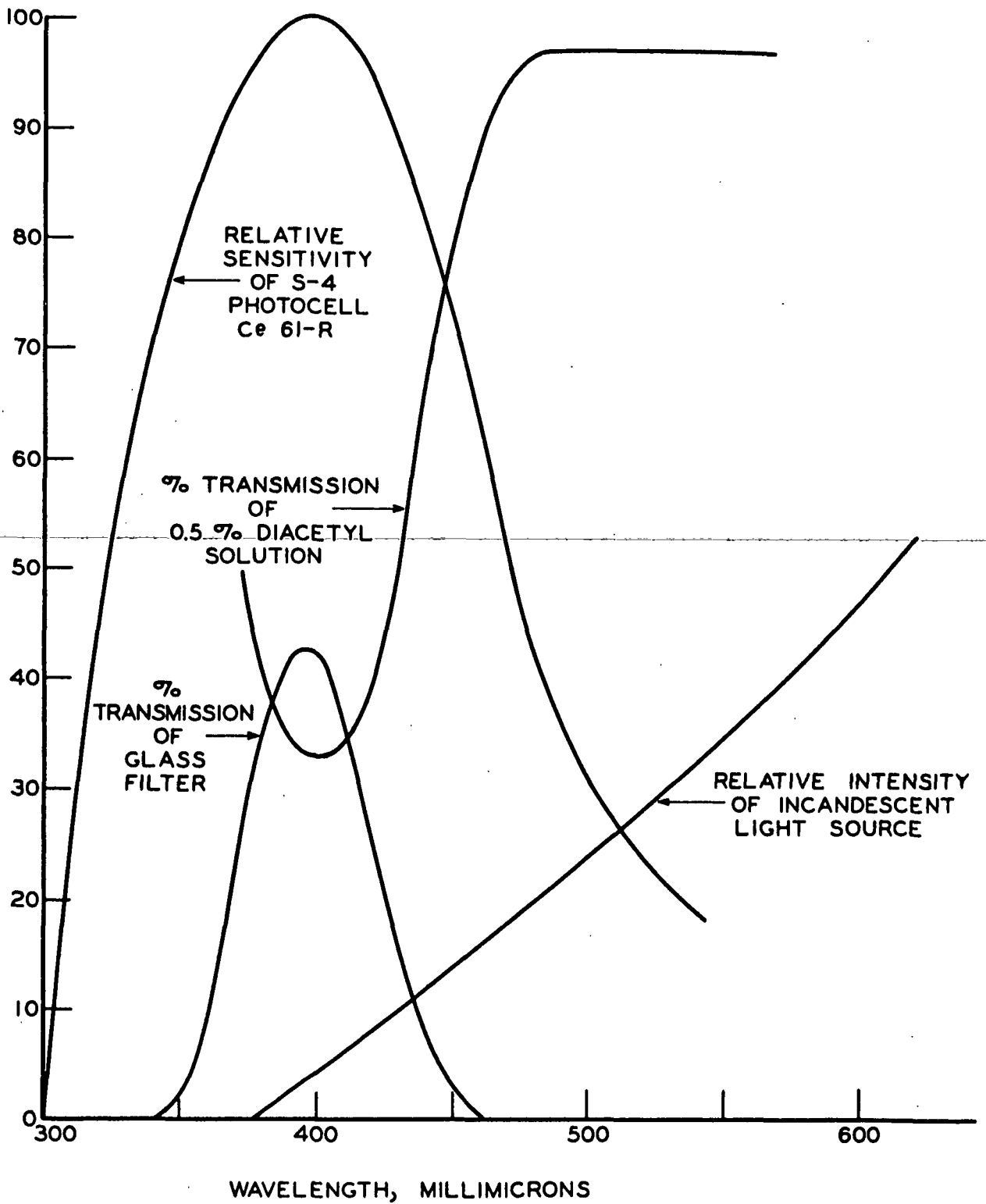


Figure 7. Characteristics of Optical Components

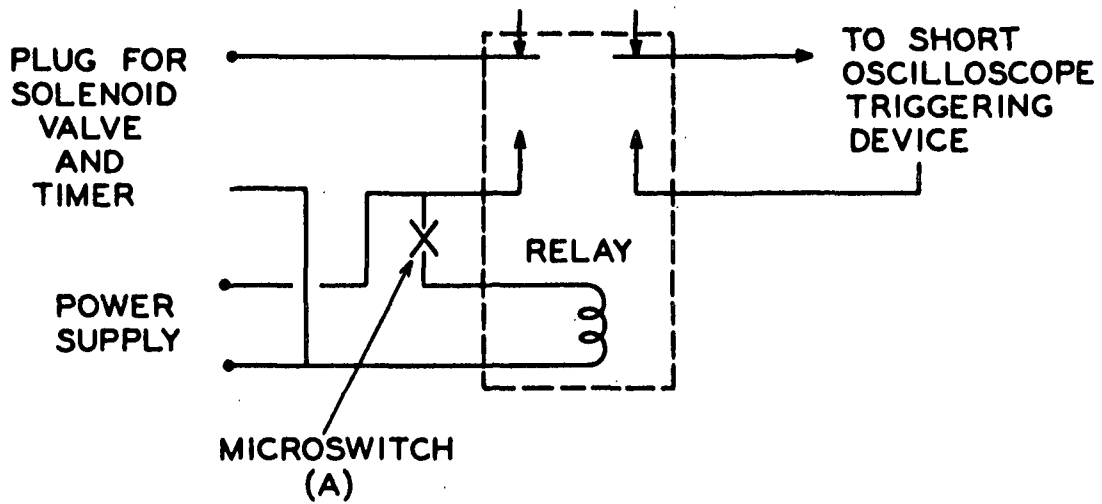


Figure 8. Synchronization of Solenoid, Timer, and Oscilloscope

EXPERIMENTAL PROCEDURES

CHARACTERIZATION OF SOLID PARTICLES

The glass beads used in this study were resistance glass shot manufactured in Germany by the Propper Mfg. Co., Inc. The nominal size of the beads was 3 mm. The average diameter of the beads was measured with a micrometer to be 3.02 mm. Fifty beads were found to weigh 1.908 g. Thus, the specific volume of the beads (assuming they are spherical in shape) was calculated to be 0.378 cc./g.

The dacron fiber used in this study was supplied by E. I. du Pont de Nemours & Company. The manufacturer gave the following specifications for this fiber:

density = 1.38 g./cc.

length = 1/4 in.

denier = 3 (ca. 18 μ diameter)

The all-skin viscose fibers used in this study were supplied by the American Viscose Co., Inc. Samples of 1, 4, 16, and 64-denier fiber were used. The following properties were determined:

1. air-dry diameter, μ
2. water-swollen diameter, μ
3. diameter swelling
4. longitudinal swelling
5. water-swollen specific volume, cc./g. (o.d.)
6. pycnometric specific volume (in water), cc./g. (o.d.)
7. porosity of the fiber.

The air-dry and water-swollen fiber diameters were measured in the normal manner, using a microscope with a calibrated eyepiece (magnification of 278X). This was done for the 1, 16, and 64-denier fibers. Only the water-swollen diameter was determined for the 4-denier fiber.

The percentage of swelling of the fibers is defined as 100 times the water-swollen dimension minus the air-dry value, divided by the air-dry value.

The longitudinal swelling was determined in the following manner. Six air-dry fibers were mounted between lantern slide plates. The slide was then placed in a photographic enlarger and a large print (24 by 36 in.) of the fibers was made. The process was then repeated with the same six fibers in the water-swollen state.

The lengths of the fiber images on the prints, in the air-dry and water-swollen states, were then measured with a map measuring device. Before making the prints, a cross was scratched on one of the slides. The procedure was calibrated by measuring the cross (on the slide) microscopically, and the image of the cross (on the print) with the map measurer. The above procedure was carried out on the 16-denier fiber.

The water-swollen specific volume (water swollen, cc./g., o.d.) of the fibers was determined in the following manner. A number of fibers were cut into approximately 5-cm. lengths. From these fibers three samples of about 50 fibers each were prepared. The three samples were weighed on a micro balance. The moisture content of a separate sample of the fibers was determined by drying the fiber at 105°C. The length

of the fibers was determined by placing them on lantern slides, projecting their image on a blackboard, and finally measuring their length with a map measurer. The map measuring device was calibrated by the same procedure as that used in the longitudinal swelling experiment. The water-swollen specific volume was then calculated from the water-swollen diameter, the air-dry length, the longitudinal swelling, and the oven-dry weight of the fibers.

The pycnometric specific volume, defined as the volume of fiber denied to water per gram of oven-dry fiber, was determined in the following manner. A sample of fibers was deaerated by placing them in hot water (ca. 50°C.) in a large vacuum desiccator and applying a vacuum to the desiccator. When the water had cooled to 35°C., the fibers were transferred to a pycnometer (this operation is carried out with the pycnometer and the fibers continuously under water). After the water temperature had decreased to 30°C., the pycnometer was sealed and weighed. The fibers in the pycnometer were then transferred to a fritted glass funnel, dried at 105°C., and weighed. The procedure was then repeated without the fibers. The pycnometric density of the fibers was then calculated from the specific volume of water at 30°C., the weight of the pycnometer containing the fibers and water, the weight of the pycnometer containing water only, and the oven-dry weight of the fibers.

The porosity of the fibers was then calculated from the water-swollen specific volume and the pycnometric specific volume.

The results of the all-skin viscose fiber characterization are shown in Table II. The plus and minus limits given in this table refer to the

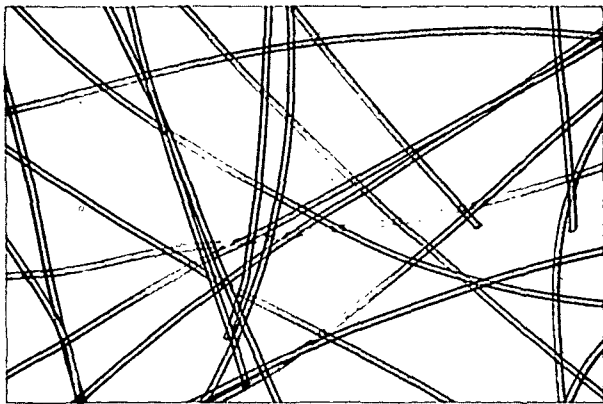
precision of the measurements. An indication of the fiber uniformity is illustrated by the fact that the 2σ limits of the individual fiber diameter measurements, for the water-swollen, 16-denier fibers, was only 7.1%. The homogeneity of the four fiber samples was indicated by the fact that they all exhibited the same swelling properties and the same water-swollen specific volume. Photomicrographs of the fibrous packing materials used in this study are shown in Fig. 9.

TABLE II
VISCOSE FIBER CHARACTERISTICS

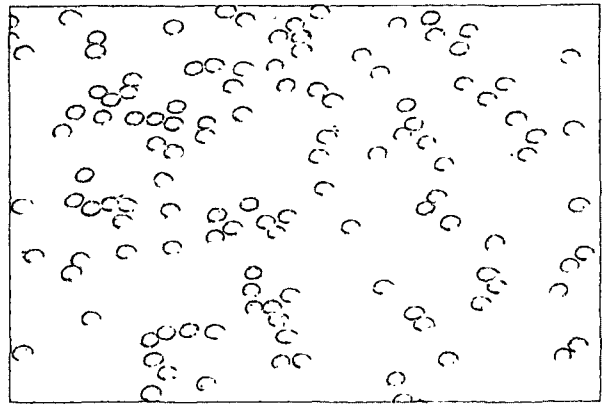
	Denier				Average
	1	4	16	64	
Av. fiber diameter					
Air dry, μ	11.07 $\pm 2.8\%$ ^a	(20.54) ^b	40.82 $\pm 2.2\%$	84.56 $\pm 1.8\%$	
Water swollen, μ	15.91 $\pm 3.3\%$	29.89 $\pm 2.3\%$	60.35 $\pm 2.3\%$	122.1 $\pm 1.2\%$	
Swelling (diameter), %	43.7	(45.5)	46.8 $\pm 13\%$	44.5 $\pm 13\%$	45.5 $\pm 5.4\%$
Swelling (length), %	--	--	6.4	--	6.4
Water-swollen specific volume, wet cc./g., o.d.	(1.626)	1.667	1.622 $\pm 6.9\%$	1.612 $\pm 1.3\%$	1.626 $\pm 5.1\%$
Pycnometric specific volume, cc./g.	--	--	0.6207 $\pm 0.3\%$	--	0.6207 $\pm 0.3\%$
Fiber porosity	--	--	0.618	--	0.618

^a \pm limits are 2σ limits (measure of precision).

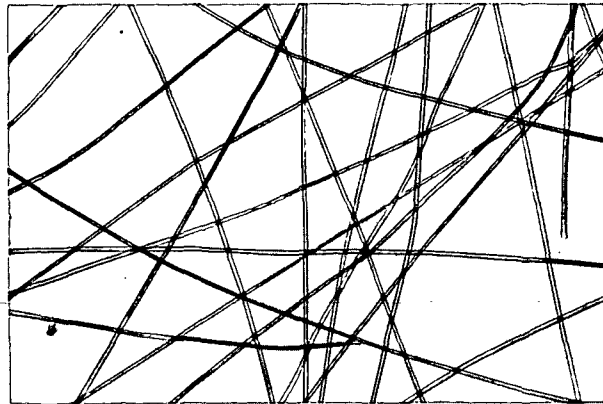
^b Values in parentheses are calculated, not measured.



Dacron--3 Denier
Magnification: 55X



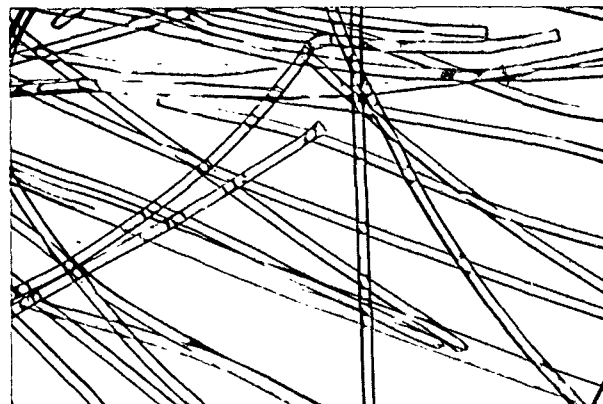
Dacron--3 Denier
Magnification: 105X



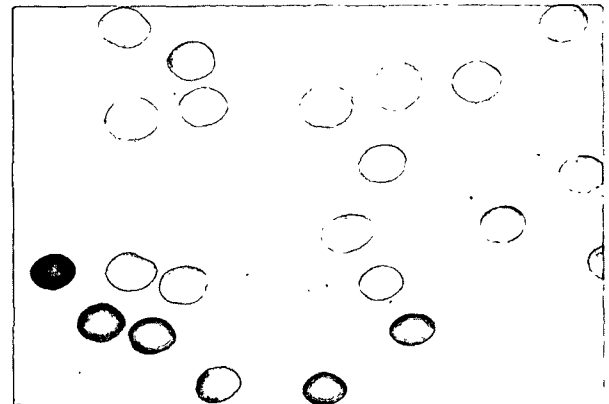
Viscose--1 Denier
Magnification: 58X



Viscose--1 Denier
Magnification: 105X



Viscose--64 Denier
Magnification: 20X



Viscose--64 Denier
Magnification: 58X

Figure 9. Photomicrographs of Packing Materials

BED PREPARATION

In order to form a bed of packed solids, the piston in Fig. 3 was lowered to its lowest position and the sliding valve was removed. In the case of the glass bead beds, the bed was formed by pouring the beads into the tube which was nearly full of water. After the bed was formed, a screen was placed above the bed, the sliding valve was replaced, the tube was filled with water, and the piston was raised until the upper screen was in contact with the bottom of the sliding valve.

In the case of the fiber beds, the tank was replaced by a pad-forming flow distributor. A dilute slurry of deaerated fibers in deaerated, deionized water, contained in a large stirred tank, was then siphoned into the pad-forming flow distributor. As the water was removed from the slurry, by opening valves (C) and (B), Fig. 3, a fiber bed was formed on the screen above the piston. It was necessary to use a very low consistency in order to avoid flocculation of the fibers in the tube above the piston. Under these conditions a bed consisting of randomly oriented fibers lying on the x-y plane should be obtained. After a fiber bed was formed, a screen was placed above the bed, the sliding valve was replaced, and the fiber bed was compressed against the bottom of the sliding valve by raising the piston.

After a bed of packed solids had been sealed in place, the bed dimensions were measured with a cathetometer. The location of the upper and lower edges of both the upper and lower screens were measured. The light-defining slits were then adjusted so as to obtain the maximum reading with the oscilloscope. After the slits were properly positioned

(at the upper edge of the upper screen and the lower edge of the lower screen), their location was measured with the cathetometer.

WASHING RUN

The beds were prepared for a washing run by cycling a diacetyl solution through the bed until the concentration of the diacetyl solution was unchanged by further contact with the bed. This was accomplished by forcing the diacetyl solution through A (Fig. 3) into the tube above the sliding valve. The solenoid valve was then opened and the solution was passed through the bed. The effluent stream was then collected and passed through the bed again. Samples of solution were analyzed colorimetrically until no change was detected upon passing through the bed.

A photograph was then taken of the oscilloscope response for each photocell with the light on (tube filled with solution) and the light blocked off (blank).

The level of the solution was then lowered until it coincided with the center of the sliding valve. The sliding valve was then closed and the tube above the valve and the tank were filled with water. The needle valve was then adjusted so that the proper flow rate would be obtained during the washing run. After the outlet overflow was connected to a collection vessel and the timer was activated, the apparatus was ready for a washing run.

Just prior to the washing run, the camera was opened. The micro-switch (A), Fig. 8, was then held depressed between two fingers and the power to the relay was turned on. The sliding valve was then opened by pushing

the sliding member against a stop. As soon as the sliding member was pushed, the microswitch (still held between the fingers) was released. This opened the solenoid valve, started the oscilloscope sweep, and started the timer. The run was completed by depressing the microswitch and closing the camera.

After the washing run was over, a photograph was taken of the oscilloscope response for each photocell (with tube containing water).

After several runs at different flow rates, the bed was removed from the apparatus, dried at 105°C., and weighed.

The data for each run consisted of:

Run number

Bed number

Flow rate

Volume of solution, cc.

Time of run, sec.

Flow rate, cc./sec.

Room temperature

Photograph of oscilloscope traces

In addition to the above data, the location of the various calibration marks, on the photograph of the oscilloscope traces, was recorded. Also, the sweep speed of the oscilloscope was recorded.

PRELIMINARY WASHING RUNS

A number of washing runs were performed using glucose as the solute. For these runs, several modifications were made in the optical system.

These were (1) the Ce 61-R, S-4 photocell was replaced with a PJ22, S-2 photocell; (2) the copper sulfate and colored glass filters were replaced with a polaroid filter; (3) a polaroid filter was placed in front of each photocell (with the optical axis of the first and second polaroids at 45° to each other).

The oscilloscope traces for a typical run in which a bed, saturated with 0.1M glucose solution was washed with water, are shown in Fig. 10 and 11. Figure 10 corresponds to the first ten seconds while Fig. 11 corresponds to the traces for 30 to 60 seconds.

From Fig. 10 and 11 it was obvious that the changes in photocell output were not proportional to the concentration of the solution in the light path. For example, the output of photocell A decreased as the concentration changed, but then quite unexpectedly returned to its original value despite the fact that the concentration had changed from 0.1M glucose to pure water. The output of photocell B started to decrease when the flow corresponded to ca. 0.5 pore volumes, but then as the glucose solution was completely displaced by pure water, the photocell output increased to its original value.

It is hypothesized that the changes in photocell output, which were recorded, were due to the scattering of light resulting from the mixing of two solutions (0.1M glucose solution, and water) with different refractive indices. When the two solutions were mixed, many interfaces were formed. Since the two solutions had different refractive indices, the light was scattered at these interfaces. As a result, the amount of light

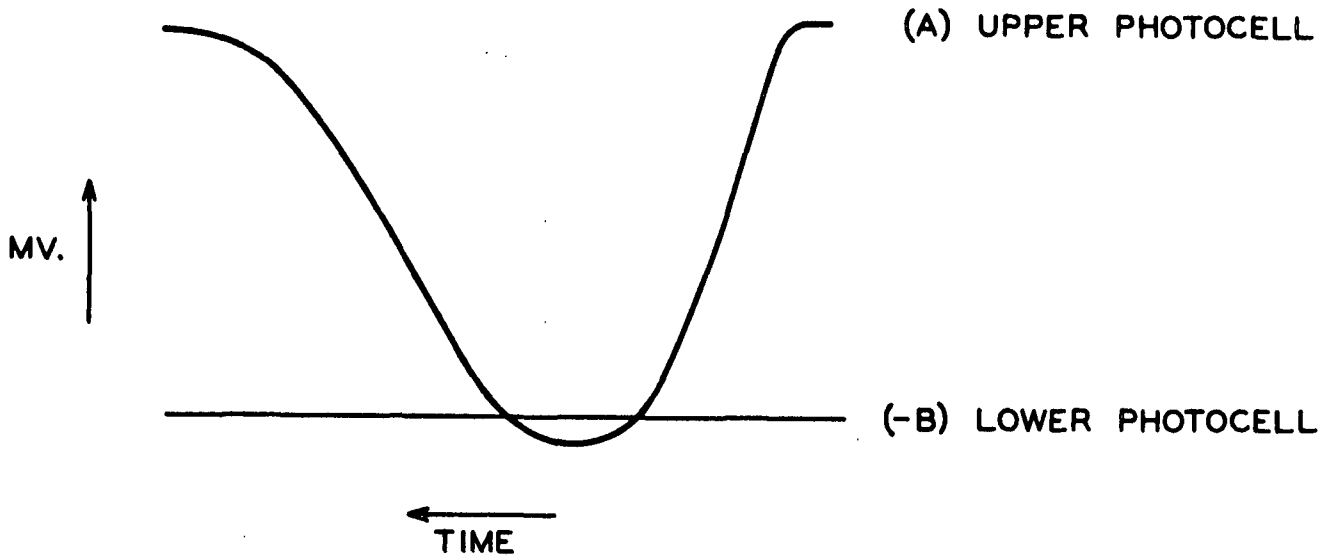


Figure 10. Oscilloscope Traces, 0-10 Seconds

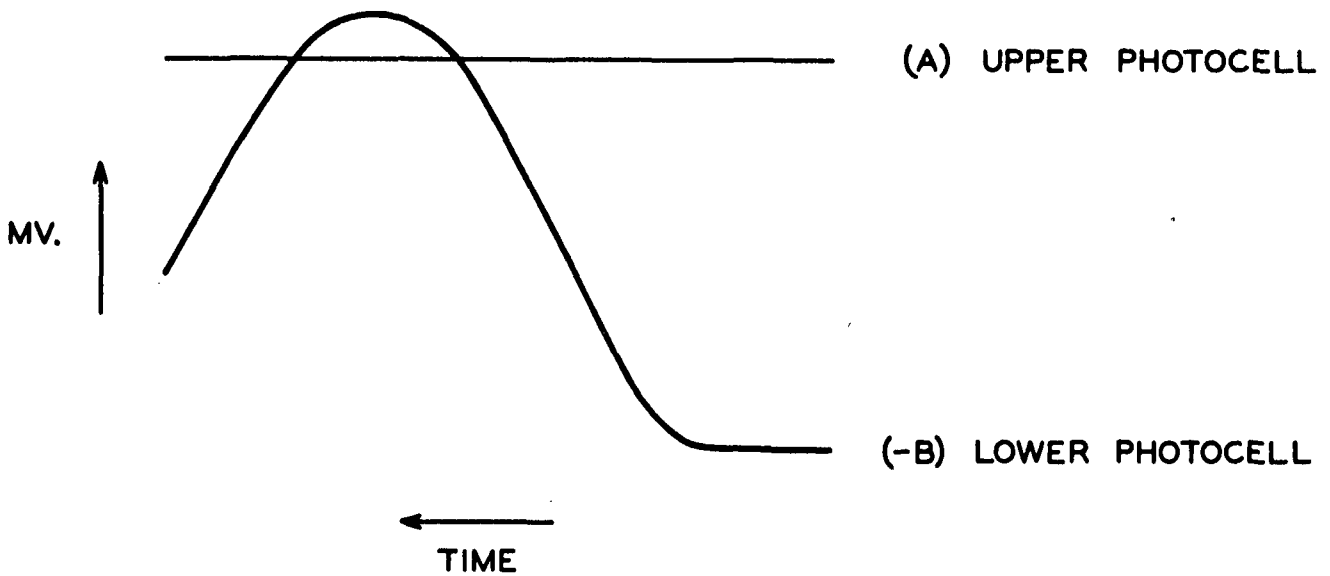


Figure 11. Oscilloscope Traces, 30-60 Seconds

falling on the photocell was greatly decreased. When the fluid was again of a constant concentration, the scattering of light was eliminated and the light intensity returned to its original value.

This phenomenon offers an indirect experimental verification that the solution which comes out of the bed of packed solids does not have a uniform concentration, but in reality consists of a mixture of fluid elements of different concentrations. Thus, when we speak of the concentration at a given level, in a bed of packed solids, we are really speaking of the average concentration at this level in the bed.

In order to minimize the scattering of light at the fluid element interfaces (formed during the washing procedure), the solute was changed from glucose to diacetyl. By using diacetyl, a much more dilute solution could be measured. This, in turn, decreased the difference in refractive index between the solution and water. The transmission of a 0.5% diacetyl solution, as a function of wavelength, was shown in Fig. 7. Some of the properties of diacetyl (or 2-3 butanedione) are listed below.

structure	molecular wt. = 86.09
$\text{CH}_3 - \begin{array}{c} \text{O} \\ \parallel \\ \text{C} \end{array} - \begin{array}{c} \text{O} \\ \parallel \\ \text{C} \end{array} - \text{CH}_3$	density = 0.9904-15/15
	boiling pt. = 88°C.
	solubility:
	25 ¹⁵ g. in 100 g. water
	infinite acetone and alcohol
	refractive index = 1.39331
	calculated refractive index of 0.3% solution = 1.3332 (refractive index of water = 1.333)
	color--yellow green
	odor--strong, buttery odor

In each washing run, using diacetyl as a solute, the relative concentration at any given time was calculated from the vertical deflection of the oscilloscope trace by Equation (45).

$$\frac{C}{C_o} = \frac{-kC}{-kC_o} = \frac{\ln(Y'/Y'_w)}{\ln(Y'_s/Y'_w)} \quad (45)$$

where

\underline{Y}' = Δy units between the point in question and \underline{Y}_o ,

\underline{Y}'_w = Δy units between the value for water and \underline{Y}_o ,

\underline{Y}'_s = Δy units between the value for the original solution,

\underline{C}_o , and \underline{Y}_o , and

\underline{k} = Beer's law constant.

The terms in Equation (45) are shown in Fig. 12.

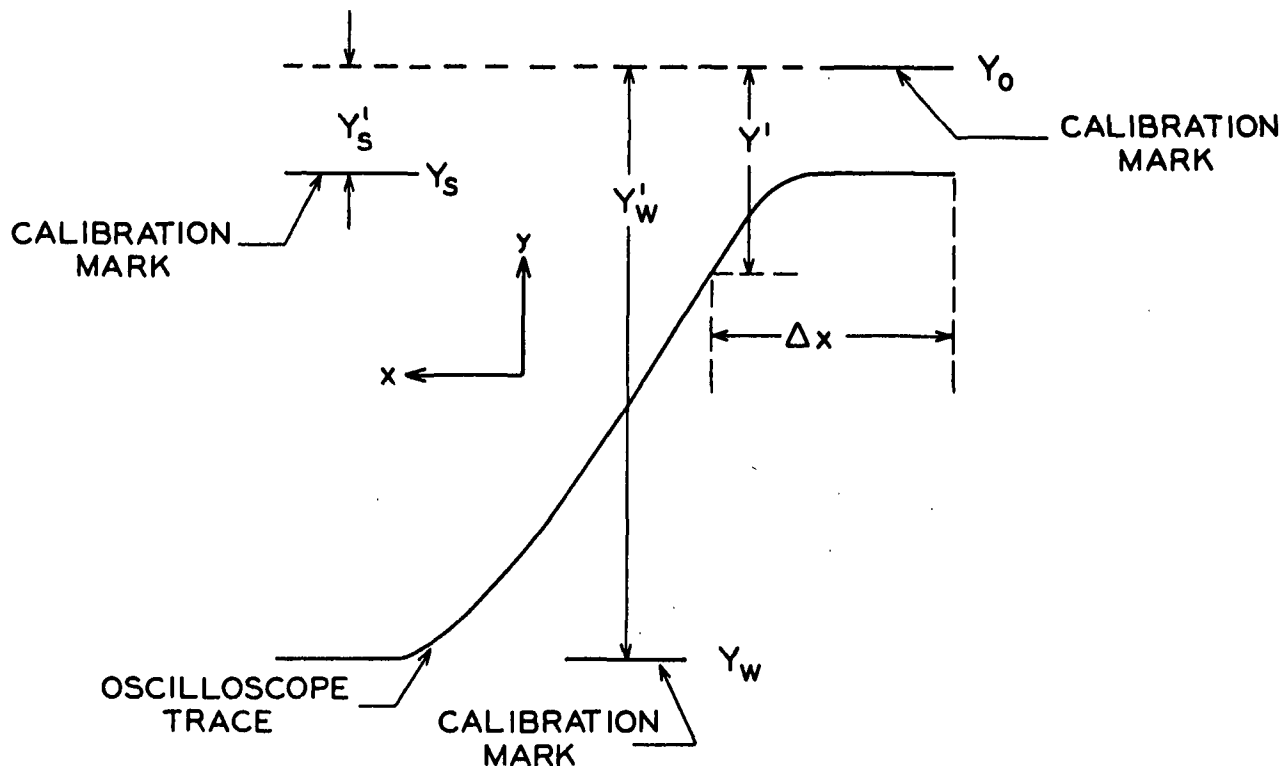


Figure 12. Oscilloscope Trace with Calibration Marks

The use of Equation (45) involved several assumptions. The first of these was that the photocell output was linearly related to the light intensity. A rough check of this assumption was made by placing a screen of known transmission (41%) in the light beam and recording the photocell output. The results of this test gave no reason to suspect that the photocell output was not linear.

A second assumption was that the solution concentration and light intensity were related by Beer's law. Beer's law was checked for aqueous diacetyl solutions from 0 to 5% diacetyl using a D.U. Spectronic photometer. The results of this test are shown in Table III.

TABLE III

A CHECK OF BEER'S LAW

Conc. ^a	Optical Density	$\frac{k}{b}$ ^b
1.25	0.110	11.38
1.67	0.149	11.21
2.50	0.215	11.62
5.00	0.425	11.78

^a Concentration in ml. diacetyl/l. solution.

^b Concentration/optical density.

Beer's law was then checked for the apparatus by passing solutions of known concentration through the apparatus and recording the oscilloscope deflections. The results of these tests are shown in Table IV.

TABLE IV
A CHECK OF BEER'S LAW

Picture No.	Concentration	$\frac{Y'_s}{Y'_w}$	$-kC$	$-k$
6	2.917	0.125	2.08	0.713
7t	2.176	0.195	1.63	0.747
7	1.796	0.263	1.33	0.740
8	1.206	0.400	0.915	0.755
1 & 2	1.166	0.421	0.865	0.740
3	1.131	0.444	0.812	0.719

The average value of k in Table IV is 0.736 ± 0.033 (2σ limits). This variability in k corresponds to a 5% error in calculating C from $\frac{Y'_s}{Y'_w}$. One advantage of Equation (45) is that it is not necessary to know the value of the Beer's law constant. Thus, any experimental error which might be involved in obtaining k is eliminated. The reason for performing the runs in Table IV, therefore, was not to determine k , but rather to establish the fact that Beer's law is valid for the system.

One other point about the light intensity-concentration relationship was checked. It was conceivable that the flow rate in the system could affect the light intensity. This possibility was checked for both water and diacetyl solution. No change in light intensity, due to the flow rate, was observed.

All of the above tests were performed at uniform concentrations. The possibility still existed, however, that light scattering occurred at fluid particle interfaces during the washing runs with the diacetyl

solutions, such as it did with all of the washing runs with the glucose solutions. If this was true then Equation (45) would not have held during the washing runs. A check on this possibility was obtained by running a material balance on the system.

In order to run a material balance on the system, the photograph of the oscilloscope trace was converted to a relative concentration (C/C_0) versus pore volume (P.V.) plot. The first step in this procedure consisted of reading the x and y axes with the aid of a microscope. The x axis was then converted to pore volumes by the following formula:

$$\frac{(\Delta x \text{ units}) \left(\frac{\text{cm.}}{\Delta \text{ unit}} \right) \left(\frac{\text{sec.}}{\text{cm.}} \right) \left(\frac{dV}{d\theta} \right)}{(\text{void volume of bed})} = \text{P.V.} \quad (46)$$

where

Δx units = horizontal distance from $t = 0$ to point in question as measured with the microscope,

$\frac{\text{cm.}}{\Delta \text{ unit}}$ = calibration of microscope measurement,

$\frac{\text{sec.}}{\text{cm.}}$ = oscilloscope setting during run,

$\left(\frac{dV}{d\theta} \right)$ = volumetric flow rate, cc./sec., and

P.V. = volume of flow/void volume of bed, dimensionless.

The y axis was converted to relative concentration by Equation (45).

By multiplying area under the C/C_0 versus P.V. plot by the void volume of the bed, the volume of solution, at a concentration C_0 , passing the point in question was obtained. Thus, for the exit stream, this procedure gave the volume of solution, at a concentration C_0 , which was

removed from the bed; while for the entrance stream, it represents the volume of solution, at a concentration \underline{C}_0 , which entered the bed. The former minus the latter represents the volume of solution, at a concentration \underline{C}_0 , which was removed from the bed. This, therefore, should represent the volume of solution, at a concentration \underline{C}_0 , which was in the bed at the start of the run; and finally, this volume should equal the void volume of the bed plus the void volume of the particles in the bed.

Three assumptions were inherent in the above procedure. The first was that all the diacetyl was removed from the bed in the washing process. The second assumption was that the diacetyl originally in the bed corresponded to the void volume of the bed plus the void volume of fibers times \underline{C}_0 . Both of these assumptions were checked in the following manner.

A bed of viscose fibers, in the proper condition (washed in the case of the first assumption, and saturated with solution of concentration \underline{C}_0 in the second), was bodily removed from the apparatus. Due to the spongelike nature of the viscose bed, it was possible to lift the bed, along with all of the solution contained therein, out of the apparatus and transfer it, without loss of solution, to a 1000-ml. flask. The mixture of fibers, solution, and 200 ml. of additional water was then distilled. The distillate was collected and colorimetrically analyzed for diacetyl.

The results of these experiments and some additional control experiments are shown in Table V.

TABLE V
DISTILLATION EXPERIMENTS

Charge to Distilling Flask	Diacetyl in Distillate, ml.	Recovery, %
500 ml. water + 0.01 ml. diacetyl	0.0066	66
500 ml. water + 0.05 ml. diacetyl	0.0482	96
washed bed including solution + 200 ml. H ₂ O	0.002	0.3 ^a
0.05 ml. diacetyl added to above	0.0499	100
bed saturated with solution, C ₀ , + 250 ml. H ₂ O	0.422	97.5 ^a

^a 100% = void volume of bed + void volume of fibers.

The third assumption in calculating the material balance was that the flow rate was constant throughout the run. The time for the flow rate to reach 99.9% of the final value (at a flow rate of 0.98 cm. per sec.) was calculated to be 0.0069 seconds. Thus, the initial effect was considered negligible.

The material balance data for the last seven beds used in this study are shown in Table VI. The bed number indicates the type of material used as well as the bed number. The notation 3D refers to a 3-denier dacron fiber, the 1V and 64V refer to 1 and 64-denier viscose fibers, respectively, and 3G refers to a 3-mm. glass bead.

The fact that negative as well as positive differences occurred in the material balances indicated that light scattering was not a major cause of difficulty in the material balances (since light scattering would

always cause \underline{V}_{mb} to be high). The large differences encountered in some of the material balances were probably due to experimental difficulties in determining $\underline{V}_G(dV/d\theta)$, and/or the sweep speed of the oscilloscope.

TABLE VI

MATERIAL BALANCE DATA

Bed No.	\underline{V}_{mb}^a	\underline{V}_G^b	Difference, % ^c
3D-15	207.4 \pm 5 ^d	188.1	+9.3
1V-14	253.6 \pm 13	215.4	+15.1
64V-13	202.1 \pm 2	215.4	-6.6
3D-12	219.9 \pm 4	203.3	+8.2
1V-11	122.5 \pm 5	120.1	+2.0
3D-10	191.9 \pm 11	209.6	-9.2
3G-9	102.2 \pm 6	104.2	<u>-2.0</u>
		Average:	+2.4

^a \underline{V}_{mb} = volume of solution, at concentration \underline{C}_0 , removed from the bed as calculated from the plots of $\underline{C}/\underline{C}_0$ versus P.V.

^b \underline{V}_G = volume of solution, at concentration \underline{C}_0 , originally in the bed as calculated from the bed geometry and particle porosity.

^c % difference = $(\underline{V}_{mb} - \underline{V}_G)100/\underline{V}_{mb}$.

^d \pm limits are 2σ limits for different runs with a given bed.

In the data reduction it was necessary to plot $\underline{C}/\underline{C}_0$ versus \underline{R} . Since

$$u = \frac{1}{A\epsilon} \left(\frac{dV}{d\theta} \right) \quad (47)$$

and

$$\epsilon = \frac{\text{void volume}}{Az} \quad (48)$$

$$u = \frac{z}{\text{void volume}} \left(\frac{dV}{d\theta} \right) \quad (49).$$

By using \underline{V}_{mb} as the void volume and then calculating \underline{R} from

$$R = \frac{u}{z} (\Delta x \text{ units}) \left(\frac{\text{cm.}}{\Delta \text{ unit}} \right) \left(\frac{\text{sec.}}{\text{cm.}} \right) \quad (50)$$

the errors in $(dV/d\theta)$ and the oscilloscope sweep speed will be cancelled since the same value of $(dV/d\theta)$ and sweep speed were used in calculating \underline{V}_{mb} as used to calculate \underline{R} . The above procedure was reasonable as long as it was believed that a material balance did exist, and the discrepancies were due to errors in \underline{V}_G , $(dV/d\theta)$, and the oscilloscope sweep speed.

A sample calculation illustrating all of the above calculations, as well as the determination of the empirical constants for Equation (44) (from a plot of $\underline{C}/\underline{C}_0$ versus \underline{R} for the entrance stream), and the determination of the longitudinal diffusivity coefficient, \underline{D}_L [from Equation (43) and a plot of $\underline{C}/\underline{C}_0$ versus \underline{R} for the exit stream] is shown in the Appendix.

RESULTS AND DISCUSSION

Before entering into a discussion of the washing runs, it seems pertinent to review the three experimental systems which were used in this study, as well as the purpose of each system. Three different solids were used. The first solid consisted of 3-mm. glass beads. The second solid consisted of 3-denier dacron fibers. The third system consisted of either 1 or 64-denier all-skin viscose fibers. In all three systems, the bed was saturated with an aqueous diacetyl (2-3 butanedione) solution and then washed with water.

The glass bead system was primarily used to check out the experimental system and verify the validity of Equation (43).

The dacron fiber system was investigated in order to indicate the important variables in a nonporous fiber system and to show the differences between a fiber system and a system of granular material.

The viscose fiber systems were investigated in an attempt to indicate the importance of the movement of solute within the fibers.

The calculations for one of the washing runs on the glass bead system are contained in the Appendix. The empirical constants for Equation (44) were adjusted so that the experimental curve for $\underline{C}/\underline{C}_0$ versus \underline{R} , for the input curve, was in agreement with Equation (44). A value of \underline{S} ($= \underline{D}_L/\underline{uz}$) was then chosen so that Equation (43) was in best agreement with the experimental curve of $\underline{C}/\underline{C}_0$ versus \underline{R} for the exit curve. The longitudinal dispersion coefficient, \underline{D}_L , was then calculated

from \underline{S} , \underline{u} , and \underline{z} . The results of the washing runs using the 3-mm. glass bead system are shown in Table VII. The value of \underline{z} for this system was 5.288 cm. The longitudinal dispersion coefficient, \underline{D}_L , is also shown as a function of the pore velocity, \underline{u} , in Fig. 13.

TABLE VII
GLASS BEAD SYSTEM

Run No.	\underline{S}	\underline{u} , cm./sec.	$\frac{\underline{D}_L}{\underline{u}}$, sq. cm./sec.
9-3	0.0435	0.374	0.0860
9-6	0.0455	0.275	0.0660
9-7	0.0475	0.162	0.0408
9-8	0.0400	0.080	0.0169
9-9	0.0295	0.043	0.0067
9-11	0.0415	0.127	0.0280
9-12	0.0435	0.205	0.0470

An inspection of Table VII indicates the assumption that $\underline{D}_{mol.}$ (ca. 5×10^{-6} sq. cm./sec.) is negligible compared to \underline{D}_L is valid even for the lowest flow rate encountered in this study.

Equation (22) states that:

$$\frac{\underline{D}_L}{\underline{u}} = \frac{1}{2\tau\underline{u}} \int_{-\infty}^{\infty} \Delta^2 \phi(\Delta) d\Delta \quad (22).$$

In the theoretical discussion we showed that $\phi(\Delta)$ was fixed if the product $\underline{u}\tau$ was constant and streamline flow was maintained in the bed. Since τ may be changed, as \underline{u} varies, to maintain the product $\underline{u}\tau$ constant, it was

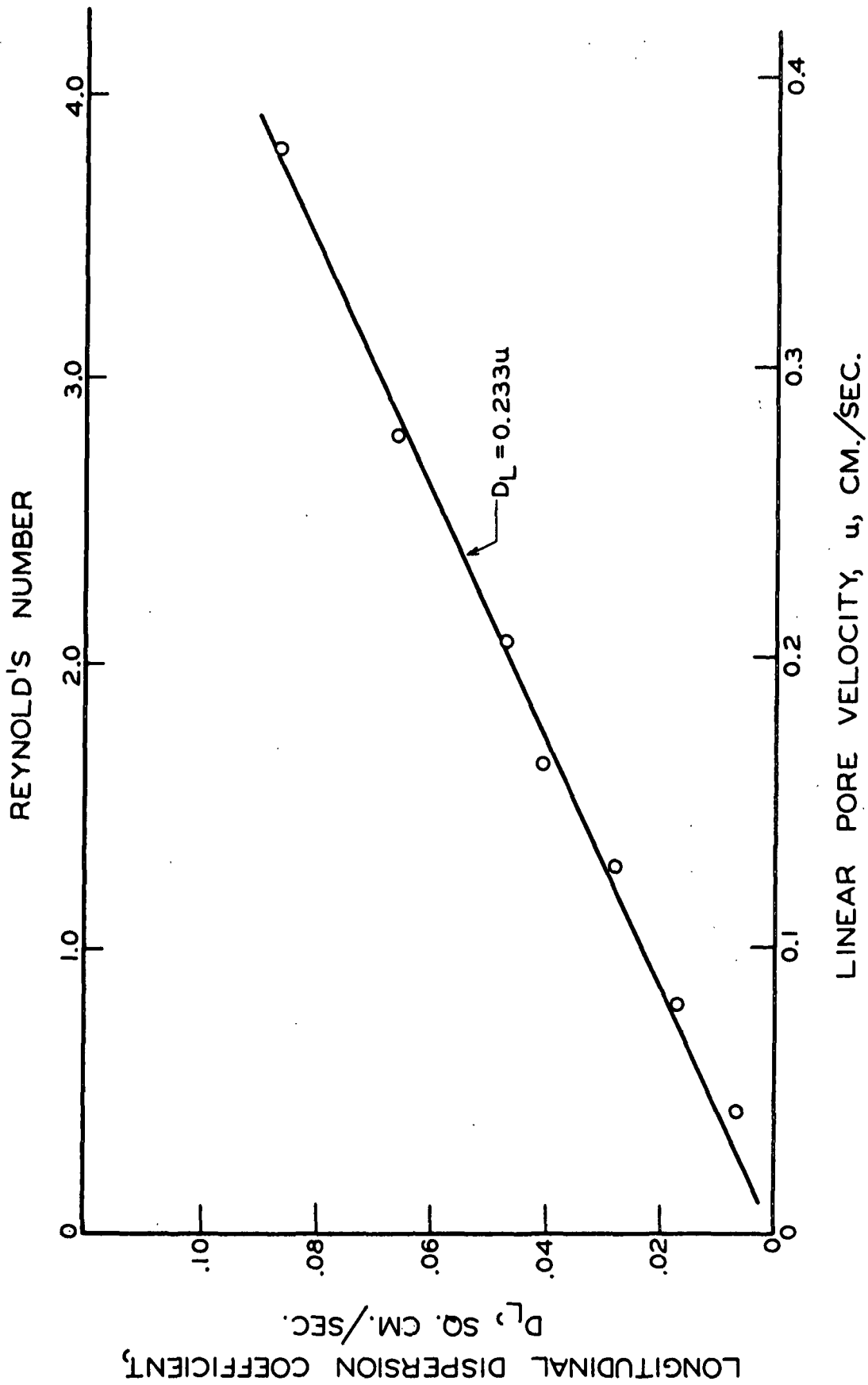


Figure 13. D_L versus u for Bed Number 3G-9

concluded that $\frac{D_L}{u}$ should be a constant if streamline flow is maintained. Several authors (2, 3, 15) found general agreement with this prediction. In Fig. 13 we can see that $\frac{D_L}{u}$ is constant for the entire range of flow rates investigated. The high Reynolds number for the higher flow rates indicates that the flow may not have been completely streamline. In these cases, however, the fact that $\frac{D_L}{u}$ remains constant indicates that any deviation from streamline flow is negligible. This is not surprising, since the transition from streamline to turbulent flow is very gradual in a bed of packed solids.

The second column in Table VII indicates that, with the exception of Run 9-9 (the very low flow rate in this run may have caused experimental difficulties), the precision of determining \underline{S} (which should be constant) was about 10% (the 2σ limits are 7% when Run 9-9 is eliminated). It was noted that a change in \underline{S} of about 10% was necessary in order to appreciably change the curve represented by Equation (43) (see Fig. 27 in the Appendix).

The fact that Equation (43) adequately describes the exit concentration data, and the fact that the expected relationship was obtained between $\frac{D_L}{u}$, as calculated from Equation (43), and u , are offered as evidence that Equation (43) is applicable to the washing of thin beds of packed solids.

The inadequacy of the step function approximation as given by Equation (29) is shown in Fig. 14 where a typical run is compared with Equations (29) and (43).

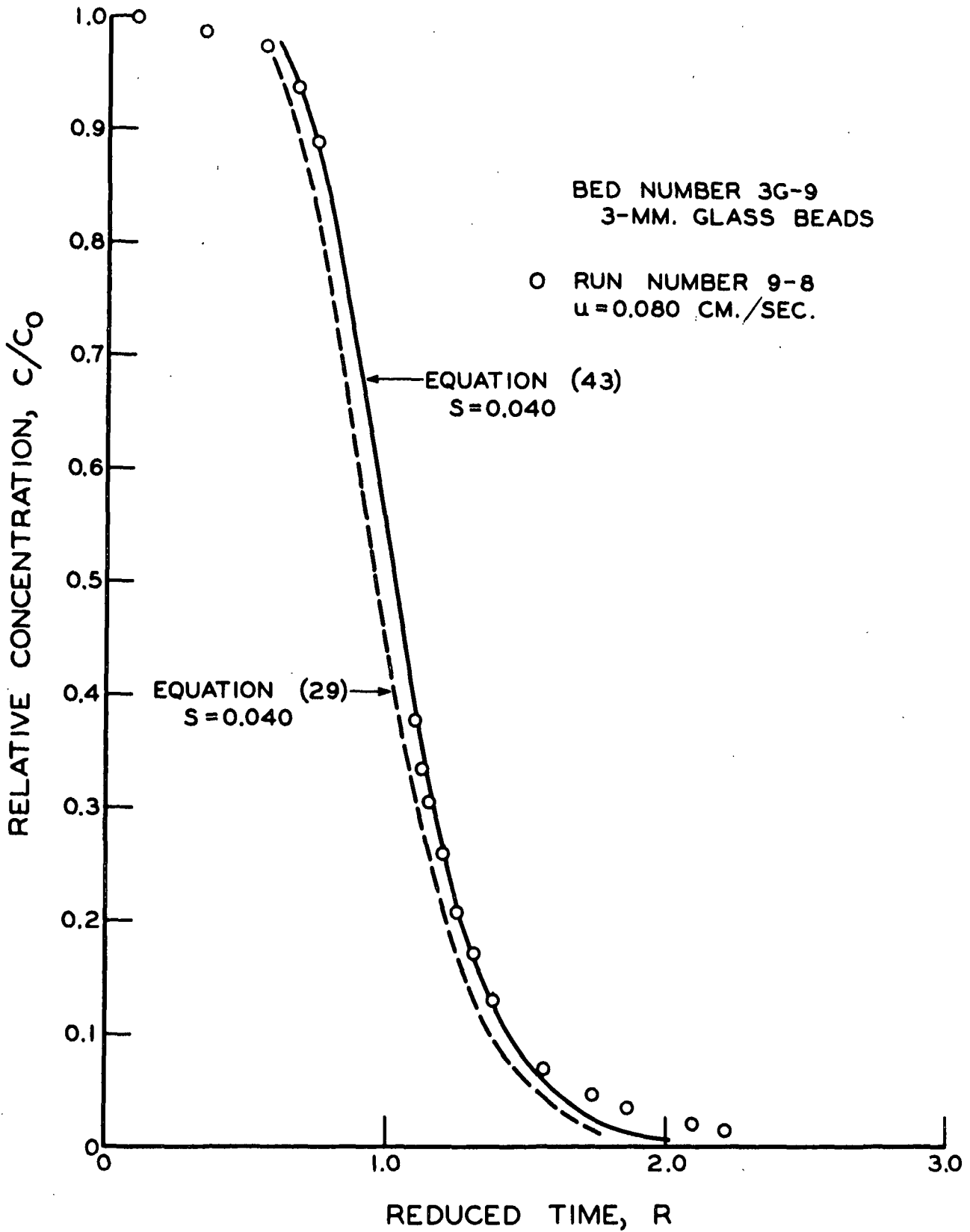


Figure 14. A Comparison of Equations (29) and (43) with Run 9-8

The value of $\underline{D_L}/\underline{u}$ obtained for 3-mm. glass beads in this study (0.233) is in close agreement with the value of 0.204 obtained by Raimondi, *et al.* (3), but is slightly lower than that obtained by most other workers. It should be noted that the precision mentioned above is for runs on the same bed of packed solids. When different beds of the same packed solids are used, it is quite possible that different values of $\underline{D_L}/\underline{u}$ will be obtained if great care is not exercised to produce the same packing and particle size distribution. The porosity of the bed used in this study was 0.45, which is appreciably higher than that used in most studies (0.36-0.41). This could account, in part, for the slightly different value of $\underline{D_L}/\underline{u}$ obtained in this study.

Three different beds of 3-denier dacron fiber were investigated in this study. All three beds were of the same thickness (5.29, 5.29, and 5.32 cm.) but of different porosities (0.916, 0.885, and 0.815 for beds no. 3D-10, 3D-12, and 3D-15, respectively). The results of the washing runs on these three beds, along with the glass bead bed (3G-9) and an estimated curve for a 17 μ glass bead bed (assuming the Peclet number is the same as that for the glass bead bed) are shown in Fig. 15.

From Fig. 15 we see that $\underline{D_L}/\underline{u}$ is a constant for each fiber bed. This is to be expected since streamline flow was maintained in these beds. The fact that Equation (43) adequately describes the exit concentration data, and the fact that $\underline{D_L}/\underline{u}$ is a constant for each fiber bed, indicates that the same basic mechanism of fluid element dispersion applies to beds of fibrous media as that which applies to beds of granular media.

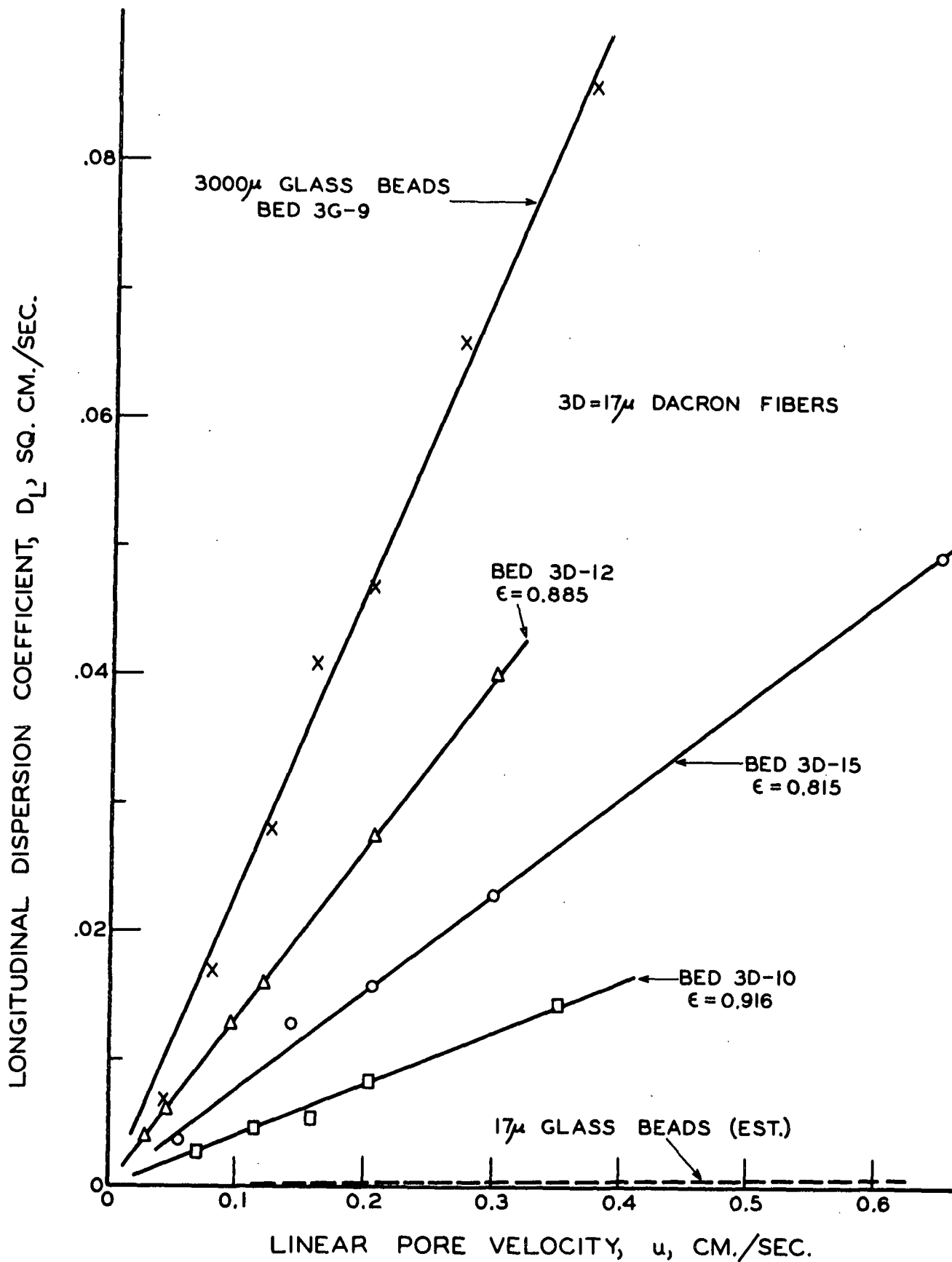


Figure 15. D_L versus u --Dacron Fiber and Glass Beads

One cause of fluid element dispersion is the fact that, under the same pressure gradient, fluid elements in large pores will travel more rapidly than fluid elements in small pores. Thus, $\frac{D_T}{u}$, which is a measure of fluid element dispersion, will depend upon the pore size distribution in a bed of packed solids. If the pore size distribution is wider, then velocity variations will be greater and $\frac{D_T}{u}$ will be larger. Raimondi, et al. found that $\frac{D_T}{u}$ was about 200 times larger for a sandstone than in packings of uniform size granular particles having the same permeability (same equivalent particle size). They stated that "This difference is due entirely to the wider pore size distribution of natural sandstones." Orlob and Radhakrishna studied the effect of entrained air on $\frac{D_T}{u}$ and found that the ratio of $\frac{D_T}{u}$ for no entrained air to $\frac{D_T}{u}$ for 15% entrained air was 30. Since the entrained air was preferentially trapped in the small pores, it effectively decreased the pore size distribution and thus decreased $\frac{D_T}{u}$. It is believed that the pore size distribution of a 17 μ fiber system is wider than the pore size distribution of a 17 μ bead system. If this is true, then $\frac{D_T}{u}$ should be greater for the 17 μ fiber beds than for the 17 μ glass bead system. From Fig. 15 we see that $\frac{D_T}{u}$ is much greater for the three fiber beds than for the 17 μ glass bead bed.

From Fig. 15 we can see that $\frac{D_T}{u}$ appears to be some function of porosity for the three dacron fiber beds. When the porosity of the bed is changed, the geometry of the bed will change. This, in turn, will alter the flow pattern in the bed, and thus it is reasonable to expect $\frac{D_T}{u}$ to depend upon the porosity. It is difficult, however, from a theoretical viewpoint, to explain the maximum observed in the $\frac{D_T}{u}$ versus ϵ relationship.

The only available data on the variation of $\frac{D_L}{u}$ (or more specifically, the Peclet number, $\frac{dpu}{D_L}$) with porosity seems to be the data of Cairns and Prausnitz (20). They studied the longitudinal mixing in a fluidized bed of spheres and found that a maximum existed in the relationship between $\frac{D_L}{u}$ and porosity for lead spheres. In their case, however, the system is complicated by the flow pattern of the solid particles. Thus, it is questionable whether their data may be used as a verification of the maximum found in the relationship between $\frac{D_L}{u}$ and porosity for the three dacron beds in this study.

Ingmanson, et al. (21) have shown that the Kozeny constant (which is used to characterize the pore shape and tortuosity of flow in porous beds) is a strong function of porosity for fiber beds over the porosity range used in this study. However, no maximum exists in this range. Parker (22) found that capillary pressure curves (from which pore size distributions may be calculated) were sensitive to porosity variations as small as 0.3%. The porosity range he investigated, however, was too limited to predict the effect of porosity on pore size distribution. McMaster (23) reported a much wider pore size distribution for a bed of $\epsilon = 0.862$ than for a bed of $\epsilon = 0.870$. He attributed this difference in pore size distribution to poor formation of the bed rather than to porosity variations. Thus, although the pore size distribution is certainly changed by varying porosity, since the area under a pore size distribution curve must change to account for the change in void volume in the bed, the exact relationship has not yet been determined.

At this time, no definite conclusions as to the effect of porosity on $\frac{D_L}{u}$ can be made. Although a maximum in $\frac{D_L}{u}$ as a function of porosity

was observed for the three beds used in this study, it is conceivable that the effect was due to poor formation of the beds. On the other hand, it seems unlikely, both from theoretical and experimental considerations, that $\frac{D_r}{u}$ is independent of porosity. Thus, it becomes apparent that one objective of future studies should be an attempt to define the relationship between $\frac{D_r}{u}$ and porosity more fully.

Three beds of all-skin viscose fibers were studied. Two of these beds were of 1-denier (16 μ) fibers while the third was of 64-denier (120 μ) fibers.

In the case of the glass beads and the dacron fibers, no sorption of diacetyl was encountered; thus, η was zero and λ , in Equation (43), was 1. In the case of the viscose fibers, however, sorption of diacetyl does occur; thus, λ is not equal to 1.

A modification of the shallow bed technique of Boyd, et al. (24) was used in an attempt to determine the apparent diffusion coefficient of glucose within the viscose fibers. In order for this technique to be useful, it is necessary for the concentration of the fluid surrounding the solid particles to be nearly zero for virtually the entire washing time, and for the particles to act independently of each other. These conditions could not be satisfied experimentally; thus, the work using this technique was stopped. The work which was done in this area is more fully discussed in the Appendix.

Although diffusion within the fiber could not be measured directly, the effect of this process can be seen by comparing the experimental

washing curves with the theoretical curve, assuming equilibrium between the fiber and the surrounding solution (very rapid diffusion from the fiber). For the case of equilibrium between the fiber and the surrounding solution, we may write

$$\eta = \epsilon_f C \quad (51)$$

where

ϵ_f = the porosity of the fiber, cc. void in fiber/cc. fiber.

The validity of Equation (51), which is based upon the assumption that no adsorption takes place, and the solution within the fiber is at the same concentration as the surrounding solution, was shown in Table V. Substituting Equation (51) in the expression for λ gives

$$\lambda = 1/(1 - \epsilon_f + \epsilon_f/\epsilon) \quad (52).$$

Two washing runs on bed 1V-11 are compared with Equation (43) in Fig. 16 and 17. The same value of $\frac{D_L}{u}$ was used in Equation (43) for these runs as was calculated from the runs on 17 μ dacron fiber at a porosity of 0.815. The porosity of this bed was 0.808 and λ was 0.892. The bed was made of 1-denier (16 μ) viscose fibers and was 3.05 cm. thick. The linear pore velocity during the run shown in Fig. 16 was 0.080 cm./sec., while the pore velocity for the run shown in Fig. 17 was 0.329 cm./sec.

The close agreement between Equation (43) and the experimental curves in both Fig. 16 and 17 indicates a number of things. First, the assumption of equilibrium was adequate for both of these runs. This is not surprising when one considers the small diameter of these fibers. Secondly, the fact

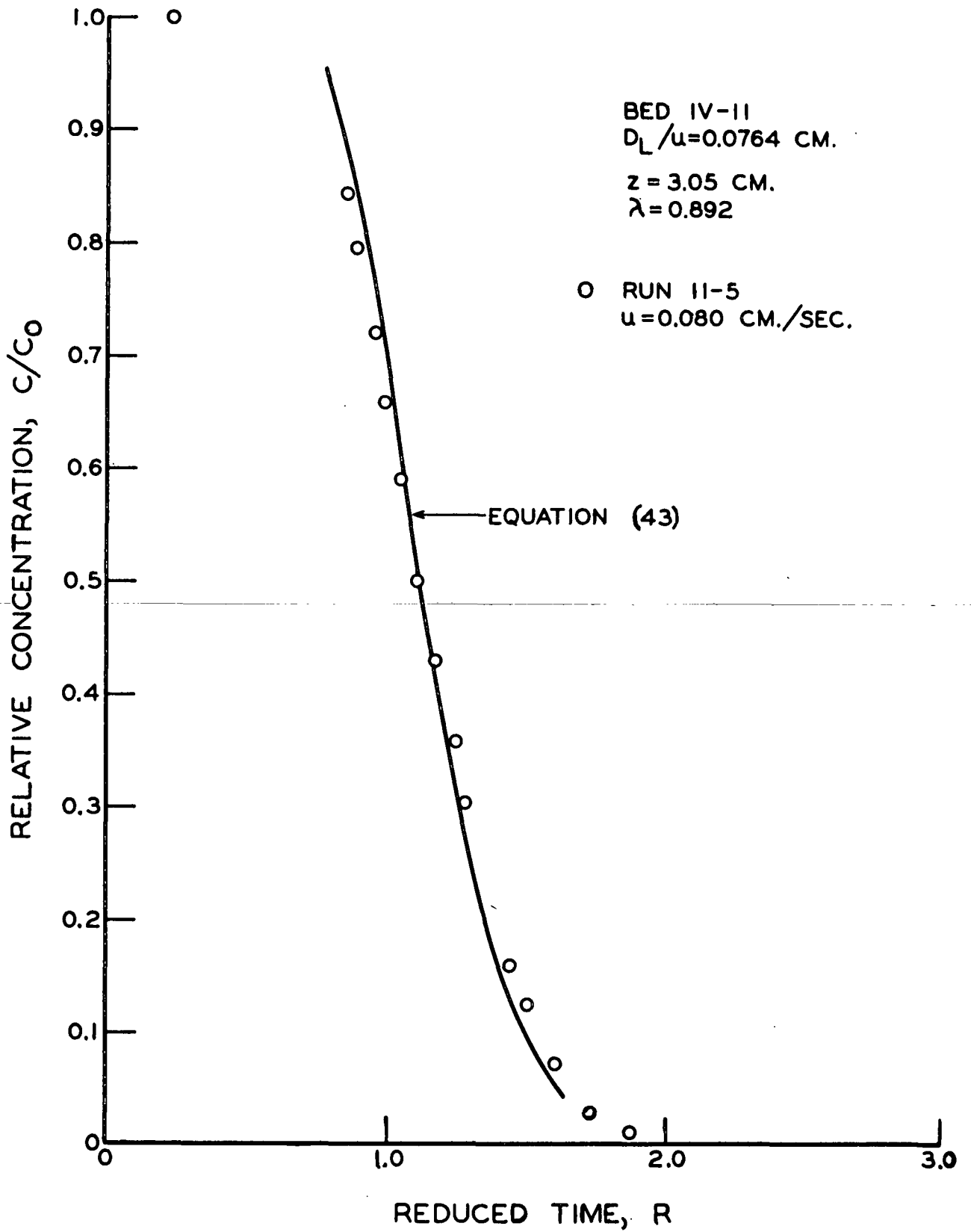


Figure 16. 1-Denier Viscose Fiber--Run 11-5

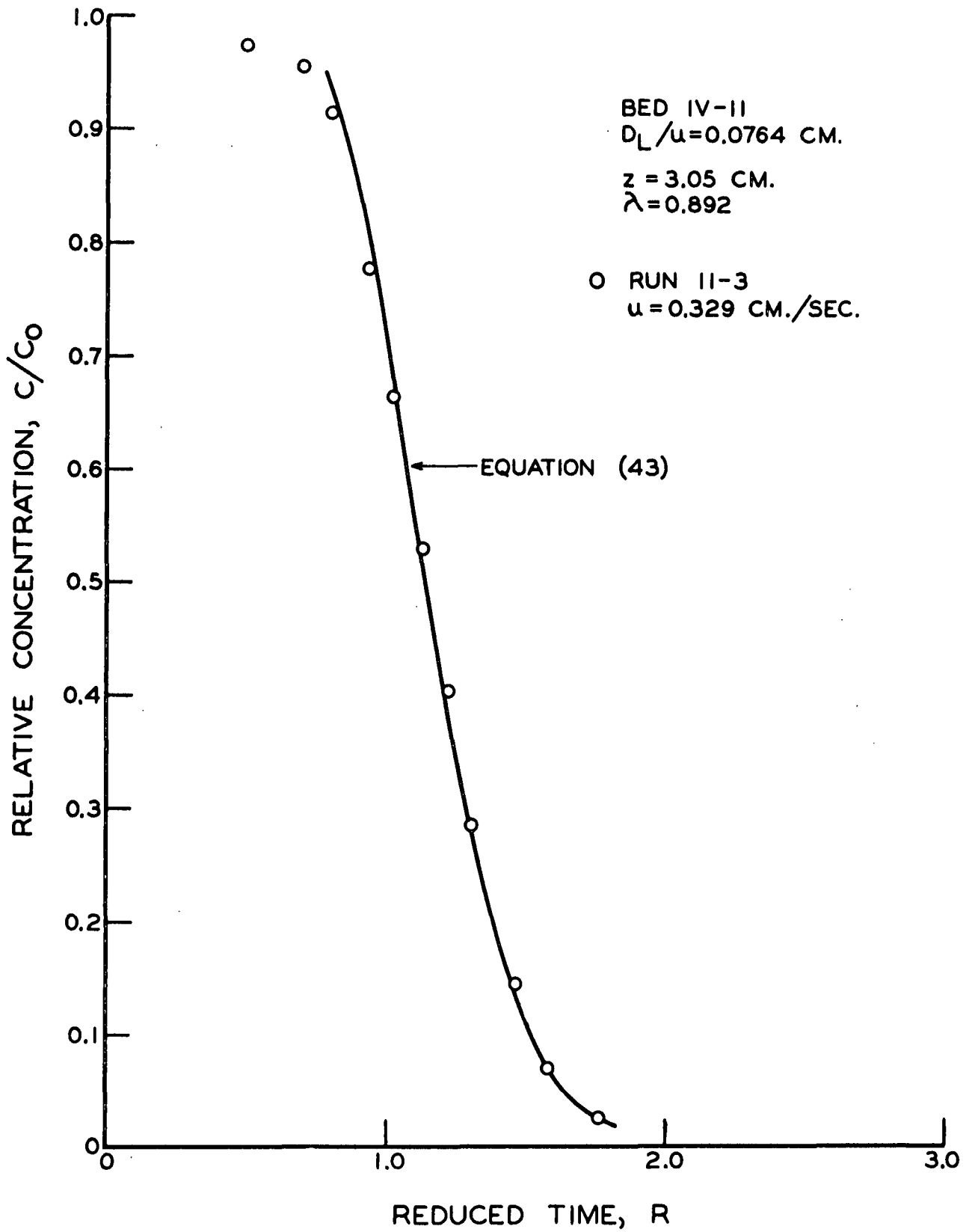


Figure 17. 1-Denier Viscose Fiber--Run 11-3

that the same value of $\frac{D_L}{u}$ was adequate for these runs, with a bed thickness of 3.05 cm., as was adequate for the runs on bed 3D-15, with a bed thickness of 5.32 cm., indicates that end effects were unimportant.

Figure 18 shows one of the runs on bed 1V-14, which was essentially the same as bed 1V-11 except that the bed thickness was 5.41 cm. Again, the assumption of equilibrium was adequate and $\frac{D_L}{u}$ was the same. This further substantiates the fact that end effects were unimportant.

Figures 19-22 show the runs on bed 64V-13. The porosity of this bed was 0.803 and λ was 0.876. The bed was made of 64-denier (120 μ) viscose fibers and was 5.39 cm. thick. The linear pore velocities for the runs shown in Fig. 19-22, respectively, were 0.042, 0.154, 0.636, and 1.316 cm./sec.

In the theoretical discussion it was predicted that, when dynamic similarity is maintained, $\frac{D_L}{u}$ should be proportional to the particle diameter. Ebach (2) and Raimondi, et al. (3) found this to be true, but Liles, et al. (15) did not find a linear relationship (i.e., $\frac{D_L}{u}$ was proportional to $d_p^{0.73}$ for three particle sizes). If $\frac{D_L}{u}$ is proportional to the fiber diameter, then $\frac{D_L}{u}$ for the 64 denier (120 μ) viscose should be eight times the value for the 1 denier (16 μ) viscose fibers. On this assumption, Equation (43) has been plotted in Fig. 19 with $\frac{D_L}{u} = 0.58$. It is quite apparent from Fig. 19 that this assumption is incorrect. Equation (43) was then plotted with $\frac{D_L}{u}$ the same as in the case of the 1-denier fiber (i.e., $\frac{D_L}{u} = 0.077$). This curve adequately represents the data.

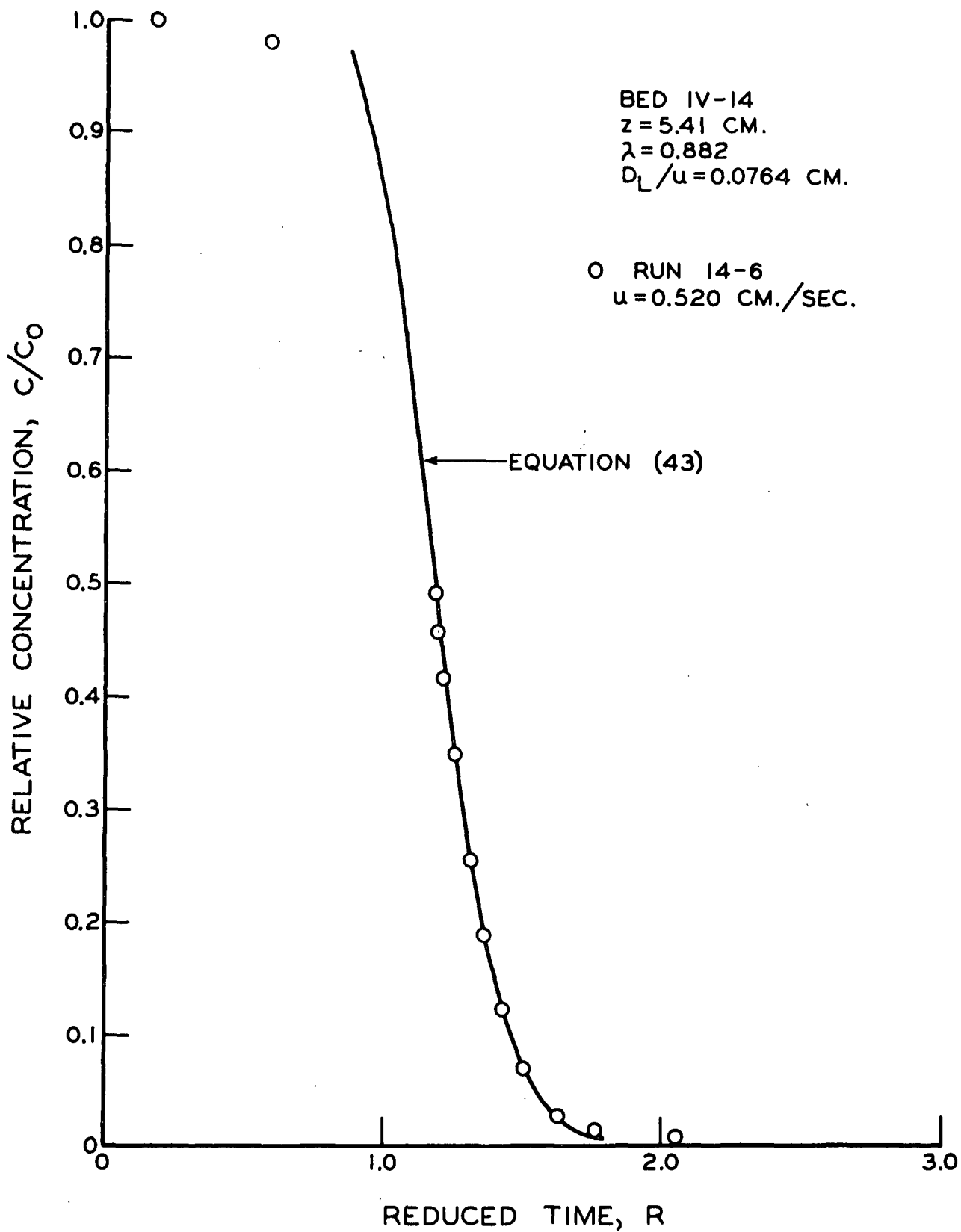


Figure 18. 1-Denier Viscose Fiber--Run 14-6

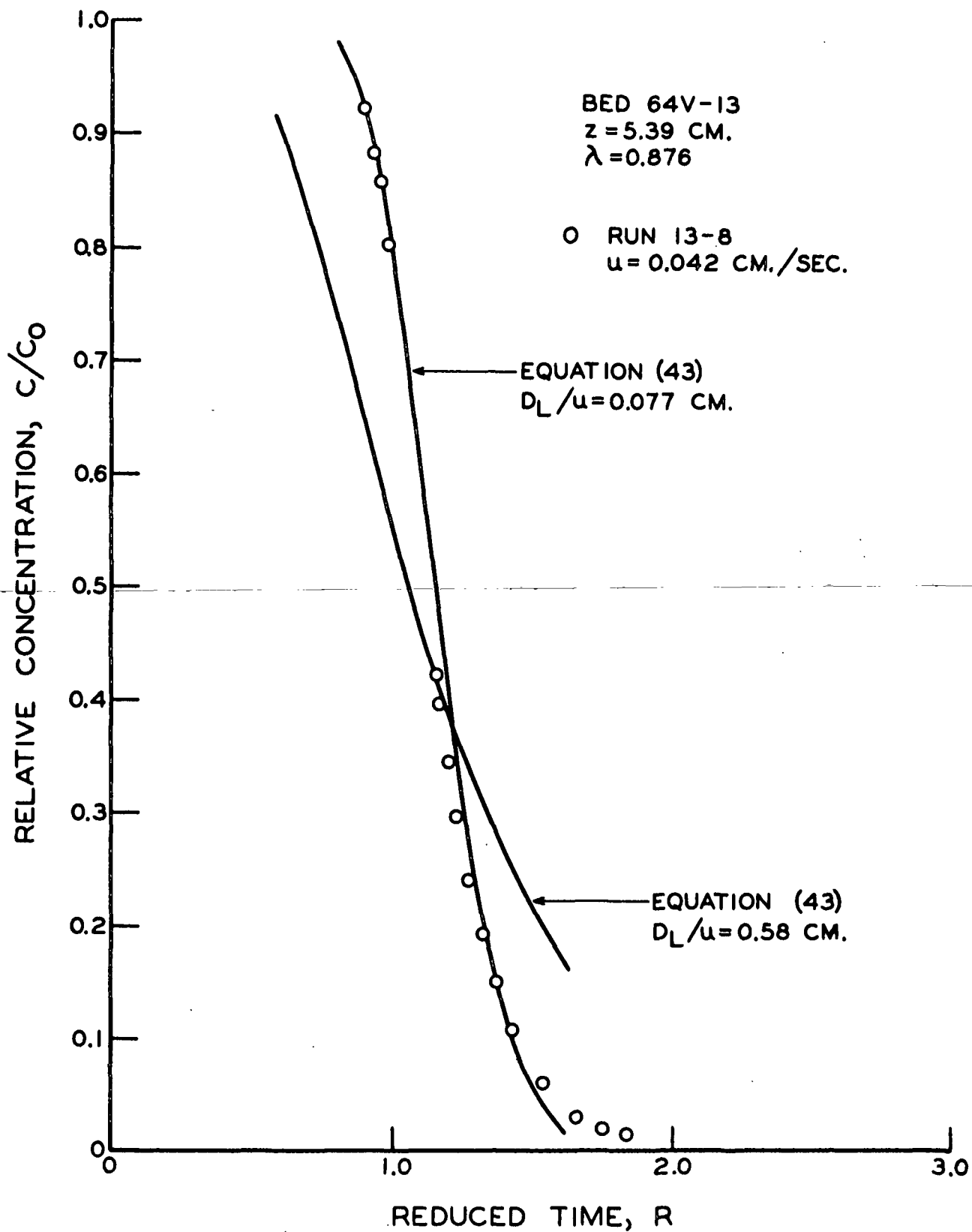


Figure 19. 64-Denier Viscose Fiber--Run 13-8

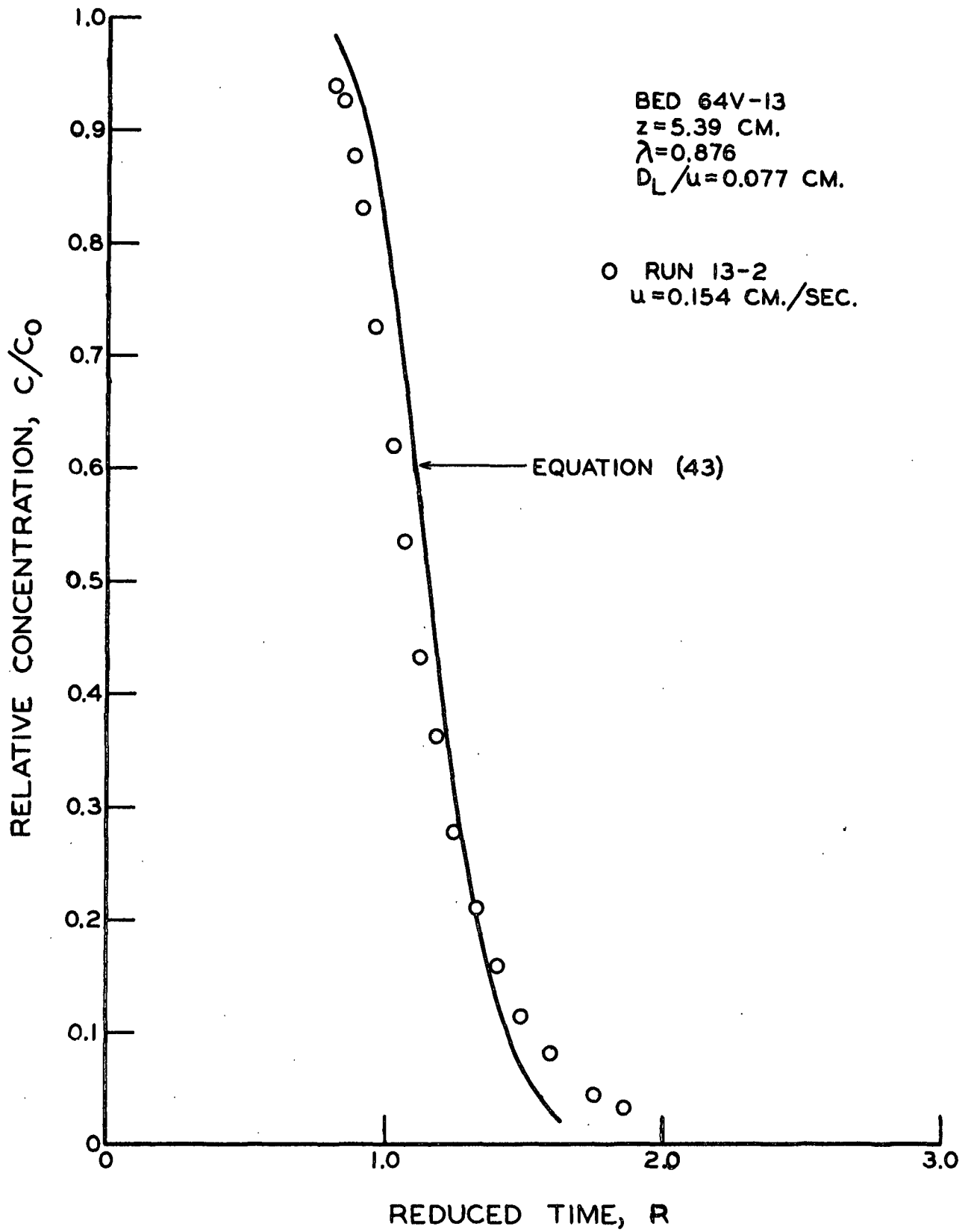


Figure 20. 64-Denier Viscose Fiber--Run 13-2

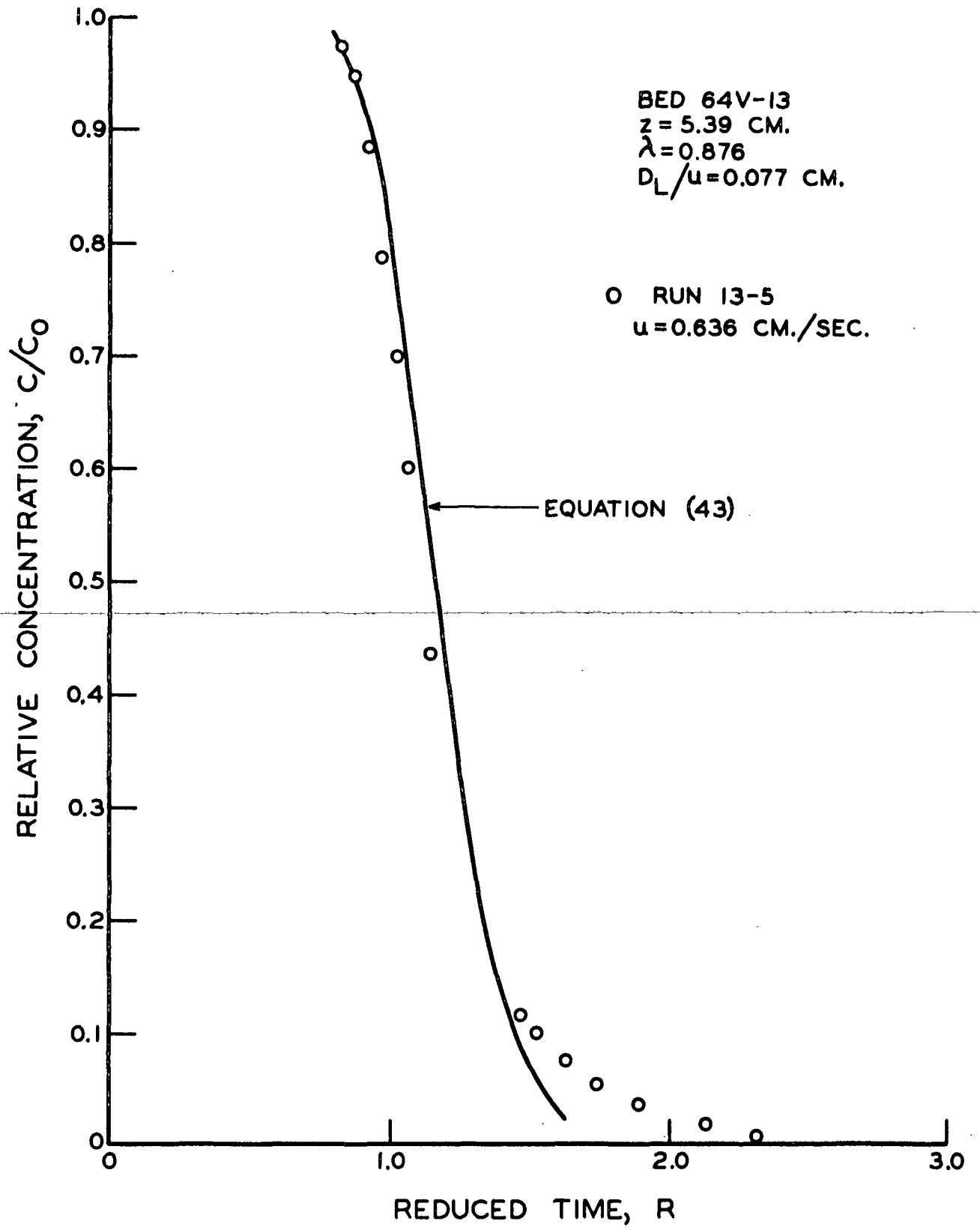


Figure 21. 64-Denier Viscose Fiber--Run 13-5

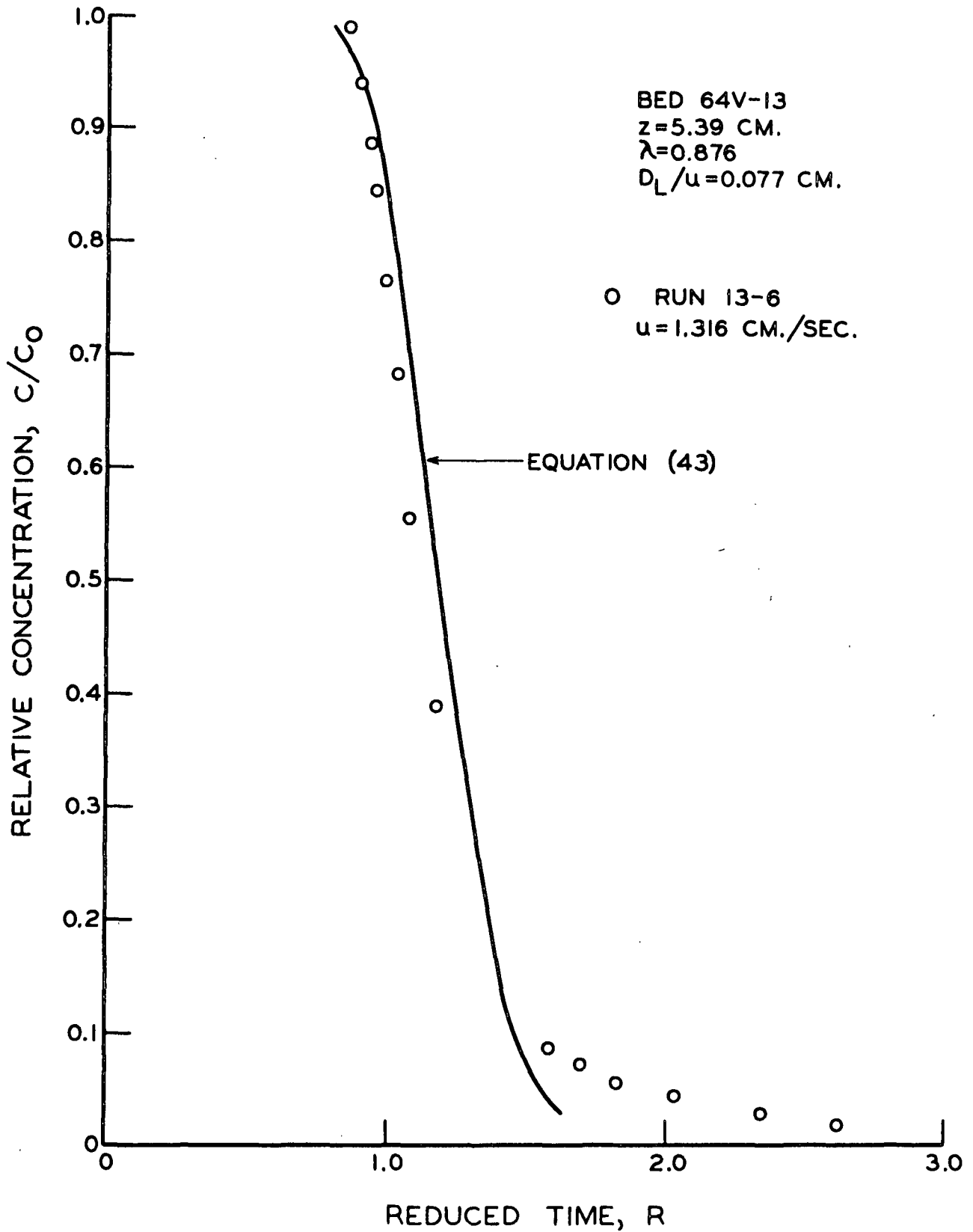


Figure 22. 64-Denier Viscose Fiber--Run 13-6

The fact that $\frac{D_L}{u}$ is apparently independent of the particle size in these beds may seem surprising since a strong relationship between $\frac{D_L}{u}$ and particle size has been demonstrated in the case of granular materials (e.g., 2, 3, 9, 15, 16). Our discussion of the effect of particle size on $\frac{D_L}{u}$, in the Historical Review, was based upon the assumption that the beds were geometrically similar. It was pointed out that not only must the particles be geometrically similar but also the packing of the beds must be geometrically similar. Neither of these assumptions were valid in our case. Although the fibers in the two beds (1V-14 and 64V-13) had a diameter ratio of 1:8, the length ratio was roughly 1:1; thus, the particles were not truly similar. It is also unlikely that the packing of the beds, even at the same porosity, was geometrically similar. In the case of spherical particles, the particles are always geometrically similar, and with reasonable care the packing will also be similar.

Another difference between a fiber system and a granular system is the porosity. In the case of a granular system, the ratio of the solid fraction to the void fraction is roughly 2:3, while in the case of these fiber systems, the ratio was 1:4. It is conceivable that the lower solid fraction in the fiber system makes the system less sensitive to changes in the size of the solid particle.

A third difference between the two systems is the fact that the fiber system has a much wider pore size distribution. This is due to the general shape of the particle (i.e., long cylinders versus spheres) rather than the size of the particle.

Thus, it appears that the packing and particle shape define the dispersion characteristics of a fiber bed and the effect of particle size is small, if not negligible.

Since Equation (43), with $\frac{D_p}{u} = 0.077$ and $\lambda = 0.876$, adequately represents the experimental data in Fig. 19, the assumption of equilibrium between the fiber and the surrounding solution appears adequate. However, as the pore velocity is increased, a perceptible breakdown of this assumption is apparent. For example, in Fig. 22 (the highest pore velocity) a definite "tail" is present in the experimental curve. Thus, with the large diameter fibers (i.e., 120 μ), the assumption of equilibrium is adequate for low flow rates but at higher flow rates the diffusion of material from the fibers is not fast enough to keep up with the rapid change in concentration of the surrounding solution.

In the case of solutes which diffuse more slowly within the fibers than the solute used in this study, the "tail" which occurred in Run 13-6 would occur at lower flow rates. Thus, for solutes which diffuse slowly within the fibers, or for high flow rates, Equation (43) will not be adequate. This is due to the fact that the expression, represented by Equation (51), for the quantity of material sorbed by the fiber is not adequate. In this case the term $\frac{\partial \eta}{\partial t}$ must be obtained from the solution of the differential equation for the diffusion of solute from the fibers under the appropriate boundary conditions.

SUMMARY AND CONCLUSIONS

An investigation of the movement of a soluble material during the washing of a number of beds of packed solids was carried out. The solids studied included glass beads, dacron fibers, and viscose fibers. The porosity of the fiber beds was maintained uniform during the washing runs by an external compacting force. The above beds were saturated with aqueous diacetyl solutions and then washed with water. A record of the input and exit stream concentrations was obtained during each run by photographing the oscilloscope response of two photocells sensing the intensity of light beams passed just above and below the bed. The intensities of the light beams were related to the concentrations of the respective streams by Beer's law.

The commonly used one-dimensional, diffusionlike differential equation was used to describe the movement of solute in these beds. In order to avoid the experimental difficulties encountered in obtaining a satisfactory step function (which is particularly difficult for thin beds, such as must be used with fibrous media), the boundary conditions were modified to include the actual input concentration history.

The input concentration history was described by an empirical equation of the form,

$$C/C_0 = (k_0 + k_1 R + k_2 R^2 + k_3 R^3 + k_4 R^4) e^{-\gamma R}$$

where

$$\frac{C}{C_0} = \text{relative concentration,}$$

$$R = \frac{ut}{z},$$

$$\underline{S} = \frac{D_L}{uz},$$

\underline{u} = pore velocity, cm./sec.,

\underline{t} = time, sec.,

\underline{z} = longitudinal distance, cm.,

\underline{D}_L = longitudinal dispersion coefficient, sq.cm./sec., and

$\underline{k}_0, \underline{k}_1', \underline{k}_2', \underline{k}_3', \underline{k}_4'$, and γ' are arbitrary constants which are adjusted so that the above equation adequately describes the relative concentration at the top of the bed as a function of time.

The equation to describe the exit concentration history was then derived to be

$$C/C_0 = 1 - \frac{1}{2} \left[\operatorname{erfc}\left(\frac{1 - R\lambda}{2\sqrt{R\lambda S}}\right) + e^{1/S} \operatorname{erfc}\left(\frac{1 + R\lambda}{2\sqrt{R\lambda S}}\right) \right] \\ + \frac{1}{\sqrt{\pi R\lambda S}} \int_1^{\infty} [k_0 + k_1'\omega_1 + k_2'\omega_1^2 + k_3'\omega_1^3 + \\ k_4'\omega_1^4] \exp\left[-\frac{1}{2S} - \gamma'\omega_1 - \frac{R\lambda}{4\omega^2 S} - \frac{\omega^2}{4R\lambda S}\right] d\omega$$

where

$$\omega_1 = \left(1 - \frac{1}{\omega^2}\right)R,$$

ω = a variable of integration, and

λ = a constant defined by the assumed relationship between the solute and the solid particle.

The above equation was found to satisfy the data for all the runs on the glass bead and dacron fiber beds and some of the runs with the viscose fiber beds. The only data that were not accurately represented by the above equation were those for a bed of large viscose fibers washed at a

high flow rate. In this case the effects of nonequilibrium intrafiber diffusion were evident, λ was not a constant, and thus the above equation did not apply.

The mixing parameter, $\underline{D}_L/\underline{u}$, was found to be a constant for all runs on any single bed regardless of the particles used to pack the bed. The value of $\underline{D}_L/\underline{u}$ (0.233 cm.) for the 3-mm. glass bead bed is in general agreement with that determined in other investigations.

The same basic mechanism of fluid element dispersion applies to beds of fibrous media as that which applies to beds of granular media; however, the physical differences in the two types of systems cause the mixing parameter, $\underline{D}_L/\underline{u}$, to behave differently in the two systems.

~~In beds of granular media, the porosity is generally fixed at~~
about 0.4. In beds of fibrous media, the porosity may vary over a considerable range; thus, an additional variable is introduced in the system. Values of $\underline{D}_L/\underline{u}$ were determined for three different porosities (0.815, 0.855, 0.916) using the dacron fibers. A considerable variation in $\underline{D}_L/\underline{u}$ was observed; however, the data were too limited to define the relationship between $\underline{D}_L/\underline{u}$ and porosity.

The mixing parameter, $\underline{D}_L/\underline{u}$, is generally believed to be directly proportional to the particle diameter for beds of granular media. In this study, the fiber diameter was changed by a factor of 8 without a noticeable change in $\underline{D}_L/\underline{u}$. In order for $\underline{D}_L/\underline{u}$ to be directly proportional to the particle diameter, it is necessary for geometric similarity to exist. In the case of the fiber beds, geometric similarity was not

maintained. The longitudinal dispersion in a bed of packed solids is a strong function of the relative width of the pore size distribution in the bed. In the case of fiber beds, the relative width of the pore size distribution appears to be governed primarily by the shape and packing of the particles rather than the size of the particles.

The difference in pore size distribution between a bed of fibrous media and a bed of granular media of the same particle diameter is believed to account for the fact that $\frac{D_L}{u}$ for the dacron fiber beds was about 60 times as great (ratios of 100, 60, and 30 were obtained for the three porosities investigated) as it would be for a bed of granular media of the same diameter.

The theoretical equation for the washing of the viscose fiber beds was written assuming equilibrium between the fibers and the surrounding solution. For this system (i.e., aqueous diacetyl and all-skin viscose fibers), the assumption of equilibrium was found to be satisfactory over the range of flow rates investigated (linear pore velocities of 0.043 to 0.520 cm./sec.) for the 1-denier fibers (16 μ diameter). For the 64-denier (120 μ) fibers, the assumption of equilibrium was satisfactory at low flow rates (e.g., 0.042 cm./sec.); however, at higher flow rates (e.g., 1.316 cm./sec.), this assumption was not satisfactory. In this case, the experimental curve exhibited an appreciable tail due to the relatively slow intrafiber diffusion of the solute.

SIGNIFICANCE OF RESULTS AND SUGGESTIONS FOR FUTURE RESEARCH

In recent years, a number of studies have been made on the movement of a solute in a bed of packed solids while a fluid is flowing through the bed. Most of these studies have been made on thick beds of granular media; however, in the pulp and paper industries we are interested in beds of fibrous media.

In the study of granular media, the step function boundary condition has often been used. In the case of fiber beds, it is extremely difficult to satisfy the step function boundary condition (since the beds are relatively thin). One of the contributions of this investigation has been to develop the equations and techniques necessary to describe and measure the washing of thin beds of packed solids for which the step function boundary condition is not satisfied.

The technique was used to perform a number of exploratory experiments on fiber beds. It was found that the same basic mechanism of fluid element dispersion applies to beds of fibrous media as that which applies to beds of granular media. The effect of the porosity of the bed, particle diameter, and intrafiber diffusion upon the mixing parameter, $\frac{D_L}{u}$, were briefly studied. Thus, the significance of this study is twofold. First, it has shown that the same basic equations may be used for fibrous media as for granular media, providing that the proper boundary conditions are used. Secondly, the studies of fibrous media provide a working basis for further and more intensive studies of the system.

Future studies should include (1) a clarification of the effect of porosity, fiber diameter, and fiber length on the mixing parameter, $\frac{D_f}{u}$, for beds of nonporous fibers, and (2) an investigation of beds of well-defined porous fibers in which intrafiber diffusion plays an important part. The experiments performed in this study on porous viscose fibers, indicate that the effect of particle diameter is much less than the predicted effect. This should be checked on beds of nonporous fibers. The effect of fiber length on $\frac{D_f}{u}$ should also be investigated. Fiber length may affect the system in two ways; it may act as a scale factor for the system, much as particle diameter does in a granular system, or it may have an effect upon the formation of the fiber bed. If the formation, or packing, of the bed is changed, then we would expect $\frac{D_f}{u}$ to be changed. We have previously discussed the fact that the mixing parameter, $\frac{D_f}{u}$, should depend upon the porosity of the bed. Some experiments were performed to investigate this relationship; however, much more work is necessary to define the relationship between $\frac{D_f}{u}$ and porosity.

A thorough understanding of the washing of beds of well-defined porous fibers, in which intrafiber diffusion plays an important part, would certainly bring us to a closer understanding of pulp washing. In a study of this type one should consider the general problem involving longitudinal dispersion (due to the flow pattern between the fibers) in conjunction with the unsteady state diffusion of a solute out of the fibers. If the diffusion within the fibers is either very rapid or very slow, the mathematical description of the problem is relatively simple. The former case was handled in this study (equilibrium between the fiber and the surrounding solution), while the latter case reduces to a study

of the diffusion of solute out of a fiber surrounded by an infinite solution of zero concentration. The mathematical description of the intermediate case is much more complex; however, Pellett (28) has obtained solutions for two cases. The first of these is based on the assumption that the surface of each fiber is in equilibrium with the bulk solution surrounding the fiber. The second case is based on the assumption that there is a fluid film surrounding each fiber which offers a finite resistance to the passage of solute from the surface of the fiber to the bulk solution. Certainly the experimental verification of these equations, which is presently under way, will bring the understanding of pulp washing much closer.

NOMENCLATURE

\underline{A}	= cross-sectional area of bed, sq. cm.
\underline{C}	= concentration of fluid, g. solute/cc. solution
\underline{C}_0	= concentration initially in bed at $\underline{t} = 0$, g. solute/cc. solution
\underline{D}_L	= longitudinal dispersion coefficient due to flow pattern, sq. cm./sec.
$\underline{D}_L/\underline{u}$	= mixing parameter, cm.
$\underline{D}_{mol.}$	= longitudinal molecular diffusion coefficient, sq. cm./sec.
\underline{D}_T	= total longitudinal dispersion coefficient, sq. cm./sec.
\underline{d}	= a diameter, cm.
\underline{d}_p	= particle diameter, cm.
\underline{h}	= $\Delta + \delta$ = a longitudinal distance, cm.
$\Delta \underline{h}$	= change in height of liquid in flow-sensing tube during a run, cm.
$\underline{K}, \underline{K}_0$	= constants in Equation (25)
$\underline{K}_\alpha, \underline{K}_\beta$	= parameters in the general solution of Equation (34)
\underline{k}	= Beer's law constant
$\underline{k}_0, \underline{k}_1, \underline{k}_2,$ $\underline{k}_3, \underline{k}_4$	= constants in Equation (32)
$\underline{k}'_1, \underline{k}'_2,$ $\underline{k}'_3, \underline{k}'_4$	= constants in Equation (44)
\underline{N}	= a number
\underline{n}	= a number
\underline{Pe}	= Peclet number = $\frac{\underline{u}\underline{d}}{\underline{D}_L}$
P.V.	= volume of flow/void volume of bed
\underline{p}	= Laplace operator

- \underline{Q} = residual glucose = glucose in fiber bed after washing, g.
- \underline{Q}_0 = glucose in fiber before washing = $\epsilon_f \underline{C}_0$, g.
- \underline{R} = $\underline{ut}/\underline{z}$
- \underline{S} = $\underline{D_L}/\underline{uz}$
- \underline{t} = time, sec.
- \underline{u} = average linear pore velocity, sq. cm./sec.
- \underline{V}_G = volume of solution at concentration, \underline{C}_0 , originally in bed as calculated from bed geometry and particle porosity, cc.
- \underline{V}_{mb} = volume of solution at concentration, \underline{C}_0 , removed from bed as calculated from plot of $\underline{C}/\underline{C}_0$ vs. $\underline{P.V.}$, cc.
- $(dV/d\theta)$ = volumetric flow rate, cc./sec.
- \underline{W}_f = o.d. weight of fiber sample, g.
- \underline{Y} = a vertical position on the photograph of oscilloscope trace
- \underline{Y}' = Δy units between point in question and \underline{Y}_0
-
- \underline{Y}_0 = position of calibration mark with light blocked off
- \underline{Y}_S = position of calibration mark with light passing through solution of concentration \underline{C}_0
- \underline{Y}'_S = $\underline{Y}_S - \underline{Y}_0$
- \underline{Y}_W = position of calibration mark with light passing through water
- \underline{Y}'_W = $\underline{Y}_W - \underline{Y}_0$
- \underline{z} = longitudinal distance variable, cm.
- α = $(\underline{u}/2 \underline{D_L}) - \sqrt{(\underline{u}/2 \underline{D_L})^2 + (\underline{p}/\lambda \underline{D_L})}$
- β = $(\underline{u}/2 \underline{D_L}) + \sqrt{(\underline{u}/2 \underline{D_L})^2 + (\underline{p}/\lambda \underline{D_L})}$
- γ = constant in Equation (32)
- γ' = constant in Equation (44)
- Δ = a longitudinal distance
- δ = a longitudinal distance

- ϵ = bed porosity
- ϵ_f = porosity of fiber
- η = quantity of solute sorbed by the solid per unit volume of solid, g. solute/cc. solid
- λ = $1/(1 - \underline{K} + \underline{K}/\epsilon)$
- ν = number of solute molecules per unit volume of fluid, molecules/cc.
- τ = an arbitrary time interval, or a variable of integration, sec.
- $\Phi(\Delta)$ = a function of Δ
- $\varnothing(\delta)$ = a function of δ
- ω = a variable of integration $=\sqrt{t/\tau}$
- ω_1 = $[1 - (1/\omega^2)]R$
- $(\Delta x \text{ units})$ = horizontal distance from $\underline{t} = 0$ to point in question as measured with the microscope
- $(\text{cm.}/\Delta \text{ unit})$ = calibration of microscope measurement, cm.
- $(\text{sec.}/\text{cm.})$ = sweep speed of oscilloscope during washing run, sec./cm.

LITERATURE CITED

1. Einstein, A. Investigations on the theory of the Brownian movement. p. 12-15. New York, E. P. Dutton, 1926.
2. Ebach, E. A. The mixing of liquids flowing through beds of packed solids. Doctoral Dissertation. Ann Arbor, Mich., University of Michigan, 1957. [Or Ebach, E. A., and White, R. R., A.I.Ch.E. Journal 4:161(1958).]
3. Raimondi, P., Gardner, G. H. F., and Petrick, C. B. Effect of pore structure and molecular diffusion on the mixing of miscible liquids flowing in porous media. Preprint 43, Fifty-second Annual Meeting, A.I.Ch.E., Dec. 6-9, 1959.
4. Carberry, J. J., and Bretton, R. H., A.I.Ch.E. Journal 4:367(1958).
5. Kramers, H., and Alberda, G., Chem. Eng. Sci. 2:173(1953).
6. Strang, D. A., and Geankoplis, C. J., Ind. Eng. Chem. 50:1305(1958).
7. Levenspiel, O., and Smith, W. K., Chem. Eng. Sci. 6:227(1956).
8. Orlob, G. T., and Radhakrishna, G. N., Trans. Am. Geo. Union 39:648 (1959).

9. de Josselin de Jong, G., Trans. Am. Geo. Union 39:67(1958).
10. Aris, R., and Amundson, N. R., A.I.Ch.E. Journal 3:280(1957).
11. Schwartz, C. E., and Smith, J. M., Ind. Eng. Chem. 45:1209(1953).
12. Wyllie, M. R. J. The fundamentals of electric log interpretation. 2d ed. New York, Academic Press, 1957.
13. Peterson, E. E., A.I.Ch.E. Journal 3:443(1957).
14. Klinkenberg, A., and Sjenitzer, F., Chem. Eng. Sci. 5:258(1956).
15. Liles, A. W., and Geankoplis, C. J., A.I.Ch.E. Journal 6:591(1960).
16. Saffman, P. G., J. Fluid Mech. 6:321(1959).
17. Lapidus, L., and Amundson, N. R., J. Phys. Chem. 56:984(1952).
18. Rafai, M. N. E. Doctoral Dissertation. Berkeley, Cal., University of California, 1956.
19. Dankwerts, P. V., Chem. Eng. Sci. 2:1(1953).

20. Cairns, E. J., and Prausnitz, J. M., A.I.Ch.E. Journal 6:400(1960).
21. Ingmanson, W. L., Andrews, B. D., and Johnson, R. C., Tappi 42:840 (1959).
22. Parker, J. D. An investigation of the permeability to water of partially saturated beds of glass fibers. Doctoral Dissertation. Appleton, Wis., The Institute of Paper Chemistry, 1958.
23. McMaster, D. G. Unpublished work. Hot-surface drying characteristics of fibrillated acrilan fiber beds. Appleton, Wis., The Institute of Paper Chemistry, 1960.
24. Boyd, G. E., Adamson, A. W., and Myers, L. S., Jr., J. Am. Chem. Soc. 69:2836(1947).
25. Nelson, N., J. Biol. Chem. 153:375(1944).
26. Somogyi, M., J. Biol. Chem. 195:13(1952).
27. Schlichting, H. Boundary layer theory. p. 503, New York, McGraw-Hill, 1960.
28. Pellett, G. L. Unpublished work. Appleton, Wis., The Institute of Paper Chemistry, 1961.

APPENDIX I

TABLE OF LAPLACE TRANSFORMS

<u>Laplace Transform</u>	<u>Inverse Transform</u>
$k f(p)$	$k F(t)$
$f(p - a)$	$e^{at} F(t)$
$\frac{1}{p}$	1
$e^{-k\sqrt{p}} \quad (k > 0)$	$\frac{k}{2\sqrt{\pi t^3}} e^{-(k^2/4t)}$
$e^{-k\sqrt{p-a}}$	$\frac{k}{2\sqrt{\pi t^3}} e^{at - (k^2/4t)}$
$\frac{1}{(p-a)^n} \quad (n=1,2,\dots)$	$\frac{1}{(n-1)!} t^{n-1} e^{at}$
$f_1(p)f_2(p)$	$\int_0^t F_1(t-\tau)F_2(\tau) d\tau$
$\frac{e^{-k\sqrt{p-b}}}{(p-a)^n}$	$\int_0^t \frac{(t-\tau)^{n-1} e^{a(t-\tau)}}{(n-1)!} \frac{ke^{b\tau - (k^2/4\tau)}}{2\sqrt{\pi\tau^3}} d\tau$

APPENDIX II

SAMPLE CALCULATIONS

RUN NO. Bu-9-8

The raw data consisted of the photograph of the oscilloscope trace, the flow rate (1.52 cc./sec.), and the sweep speed of the oscilloscope trace (5 sec./cm.).

In addition to the above data, the bed geometry was known. The bed geometry for pad no. 3G-9 is shown in Fig. 23.

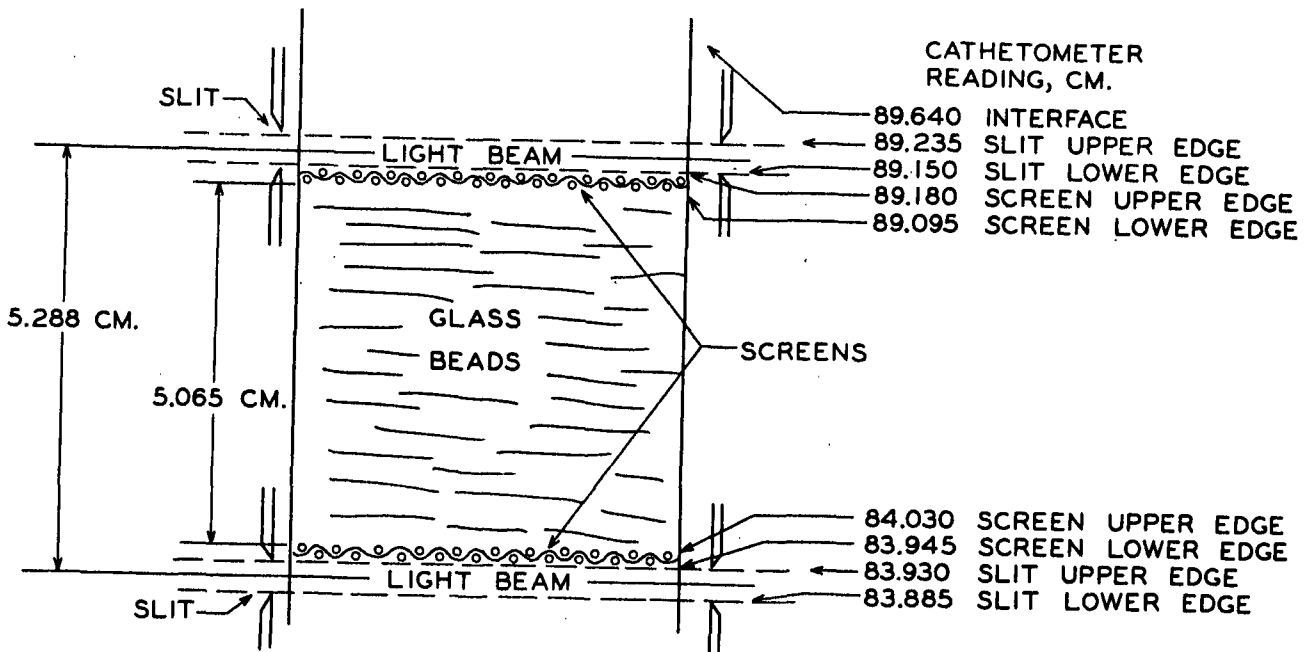


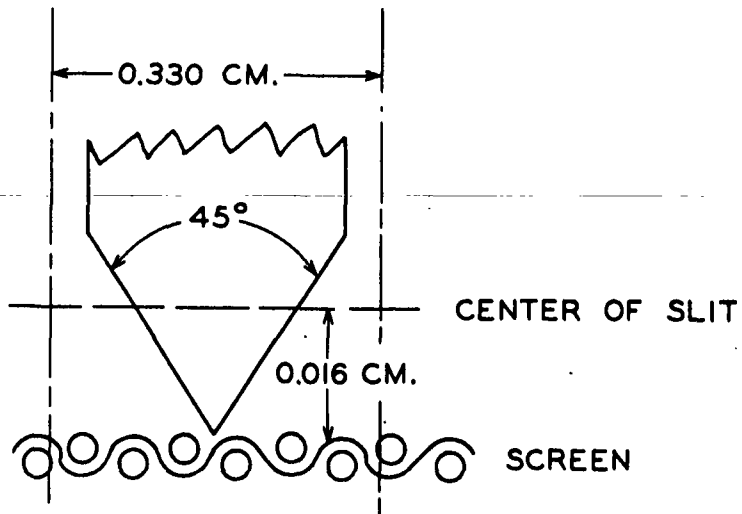
Figure 23. Bed Geometry

The void volume of the bed was broken down into five parts. These were:

- (1) the valve,
- (2) the upper screen,
- (3) the void space between the beads,
- (4) the lower screen, and
- (5) the piston.

These five parts were calculated as follows:

1. The Valve



$$\text{solid portion} = [0.016 \tan (22.5^\circ)][0.016] = 0.000106$$

$$\text{total} = (0.330)(0.016) = 0.00528$$

$$\text{void volume} = \frac{0.00528 - 0.00011}{0.00528} (0.016)(43.54) = 0.63 \text{ cc.}$$

2. Upper Screen

$$\text{void volume} = (0.7)(43.54)(0.085) = 2.6 \text{ cc.}$$

3. Void Space Between Beads

$$\text{av. bead diameter} = 0.302 \text{ cm.}$$

wt. of 50 beads = 1.908 g.

$$\text{sp. vol. of beads} = \frac{4}{3} \pi \left(\frac{0.302}{2} \right)^3 \frac{50}{1.908} = 0.378 \text{ cc./g.}$$

$$\text{void volume} = (5.065)(43.54) - (0.378)(328.2) = 96.7 \text{ cc.}$$

4. Lower Screen

$$\text{void volume} = (0.7)(43.54)(0.085) = 2.6 \text{ cc.}$$

5. Piston

(same as valve except center line of slit was 0.030 cm. instead of 0.016 cm. from screen)

$$\text{solid} = [0.030 \tan(22.5)][0.030] = 0.00037$$

$$\text{total} = [0.030][0.330] = 0.0099$$

$$\text{void volume} = \frac{0.0099 - 0.00037}{0.0099} (0.030)(43.54) = 1.26$$

$$\text{Void volume of bed} = (1) + (2) + (3) + (4) + (5) = 104.2.$$

The calibration of the microscope gave 4.03 Δ units/cm. Equation (46) now becomes:

$$\text{P.V.} = \frac{\Delta x \text{ units} (1/4.03)(5)(1.52)}{104.2} = 0.0181 \Delta x \text{ units} \quad (46).$$

Tables VIII and IX were obtained from the photograph and Equations (45) and (46). The input curve is shown in Fig. 24. The exit curve is shown in Fig. 25. The areas under the curves in Fig. 24 and 25 are 0.0553 and 1.018, respectively. Multiplying each of these areas by the void volume gives 5.8 and 106.0 cc., respectively. Thus, the quantity of diacetyl (expressed as cc. of solution of concentration C_0) removed from the bed is 106.0 - 5.8 = 100.2 cc. This corresponds to $(100.2/104.2) \times 100 = 96.2\%$ of that calculated from the void volume of the bed.

TABLE VIII
INPUT CURVE

<u>x</u>	<u>Δx</u>	P. V.	<u>Y</u>	<u>C/C₀</u>
60.5	0.0	0.0000	10.7	0.847
60.3	0.2	0.0036	11.0	0.822
59.7	0.8	0.0145	11.5	0.790
57.5	3.0	0.0542	15.6	0.566
57.1	3.4	0.0615	18.4	0.449
56.7	3.8	0.0687	21.0	0.357
56.3	4.2	0.0760	24.3	0.255
55.9	4.6	0.0832	26.8	0.189
55.0	5.5	0.0995	30.3	0.105
54.5	6.0	0.109	32.0	0.068
53.8	6.7	0.121	33.4	0.039
52.8	7.7	0.139	34.3	0.022
48.8	11.7	0.212	35.0	0.008
39.9	20.6	0.372	35.4	0.000

$$\frac{Y}{I_W} = 35.4$$

$$\frac{Y}{I_S} = 8.8$$

$$\frac{Y}{I_O} = 1.8$$

TABLE IX
EXIT CURVE

<u>x</u>	<u>Δx</u>	P. V.	<u>Y</u>	<u>C/C₀</u>
60.4	0.1	0.00	13.9	1.000
42.5	18.0	0.36	14.0	0.986
30.8	29.7	0.54	14.1	0.973
24.8	35.8	0.65	14.4	0.938
20.8	39.7	0.72	14.8	0.884
60.5	58.0	1.05	21.1	0.376
59.2	59.3	1.07	21.8	0.336
57.9	60.6	1.10	22.4	0.305
55.4	63.1	1.14	23.3	0.260
52.5	66.0	1.19	24.4	0.210
49.5	69.0	1.25	25.3	0.171
45.8	72.7	1.32	26.3	0.130
42.0	76.5	1.38	27.0	0.103
36.0	82.5	1.49	27.9	0.069
27.2	91.3	1.65	28.5	0.048
20.9	97.6	1.77	28.9	0.034
60.5	110.3	2.00	29.3	0.020
54.0	116.8	2.11	29.5	0.013

$$\frac{Y}{-W} = 29.9$$

$$\frac{Y}{-S} = 13.9$$

$$\frac{Y}{-O} = 9.1$$

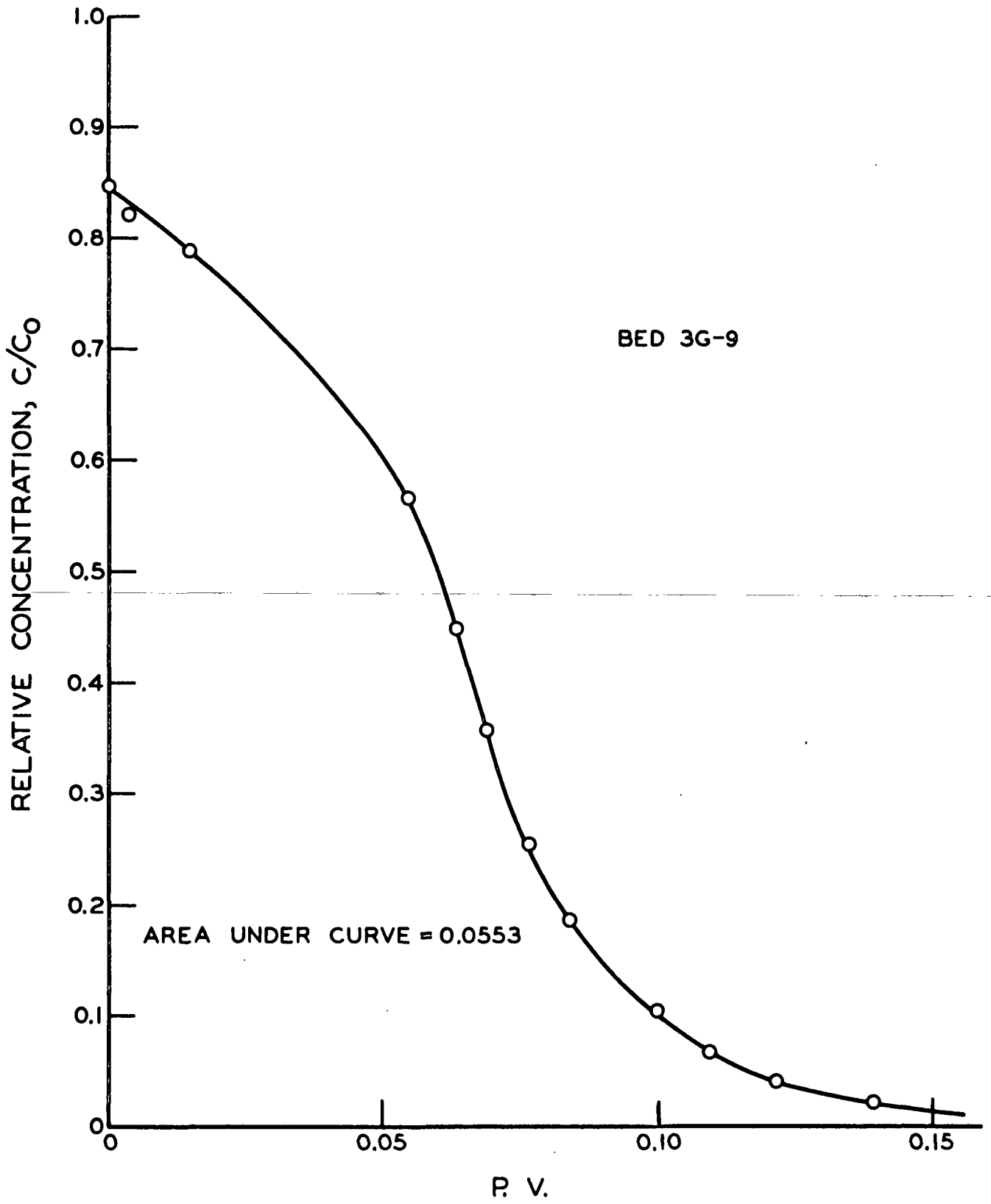


Figure 24. Input Curve--Run 9-8

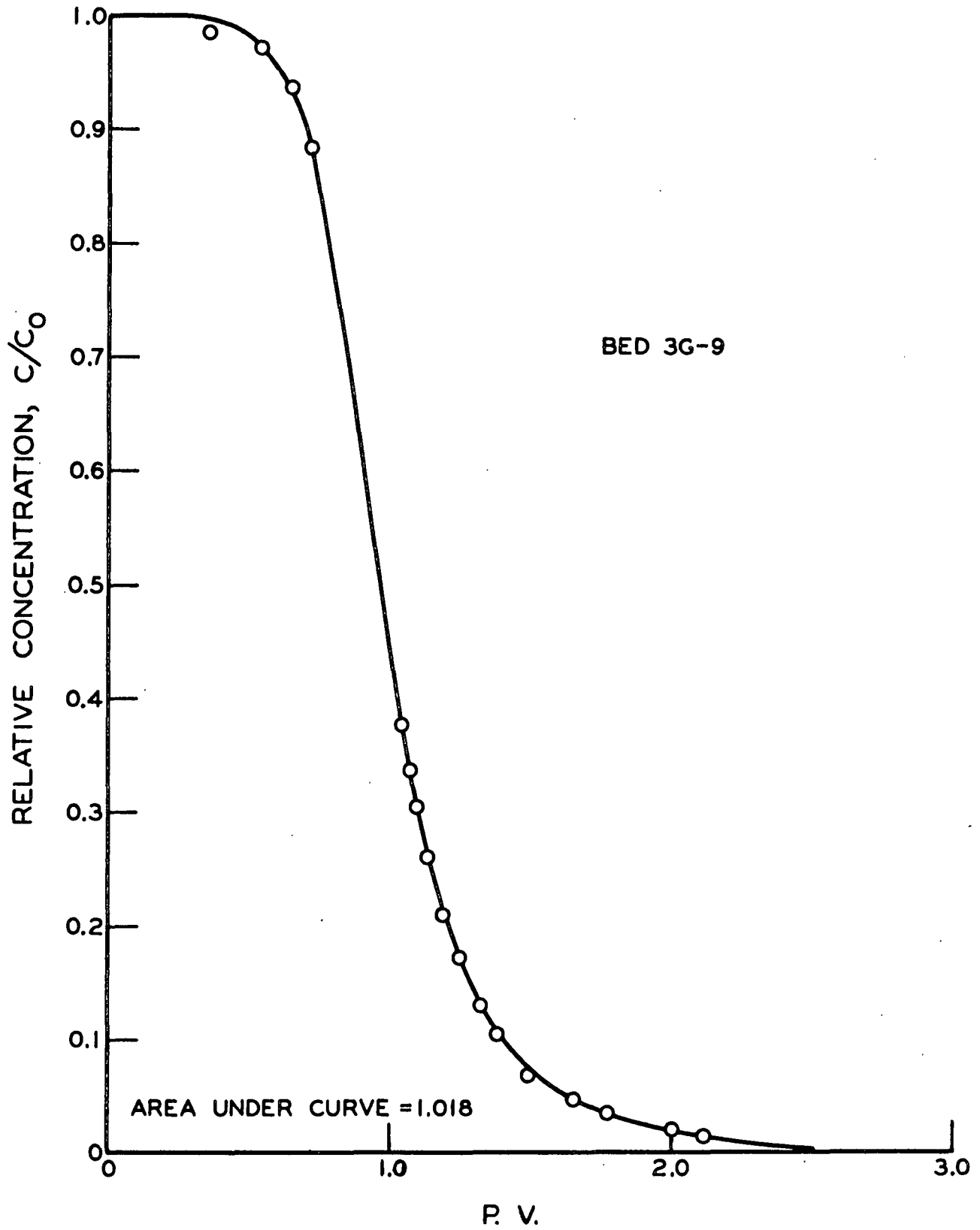


Figure 25. Exit Curve--Run 9-8

In order to calculate the constants in Equation (44), Fig. 24 must be converted to a plot of $\underline{C}/\underline{C}_0$ versus \underline{R} . Equation (49) gives:

$$u = \frac{5.288}{100.2} (1.52) = 0.080 \text{ cm./sec.}$$

Thus, from Equation (50),

$$R = \frac{0.080}{5.288} \left(\frac{1}{4.03} \right) (5) (\Delta x \text{ units}) = 0.0188 \Delta x \text{ units.}$$

Figures 24 and 25 are shown replotted as $\underline{C}/\underline{C}_0$ versus \underline{R} in Fig. 26 and 27. Equation (44) with $\underline{k}_0 = 0.84$, $\underline{k}_1' = 10$, $\underline{k}_2' = 2300$, $\underline{k}_3' = -24,000$, $\underline{k}_4' = 65,000$, and $\gamma' = 40$ is shown in Fig. 26. Since this is a reasonable fit of the input concentration data, these constants were used in Equation (43). With no adsorption, $\eta = 0$ and $\lambda = 1$; therefore, the only unknown in Equation (43) was \underline{S} . In order to determine \underline{S} , Equation (43) was plotted for several values of \underline{S} and the curves were compared with the exit concentration data. This is shown in Fig. 27. A value of $\underline{S} = 0.040$ gave a reasonable fit between Equation (43) and the data; therefore

$$\underline{D}_L = \underline{uzS} = (0.080)(5.288)(0.040) = 0.0169 \text{ sq. cm./sec.}$$

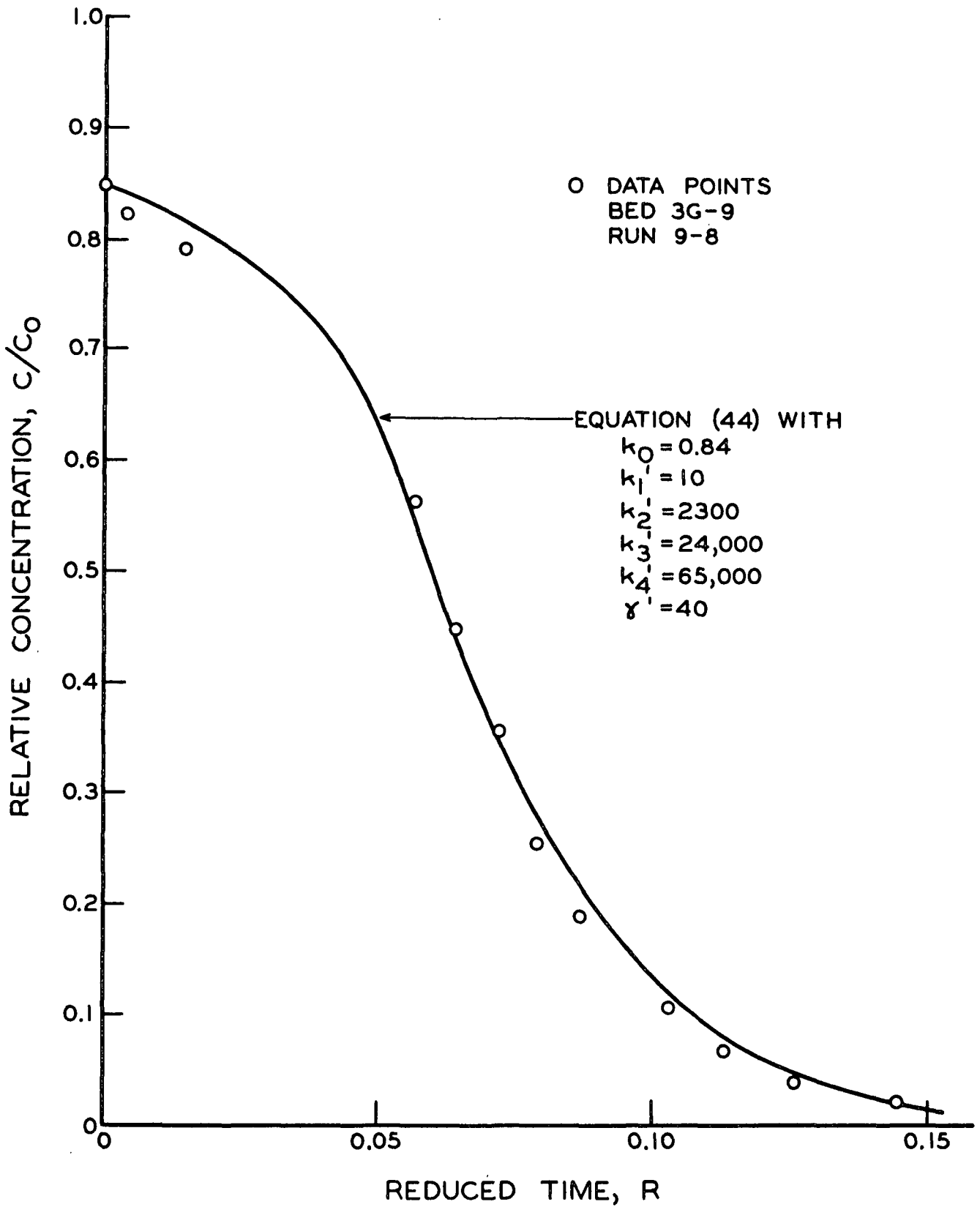


Figure 26. Input Curve--Run 9-8

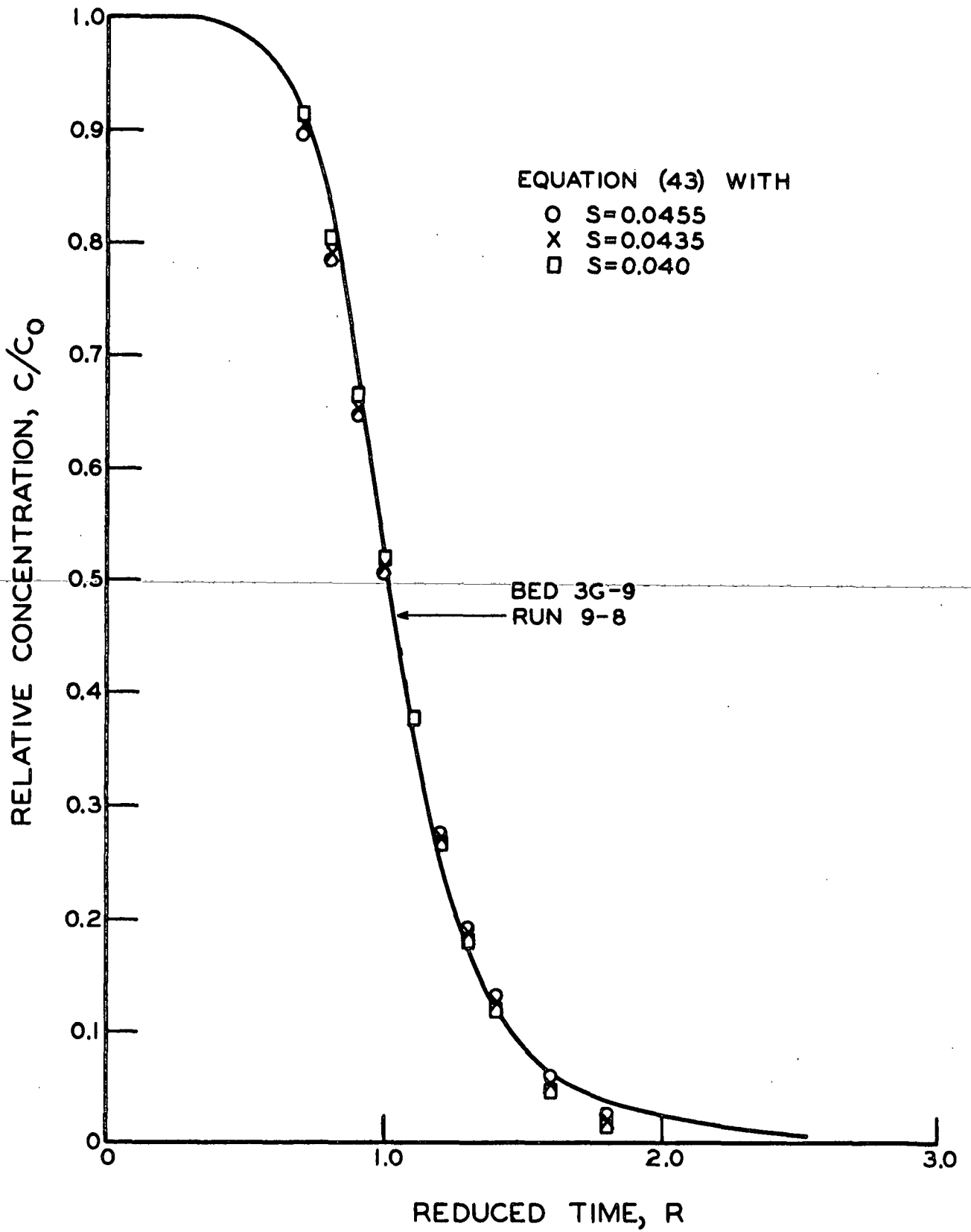


Figure 27. Exit Curve--Run 9-8

APPENDIX III
INTRAFIBER DIFFUSION

An unsuccessful attempt was made to measure the apparent diffusion coefficient of glucose in the viscose fibers. A modification of the shallow bed technique of Boyd, et al. (24) was used. In their work, Boyd, et al. washed small beds of ion-exchange resin (10-100 mg.) with various salt solutions. They measured the amount of cation exchanged in various time intervals (1.3-60 sec.). They then calculated which of three possible mechanisms (i.e., the exchange reaction, the diffusion of ions through the particle, or the diffusion of ions through a "film" around the particle) was controlling under the experimental conditions used.

There were several major differences between the solute-solvent-particle system used by Boyd, et al. and that used in these studies. The first of these was the fact that the solute used in this study was nonionic and nonadsorbed, while they used ionic, highly adsorbed solutes. This had two effects. First, the ratio of the intrafiber diffusion coefficient to the molecular diffusion coefficient in solution was probably greater in our case than theirs. Secondly, the ratio of the solute concentration in the solid to that in solution, at equilibrium, was much less (1/10) in our case than theirs.

A second major difference was the particle size used. The particle radius used by Boyd, et al. was about 180 μ , while the particle radius in our case was 30 μ . Thus, the rate of diffusion was probably faster in our

case than theirs. Boyd, et al. used washing times of 1-60 seconds, while we used washing times of 0.1-0.8 second.

A third difference between our system and that of Boyd, et al. was the fact that their beds were incompressible, while ours were compressible.

Due to the above differences, several modifications in technique were necessary before the technique could be used. First, it was necessary to develop a means of measuring extremely short washing times (0.1-0.8 sec.) and, secondly, it was necessary to use very high flow rates. High flow rates were needed since it was necessary to bring a relatively large volume of wash fluid into contact with the fibers in a very short time. The apparatus which was used is shown in Fig. 28.

A high flow rate was obtained by the compressed nitrogen head. By turning valve (3) 180°, a short washing time was obtained. By closing valve (7) at the end of a run, the fibers containing the residual glucose were separated from the rest of the system. The residual glucose was washed out by using valves (4), (5), and (6). Valve (8) was used to adjust the liquid height in the flow-sensing tube at the start of a run. The use of a ball valve with the insert shown in Fig. 28 served two purposes. First, it allowed the fibers to be isolated at the end of a run and, secondly, it allowed the fibers to be surrounded by a glucose solution contained between the foil at each end of the insert while at the same time keeping the glucose solution in the system to a minimum.

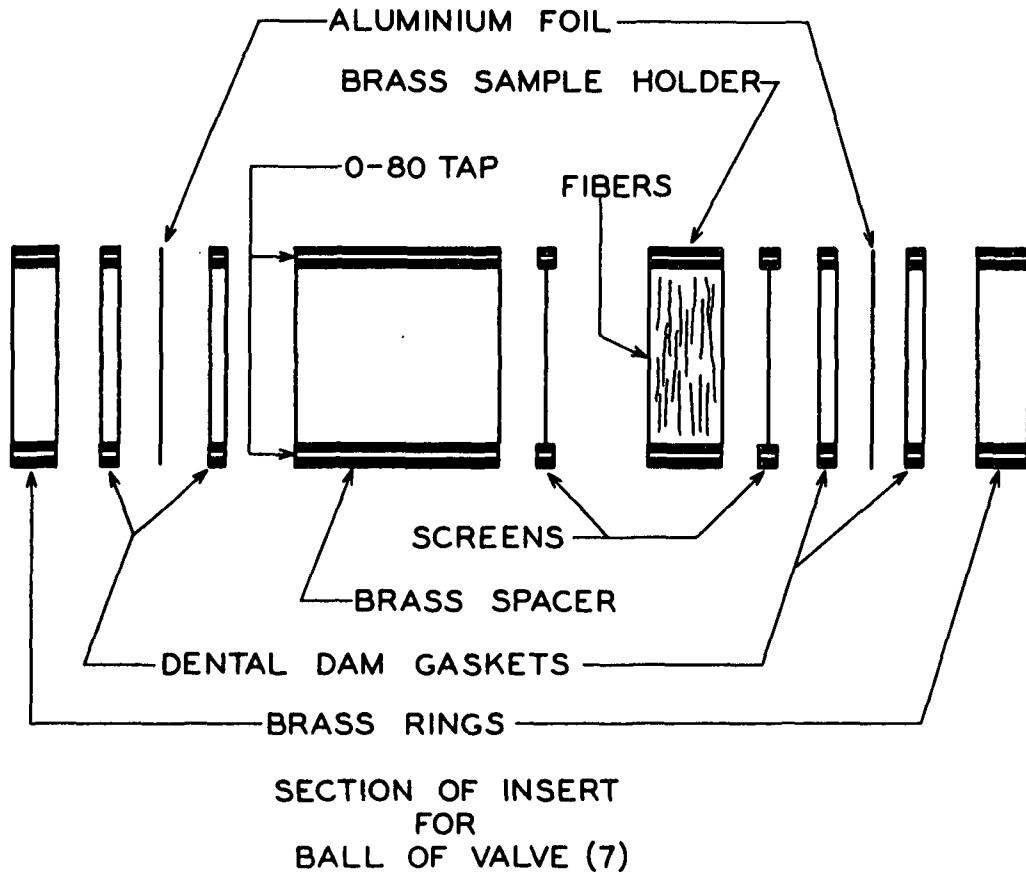
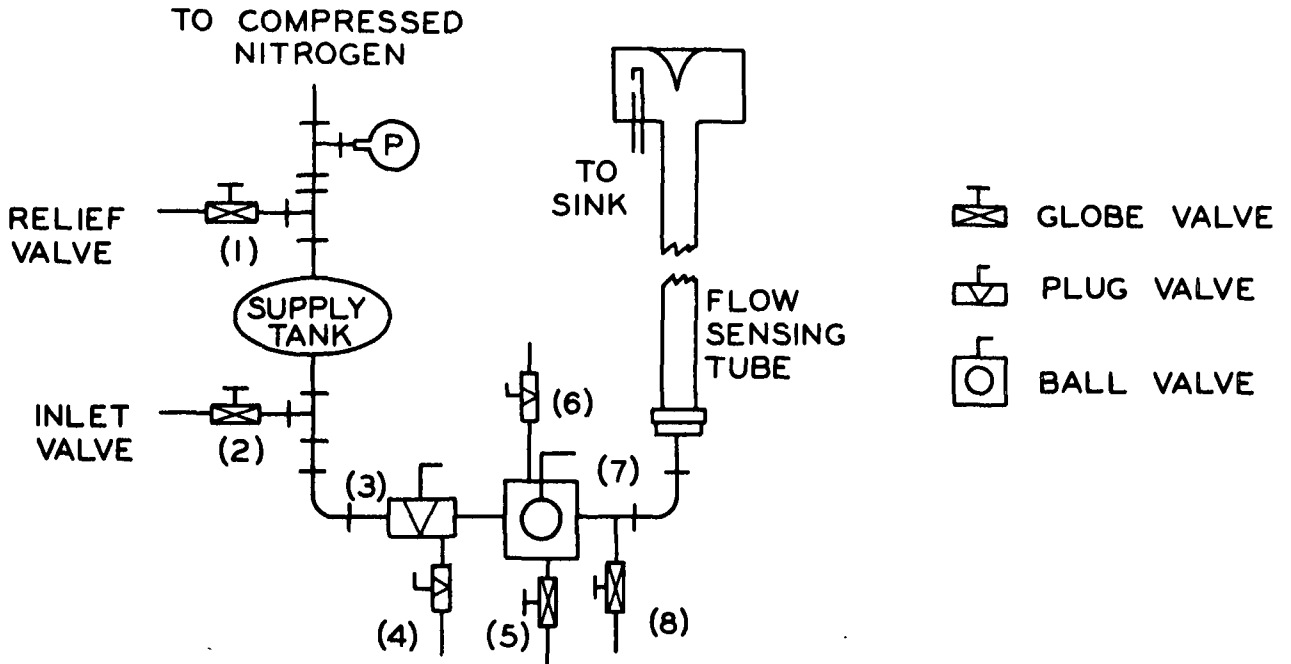


Figure 28. Apparent Diffusion Coefficient Apparatus

The system for measuring the washing time is shown in Fig. 29. This system was based upon the fact that as the level in the flow-sensing tube changed, the resistance of the cell changed. As this arm of the bridge changed, the bridge was unbalanced and the amplitude of the oscilloscope trace changed. Thus, by photographing the oscilloscope trace, a record of liquid level versus time was obtained. The oscilloscope trace was triggered by a microswitch connected to valve (3). When the valve was turned, the trace was triggered. By proper interpretation, this record enables one to tell when the washing started and stopped.

The procedure used to carry out a washing run is outlined below.

1. A large pad of fibers (3-in. diameter) was formed and from this a 1/2-in. diameter sample was cut.
2. The sample was placed in the insert of the ball, rinsed with glucose solution, and then deaerated under vacuum at room temperature for 30 minutes while setting in the glucose solution.
3. The fibers and glucose solution were then sealed in the ball with aluminum foil, while under the glucose solution. The ball was then rinsed with water and then soaked in water for 15 minutes.
4. The ball was then rinsed again with water and placed in the ball valve.
5. The right side of ADCA (Fig. 28) was filled with salt solution through valve (8) and the level adjusted to the desired height (so that the bridge circuit could be balanced).
6. The left side of ADCA was filled through valves (4) and (5).

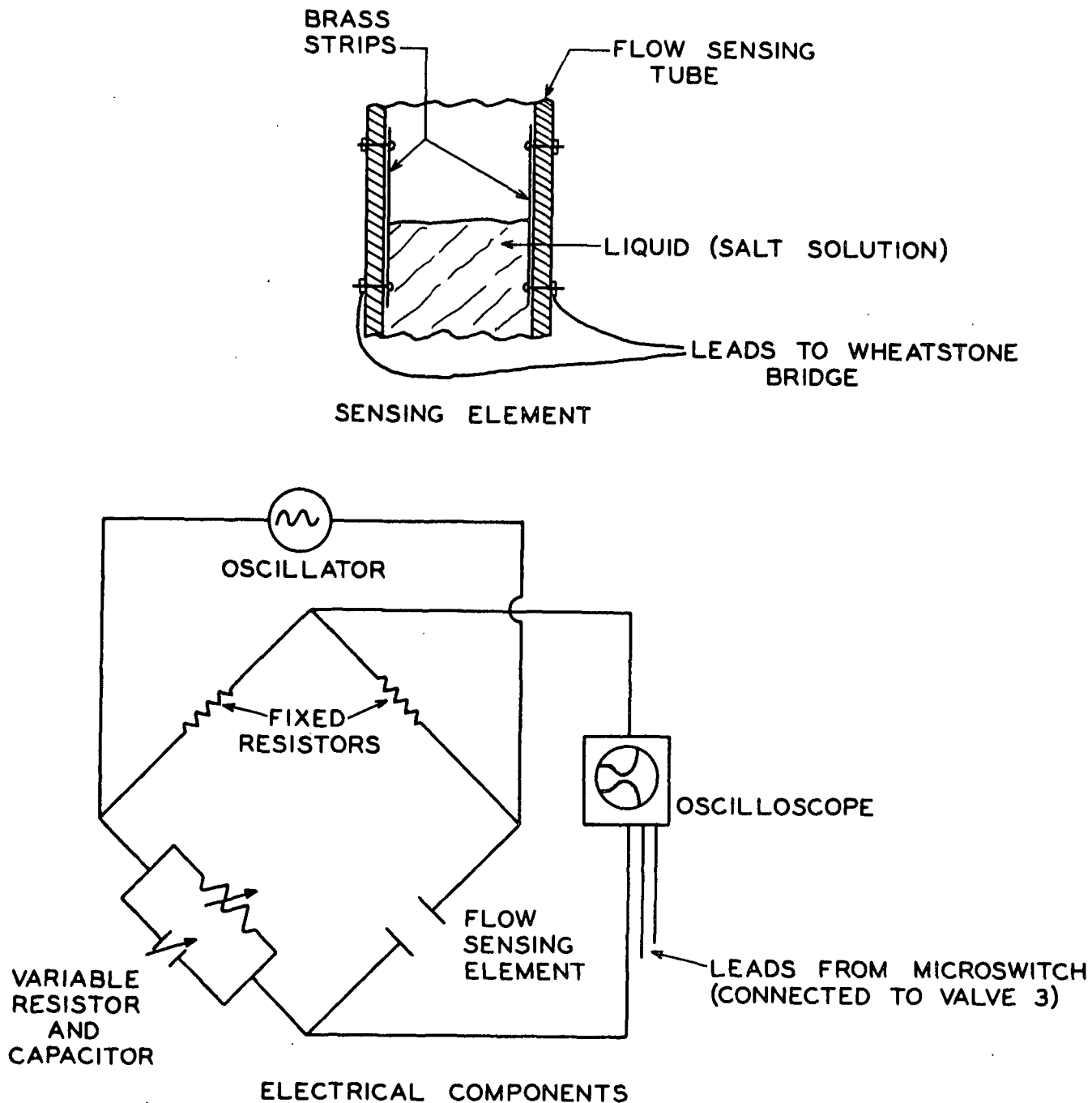
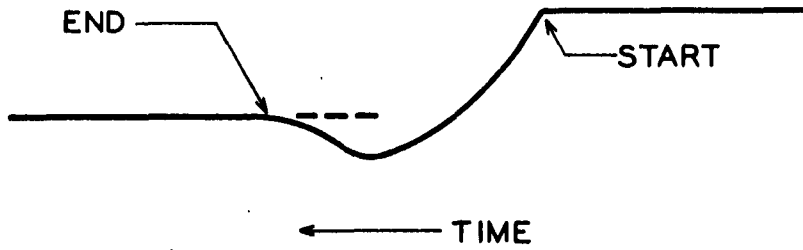


Figure 29. Components of Washing Time Device

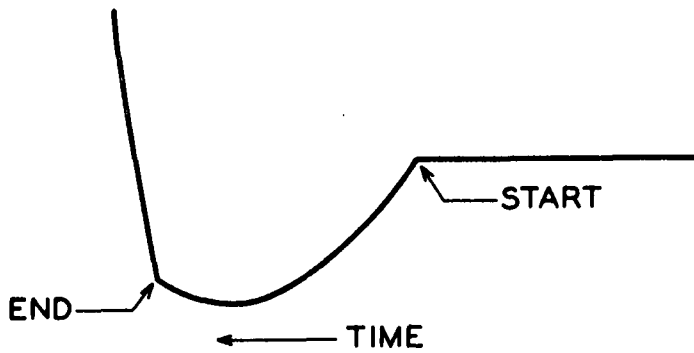
7. All valves were closed and the nitrogen head was placed upon the supply tank.
8. In rapid succession, the ball valve (7) was opened, the camera opened, valve (3) rotated 180°, the ball valve (7) closed, the camera closed, and the pressure released by opening (1).
9. The right side of ADCA was then drained.
10. The portion between (3) and (7) was drained and quantitatively rinsed to obtain the residual glucose.
11. The pressure, temperature, oscilloscope settings (mv./cm. and sec./cm.), and rise of liquid level in the flow-sensing tube were recorded.
12. The picture was developed and then, if the picture was satisfactory:
13. The washings were concentrated and the residual glucose determined by the Nelson-Somogyi method (25, 26).
14. Steps 2 through 13 were then repeated for several runs and then the fibers in the ball were quantitatively transferred to a sintered funnel, dried at 105°C., and weighed.

The above procedure was called "normal" and gave an oscilloscope trace like that shown in the upper part of Fig. 30. The start of such a run was easily distinguished; however, the end point was more difficult to define.

A number of runs were also made with a slightly different procedure called an "air purge" run. In this case, the liquid in the supply tank



"NORMAL RUN"



"AIR PURGE RUN"

Figure 30. Oscilloscope Traces

was decreased so that, at the end of a run, a rush of nitrogen would pass through the bed. Step 8 of the above procedure thus became:

8A. In rapid succession, the ball valve (7) was opened, the camera opened, the valve (3) rotated 90°, the ball valve (7) closed, the camera closed, and the pressure released by opening (1).

All other steps were the same. With this procedure, the lower trace in Fig. 30 was obtained. Both the start and end of a run were easily distinguished with this procedure.

All runs were made using 16-denier (60 μ diameter) all-skin viscose fibers. The runs in Table X were made using the "normal" procedure, while those in Table XI were made using the "air purge" procedure. The results of these runs, along with a theoretical curve, are also shown in Fig. 31. The theoretical curve is based upon the assumption that the fibers act as discrete, infinite cylinders, of 30 μ radius, surrounded by solution of zero concentration for the duration of the washing time, and the intrafiber diffusion coefficient is 0.7 times the diffusion coefficient in solution.

A look at Tables X and XI, or Fig. 31, reveals that the assumption that the fibers were surrounded by solution of zero concentration almost immediately after the flow was started is incorrect (since, even at the end of the run, more glucose was in the bed than the fibers could hold). It is believed that this difficulty was probably due to channeling in the bed of fibers.

TABLE X

VISCOSE FIBER RUNS WITH "NORMAL" PROCEDURE

Pad	Run	\underline{C}_0 , μg./ml.	\underline{W}_f , mg.	\underline{Q}_0 , μg.	\underline{Q} , μg.	\underline{t} , sec.	$\underline{Q}/\underline{Q}_0$	$\underline{\Delta h}$, cm.
2	1	17.39	28.7	503	928	0.20	1.85	(3.0) ^a
2	2	17.39	28.7	503	707	0.20	1.41	(6.9)
2	3	17.43	28.7	504	629	0.47	1.25	(7.9)
2	6	18.43	28.7	533	727	0.43	1.37	5.8
2	7	18.43	28.7	533	1271	0.18	2.38	2.0
2	8	18.43	28.7	533	502	0.78	0.94	11.5
3	1	17.71	26.4	475	808	0.18	1.70	3.5
3	2	17.71	26.4	475	497	0.40	1.05	9.8

\underline{C}_0 = concentration of glucose solution surrounding the fibers before washing

\underline{W}_f = weight of fiber sample

\underline{Q}_0 = glucose in fiber before washing (= fiber porosity times \underline{C}_0)

\underline{Q} = glucose in fiber bed after washing (residual glucose)

\underline{t} = washing time

$\underline{\Delta h}$ = change in height of liquid in flow-sensing tube during a run
(11.4 $\underline{\Delta h}$ = cc. wash fluid used)

^a Values in parentheses are estimated from the oscilloscope traces. The other values were measured directly.

TABLE XI

VISCOSE FIBER RUNS WITH "AIR PURGE" PROCEDURE

Pad	Run	$\frac{C}{O}$, μg./ml.	$\frac{W}{f}$, mg.	$\frac{Q}{O}$, μg.	$\frac{Q}{}$, μg.	$\frac{t}{}$, sec.	$\frac{Q}{Q_0}$	$\frac{\Delta h}{}$, cm.
4	1	18.19	27.1	500	571	0.07	1.14	5.0
4	2	18.19	27.1	500	515	0.52	1.03	13.5
4	3	18.19	27.1	500	531	0.41	1.06	12.5

$\frac{C}{O}$ = concentration of glucose solution surrounding the fibers before washing

$\frac{W}{f}$ = weight of fiber sample

$\frac{Q}{O}$ = glucose in fiber before washing (= fiber porosity time $\frac{C}{O}$)

$\frac{Q}{}$ = glucose in fiber bed after washing (residual glucose)

$\frac{t}{}$ = washing time

$\frac{\Delta h}{}$ = change in height of liquid in flow-sensing tube during a run
(11.4 $\frac{\Delta h}{}$ = cc. wash fluid used)

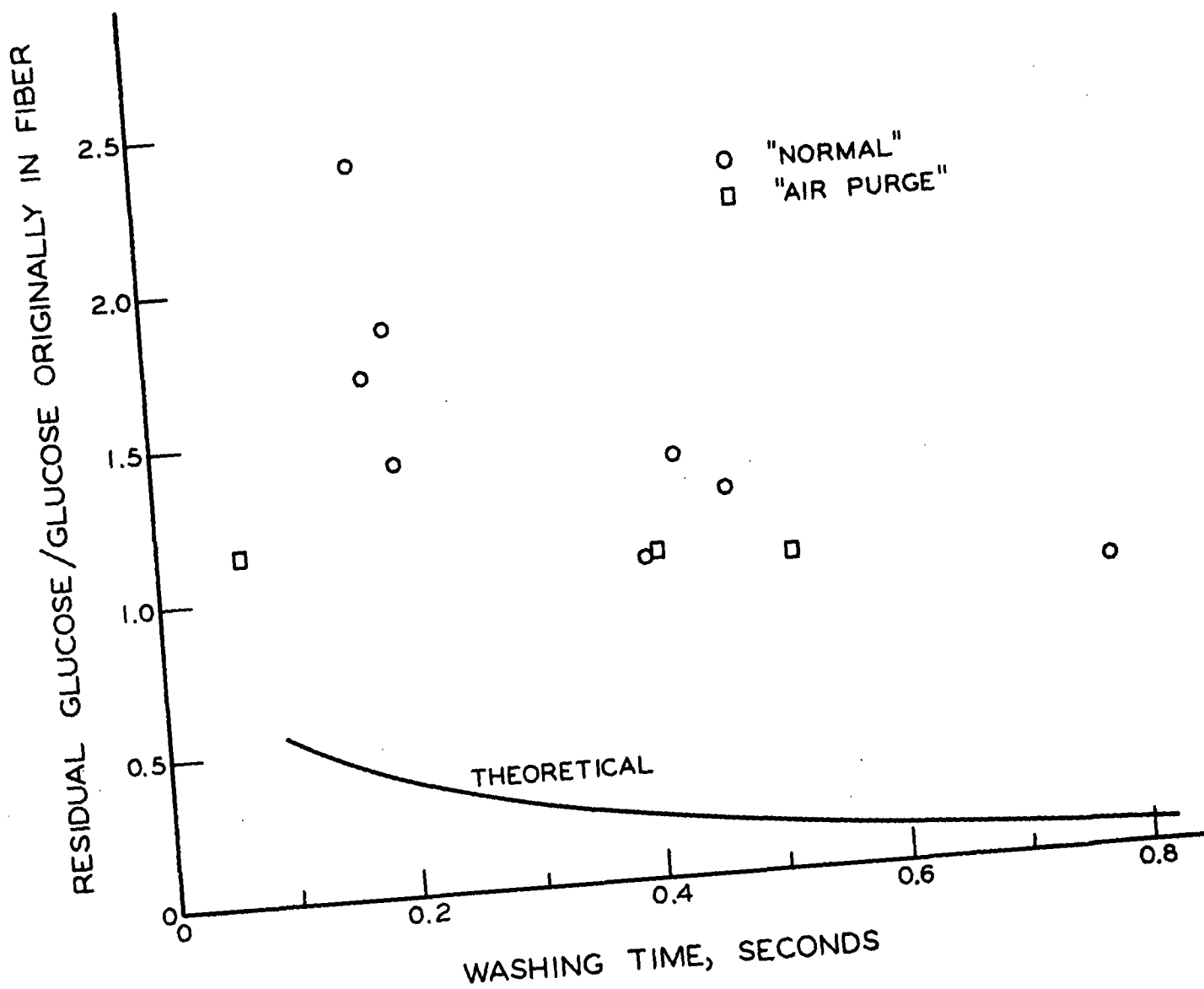


Figure 31. Apparent Diffusion Coefficient Data